



universität
wien

DIPLOMARBEIT

Titel der Diplomarbeit

Development of the central nervous system in the
Hawaiian bobtail squid (*Euprymna scolopes*) based
on histology and x-ray microtomography

Verfasserin

Alexandra Kerbl, Bakk. phil.

angestrebter akademischer Grad

Magistra der Naturwissenschaften (Mag. rer.nat.)

Wien, 2012

Studienkennzahl lt. Studienblatt: A 439

Studienrichtung lt. Studienblatt: Zoologie

Betreuer: Ao. Univ.-Prof. Mag. Dr. Manfred G. Walzl

CONTENT

ABSTRACT	5
KEYWORDS	5
ZUSAMMENFASSUNG	7
SCHLÜSSELWORTE	8
INTRODUCTION.....	9
MATERIALS & METHODS	13
Specimen	13
Specimen preparation for Micro-CT	14
Specimen preparation for histology	15
3D-reconstruction	17
RESULTS	19
Embryonic development of <i>Euprymna scolopes</i>	19
Nervous system development	27
Ganglionic placode formation and accumulation around the oesophagus (stage 19-22)	27
Neuropile development and lobe differentiation (stage 23-25)	30
Further lobe differentiation (stage 26-hatching)	31
The central nervous system of a hatching <i>Euprymna scolopes</i>	34
Volumetric measurements of the developing sepiolid brain	37
DISCUSSION	41
Cephalopod nervous system development	41
Patterns of neuropile differentiation in cephalopod central nervous systems.....	45
Nervous systems in cephalopods.....	46
<i>Euprymna scolopes</i> as model organism of decabrachiate brain development.....	49
Micro-CT in cephalopod nervous system research.....	50
CONCLUSION	54
ACKNOWLEDGEMENTS.....	56
REFERENCES	57
SUPPLEMENTARY INFORMATION	II

SUPPLEMENTS I: Kerbl, A., S. Handschuh, M.-T. Nödl, B. Metscher, M. Walzl & A. Wanninger (subm.). Micro-CT as non-destructive technique to determine ganglionic growth during cephalopod development. *Journal of Experimental Marine Biology and Ecology*¹ IIII

SUPPLEMENTS II: Curriculum Vitae XXVI

¹This article includes all of the 3D-reconstructions done during my diploma thesis as well as the main part of the micro-CT-analysis. Therefore, it is a vital part of the work I have done.

ABSTRACT

The cephalopod central nervous system is believed to have evolved by fusion of paired ganglia. As such, the cephalopod “brain” may contain the cerebral, brachial, pedal, palliovisceral and buccal ganglia as well as the optic lobes. In contrast to vertebrates, where the brain develops by neurulation from a neural tube, the mollusk (including cephalopod) ganglia form as individual placodes in the blastoderm of the embryo, which fuse during subsequent development. Only few studies have focused on the early development of the cephalopod nervous system. Herein, I want to re-assess cephalopod gangliogenesis in the emerging model decabrachiate *Euprymna scolopes* using state-of-the-art micro-CT and traditional histology in combination with digital 3D reconstruction techniques. Nervous system development in *Euprymna* starts at stage 19, when the ganglionic placodes are formed as thickened places in the blastoderm at the animal pole of the egg. The neuropile, the fiber material inside the ganglia in adult animals, differentiates later, after the ganglia are accumulated in a ring-like structure around the oesophagus (stage 22). The single ganglia melt together to one mass and give rise to a series of lobes, which are parts of motoric and sensory systems inside the brain. Most striking are the lateral optic lobes, which have a characteristic structure in their interior formed by the tree-like extension of the nervous fibers and account for about a third of the total brain volume. Arm and tentacular nerves show the specific structure of a ganglionic series, whereas the peripheral parts (gastral ganglion and stellar ganglia) are formed later and appear approximately at stage 26. Previous neuro-anatomical studies have examined common genera such as *Loligo*, *Sepia* or *Octopus*. The overall formation pattern in coleoids is largely similar among species, although the temporal succession of individual processes such as ganglionic accumulation and lobe differentiation differs. The ganglionic layout is quite common in *Loligo*, *Sepia* and *Euprymna*, whereas *Octopus* abberates due to a higher concentration of the ganglia. In an early stage, the decabrachiate brain more closely resembles the nautiloid adult brain than the coleoid one. Therefore, investigating brain development in coleoid cephalopods contributes to our knowledge about the ancestral conditions in this group and will answer questions about the development of complex brains.

KEYWORDS

Sepioids – nervous system – development – histology – x-ray microtomography – Micro-CT

ZUSAMMENFASSUNG

Das Zentralnervensystem der Cephalopoden entstand vermutlich durch die Verschmelzung paariger Ganglien. Das „Gehirn“ besteht daher vermutlich aus zumindest Teilen des Cerebral-, des Brachial-, des Pedal-, des Palliovisceral- und des Buccalganglions sowie der optischen Loben. Es gibt nur wenige Studien, die sich mit der Frühentwicklung des Nervensystems der Cephalopoden befassen. Das Ziel dieser Diplomarbeit ist es, diese an dem aufstrebenden Modellorganismus *Euprymna scolopes* zu demonstrieren. Eine Kombination aus Micro-CT und Histologie zusammen mit computerunterstützter 3D-Rekonstruktion soll Aufschluss über die Gangliogenese geben. Die Entwicklung des Nervensystems setzt bei *Euprymna* später als bei *Todarodes* im Stadium 19 ein, wenn sich die Plakoden der Ganglien als Verdickungen des Blastoderms ausbilden. Das Neuropil (das Nervenfasermaterial der Ganglien) differenziert sich erst später, nachdem die Ganglien nach innen verlagert und um den Oesophagus akkumuliert wurden (Stadium 22). Die einzelnen Ganglien verschmelzen zu einer ringartigen Struktur und bilden Loben aus, die im adulten Tier gemeinsam durch verschiedene Verschaltungen die motorischen und sensorischen Zentren darstellen. Am auffälligsten sind die lateralen optischen Loben, die eine charakteristische, bäumchenartige Struktur in ihrem Inneren aufweisen, die vom Neuropil gebildet wird. Sie machen etwa ein Drittel des gesamten Gehirnvolumens aus. Die Arm- und Tentakelnerven zeigen die spezifische, zweischichtige Struktur einer Ganglienkette. Periphere Anteile des Nervensystems wie das Gastralganglion oder die Stellarganglien differenzieren sich erst später (Stadium 26). Bisherige neuroanatomische Studien untersuchten vor allem allgemein bekannte Gattungen wie *Loligo*, *Sepia* oder *Octopus*. Der generelle Ablauf ist innerhalb der Coleoiden sehr ähnlich, jedoch kommt es häufig zu einer zeitlichen Änderung von individuellen Prozessen wie der Ganglienakkumulation und der Lobendifferenzierung. Die Anordnung der Ganglien bei *Loligo*, *Sepia* und *Euprymna* ist sehr ähnlich, während es bei *Octopus* zu einer stärkeren Konzentration der Ganglien kommt. In den frühen Stadien erinnert das Gehirn der decabrachiatischen Cephalopoden aufgrund der Anordnung der Ganglien und ihrer Verbindungen sehr an das adulte Gehirn von *Nautilus*. Daher kann die weitere Untersuchung der Entwicklung des Nervensystems in coleoiden Arten dazu beitragen, unser Wissen über die ursprünglichen Zustände innerhalb dieser Tiergruppe zu erweitern und daher auch Fragen zur Entwicklung komplexer Nervensysteme beantworten.

SCHLÜSSELWORTE

Sepiolidae – Nervensystem – Entwicklung – Histologie – Micro-CT

INTRODUCTION

Cephalopods are commonly known for their behavioural patterns and their ability to camouflage (e.g. Adamo & Hanlon 1996; Agin *et al.* 2006; Hanlon 2007). These abilities make them on the one hand special in the molluscan group and in most of the invertebrates, but require on the other hand a high developed nervous system (Wilson 1959; Tublitz *et al.* 2006). Indeed, the cephalopod brain is highly concentrated, so that it nearly resembles the brain in vertebrates (Packard 1972). In contrast to vertebrates, though, it develops not by neurulation, but from individual ganglionic placodes (e.g. Marquis 1989; Shigeno *et al.* 2001a, b; 2008). The central nervous system as consisting of different ganglia is common in all molluscs, whereas the concentration is variable between the groups, as are the general bodyplans. The taxa inside the cephalopods (e.g. nautiloids, octopods, sepiolids) are of variable shape, as are the nervous systems.

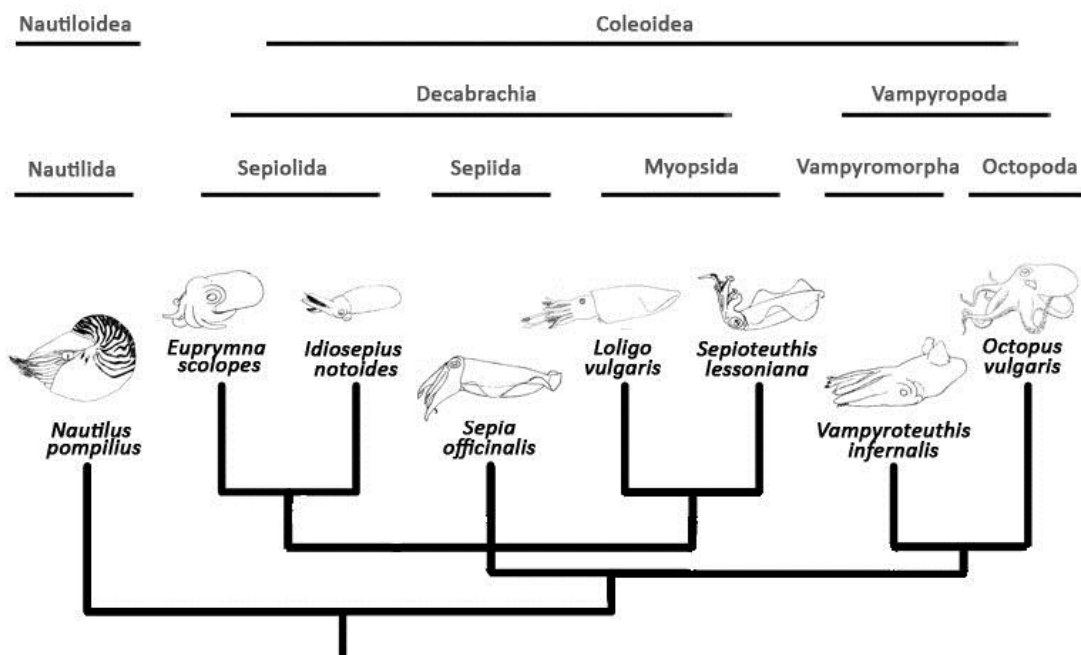


Fig. 1. Cephalopod groups with respect to the most important species in nervous system research based on recent publications (Allcock *et al.* 2011, Kröger *et al.* 2011). This tree intends to show some of the relationships between taxa without including data about either distance between them, branching points or support for the presented theory. Not all cephalopod groups are included here, so the oegopsids and the bathyteuthids are missing next to some other small groups. Although *Octopus vulgaris* has been in the focus of brain research for a very long time, decabrachiate species gain importance as they are supposed to give insight in the basal coleoid conditions. Nowadays, *Nautilus* is considered to display derived features as well.

In the cephalopod group are two major subgroups: the nautiloids with their external, chambered shell with *Nautilus pompilius* Linnaeus, 1758 being the most popular representative, and the coleoids, which have moved the shell in their interior and reduced it in the process (Allcock *et al.* 2011, Kröger *et al.* 2011, Fig. 1). The coleoid group consist of most of the taxa we know today, mainly octopods, cuttlefish and squid as well as some enigmatic forms such as *Spirula spirula* Linnaeus, 1758 (probably at the base of recent coleoids, Warnke *et al.* 2003) or *Vampyroteuthis infernalis* Chun, 1903 (grouped next to octopods forming the Vampyropoda-group, e.g. Kröger *et al.* 2011). Besides the rough discrimination in octopods (now grouped together with Vampyromorpha to form the Vampyropoda, Kröger *et al.* 2011) and decabrachia due to the different arm number, systematic in especially the decapodiform group are problematic. Whereas former phylogenetic trees groups based on morphology grouped myopsid and oegopsid cephalopods in a teuthid group (e.g. Naef 1913), molecular analysis indicate a greater distance between these two groups (Strugnell & Nishigushi 2007, Allcock *et al.* 2011). Sepiolids and sepiids, though, seem to be sister groups of the taxon consisting of myopsids, oegopsids and bathyteuthids. The position of Idiosepiids remains uncertain (Bonnaud *et al.* 2005), as they can be either part of the sepiolid group or a separated taxon placed as sister taxon to oegopsids and bathyteuthids (Allcock *et al.* 2011). Recently, the position of the cephalopod group in the molluscan taxon has been under debate. Whereas previous studies focussing mainly on morphology stated the gastropods as their most probable sister group (Salvini-Plawen 1980, Salvini-Plawen & Steiner 1996), molecular data suggest the whole conchiferan group (monoplacophorans, gastropods, bivalves and scaphopods) to be their sister group (Kocot *et al.* 2011, Smith *et al.* 2011). In the later theory, cephalopods would have developed independently from the other groups, and similarities between gastropods and cephalopods might result from convergent evolution.

Starting in the middle of the last century, there was a lot of interest in the anatomy of the nervous system in different groups inside the cephalopods. It was especially JZ Young in collaborations with other teuthologists, who first described the different components of the cephalopod brain in high detail (Young 1932, 1964, 1973, 1975, 1976, 1977; Messenger 1978; Young 1978, 1985). The origins of electrophysiologic measurements in nerve cells and the discovery of the membrane potential date back to these early days in cephalopod research (Martin & Rungger 1966; Martin 1969; Young 1985). However, such experiments are not that common any more (Pozzo-Miller *et al.* 1998). Although the homology of the cephalopod ganglia to other molluscan ganglia is critical, the structures in cephalopods are named according to their arrangement in gastropods. The brain can be distinguished in a supra- and a

suboesophageal mass, which are composed of either the cerebral ganglion or the fused masses of the pedal and the palliovisceral ganglion. The optic lobes are situated laterally to the other masses and therefore close the ringlike brain, which embraces the oesophagus (e.g. Budelmann *et al.* 1997).

Although there was and is much interest in the structure of the cephalopod brain, just few species have been examined to this respect. These are nautilids (Shigeno *et al.* 2008), “teuthids” (Shigeno *et al.* 2001a, b), sepiolids (Yamamoto *et al.* 2003) and octopods (Marquis 1989). Although there are investigations of the adult nervous system in sepiids (Martin & Rungger 1966; Budelmann & Young 1987; Di Cosmo *et al.* 2000; Quast *et al.* 2001), there are no data on their development. Nevertheless, investigated species allow to distinguish three phases in nervous system development, which mainly can be characterized using histological techniques. This development starts with the ganglionic formation and the accumulation around the oesophagus (phase I) and via neuropile formation and lobe differentiation (phase II), the brain finally increases size and differentiates before hatching (phase III). Unfortunately, none of the species mentioned above shows all the requirements for a general model organism due to critical rearing conditions, territorial behaviour or modified body plans.

The Hawaiian bobtail squid (*Euprymna scolopes* Berry, 1913) has a long history as model organism in symbiosis research due to its symbiotic relationship with the marine bacterium *Vibrio fischerii* (e.g. Hanlon *et al.* 1997; Claes & Dunlap 2000; Nyholm *et al.* 2000; Guerrero-Ferreira & Nishiguchi 2007; McFall-Ngai *et al.* 2010). The tiny sepiolid cephalopods (Fig. 1) live in the shallow waters of the Hawaiian archipelago (Kimbrell *et al.* 2002) and are nocturnal benthic predators (Moynihan 1983; Shears 1988). Recently, there have been attempts to use *Euprymna* as model organism in decabrachiate development (Lee *et al.* 2009g), as there are already some protocols developed for conducting genomic and molecular expression studies (Lee *et al.* 2009f, c, d), as well as confocal (Lee *et al.* 2009e) and developmental investigations (Lee *et al.* 2009a, b). Nothing is known about their internal organization or their histology so far. This includes the nervous system in general and its development in special. It is therefore the aim of this study to investigate the development of the nervous system in this species using both histological techniques and micro-CT in a combined approach.

MATERIALS & METHODS

Specimen

Adult specimens of *Euprymna scolopes* Berry, 1913 (Cephalopoda: Sepiolidae, Fig. 1) were sampled alive near the coast of Manoa, Hawaii, by Marie-Therese Nödl. They were kept in through-flow aquaria at the University of Manoa, Hawaii, where they laid their eggs in clutches. These were removed and separated from each other. For an approximate staging of the embryos, the tables of both Arnold *et al.* (1972) and Lee *et al.* (2009b) were used as well as the same temperature. When reaching a desired stage, they were fixed in 4% glutaraldehyde in 0.1M cacodylate buffer (overnight at 4°C) and afterwards preserved in 75% methanol for micro-CT-application (Fig. 2). The chorion (a tough membrane secreted by the egg, Young *et al.* 2012) was manually removed from the embryos as soon as a thin extraembryonal epithelium was covering the yolk mass (stage 21). For this study, embryos of stages 17 to 30 (hatching stage) were used. These stages have been chosen as previous histological studies (Marquis 1989; Shigeno *et al.* 2001a, b; 2008) found evidence of embryonic nervous system development in other species during that period. Another series of embryos was fixed in Bouins fluid and preserved in 75% ethanol for histological preparation (Fig. 2). See Table 1 for a detail listing of all embryos used. The specimens were sent to Austria preserved in 75% methanol or 75% ethanol. All further steps were conducted at the Department of Integrative Zoology at the University of Vienna in Austria.

Table 1. Embryos of different developmental stages used in this study. Most of the embryos treated for x-ray microtomography were afterwards used in the histologic analysis as well. A more narrow assignment of the different specimens to one stage was conducted after data analysis. Outer morphologic characters proved to be problematic, as some details could not be observed in light-microscopic images.

Developmental Stage	16-17	19-22	22-24	23-26	25-28	27-30
Micro-CT	2	2	3	2	2	6
Histology	3	6	8	4	4	6

Specimen preparation for Micro-CT

Specimen preserved in 75% methanol were used for X-ray microtomography. As cephalopod tissues do not have much signal in themselves, such as mineralized structures (bones, mineralized material), an iodine-solution (I2M, 1% elemental iodine in 100% methanol) is used (Metscher 2009a, b; 2010). The specimens were stained for approximately 22hrs and afterwards rinsed at least three times with 75% methanol (Fig. 2). The unbound iodine has to be removed from the specimen and the surrounding medium to decrease scanning artifacts. Additionally, one specimen was stained with phosphotungstic acid (PTA, Metscher 2009a). Single cephalopod embryos were mounted in heat-sealed pipette tips to avoid movement as well as air bubbles. Both of them decrease the final quality of the scan. The pipette tip was sealed with UHU Patafix (UHU, Bühl, Germany) and Parafilm (PECHINEY PLASTIC PACKAGING, Inc., Chicago, IL, USA) to avoid vaporization (Metscher 2009a, b).

The heat-sealed pipette tips were mounted on the object platform, which is located inside the Xradia MicroXCT scanner (XRADIA Inc., Pleasanton, CA, USA). In principle, a micro-CT-scanner works like a CT-scanner in human medicine, so the X-ray source produces projection images in different virtual layers of the sample on the detector. Different to the human CT-scanner, the X-ray source as well as the detector are stable and the sample rotates around its own axis. The detector system is composed of a set of light microscopy objectives (each equipped with a scintillator crystal at its frontal lens that absorbs X-rays and converts the energy into visible light), a tube lens system and a CCD camera. The Xradia system-specific control software was used to set the source and detector distances to achieve a geometric magnification suitable for the specimen size. Both geometric and objective magnification can be used to optimize the depiction of important details and to determine an ideal field of view. In this study, a 4x objective magnification was used for all specimens. The field of view for a scan is adjusted such that it covers either the total or just a part of the specimen. For specimens too large to be scanned in one scan, two regions were scanned separately and stitched together using the Xradia stitching plugin. With this method, a higher resolution can be achieved even in relatively large objects than with one individual scan. Exposure time and source voltage and current may be adjusted depending on the object and the contrasting agents applied. In our case, we used 15 sec exposure per projection image, and source settings of 60 keV and 8 W. During the scan, the specimen is rotated around its own vertical axis by slightly more than 180°. For this rotation range, 4 images were taken per 1° rotation, resulting in about 720 projection images for each scan. Thus, specimens were entirely scanned within 5-12 hrs.

Tomographic cross sections were reconstructed from projection images using the included XMReconstructor software (XRADIA Inc., Pleasanton, CA, USA) and saved as 8-bit greyscale TIFF image stacks. Exporting the data in a standard image format is necessary for later import in 3D software packages such as Amira (VISAGE IMAGING Inc., San Diego, California, USA) and allows an inspection with traditional image processing applications. After reconstruction, a medianfilter with kernel size 3 was used to reduce background noise. The process of reconstruction results in perfectly aligned and size-calibrated image stacks with isotropic voxels ranging in a size range of 2.5 to 3.8 microns (Fig. 2).

Specimen preparation for histology

Specimen preserved in 75% ethanol were used for the histological preparation. Therefore, the samples were dehydrated by a graded ethanol series and embedded in epoxy resin (Araldite, MERCK, Darmstadt, Germany), including infiltration with propylene oxide. The epoxy resin blocs were polymerized at 60°C for 20h and afterwards sectioned to semithin section series (1µm section thickness), using an Reichert-Jung Ultracut E-microtome (REICHERT, Germany). The sections (thickness 1µm) were stained with toluidineblue at 80°C for 30sec. They were sealed with Araldite and images were taken using a Nikon Eclipse E800-microscope (NIKON Corporation, Tokyo, Japan) in combinations with a Canon D5-SM-camera (CANON Inc., Tokyo, Japan). Finally, images were processed with the program Adobe Photoshop CS5 (ADOBE Systems Inc., San Jose, California, USA) to reduce gradients and label specific structures (Fig. 2).

Next to the ethanol-preserved specimens originally fixed with Bouins fluid, the scanned specimens (preserved in methanol and originally fixed with glutaraldehyde) were rinsed with ethanol and otherwise treated similar to the unscanned embryos (Fig. 2). This additional step was needed to test for the possibility of combined approaches and increased the amount of specimen analyzed using histology.

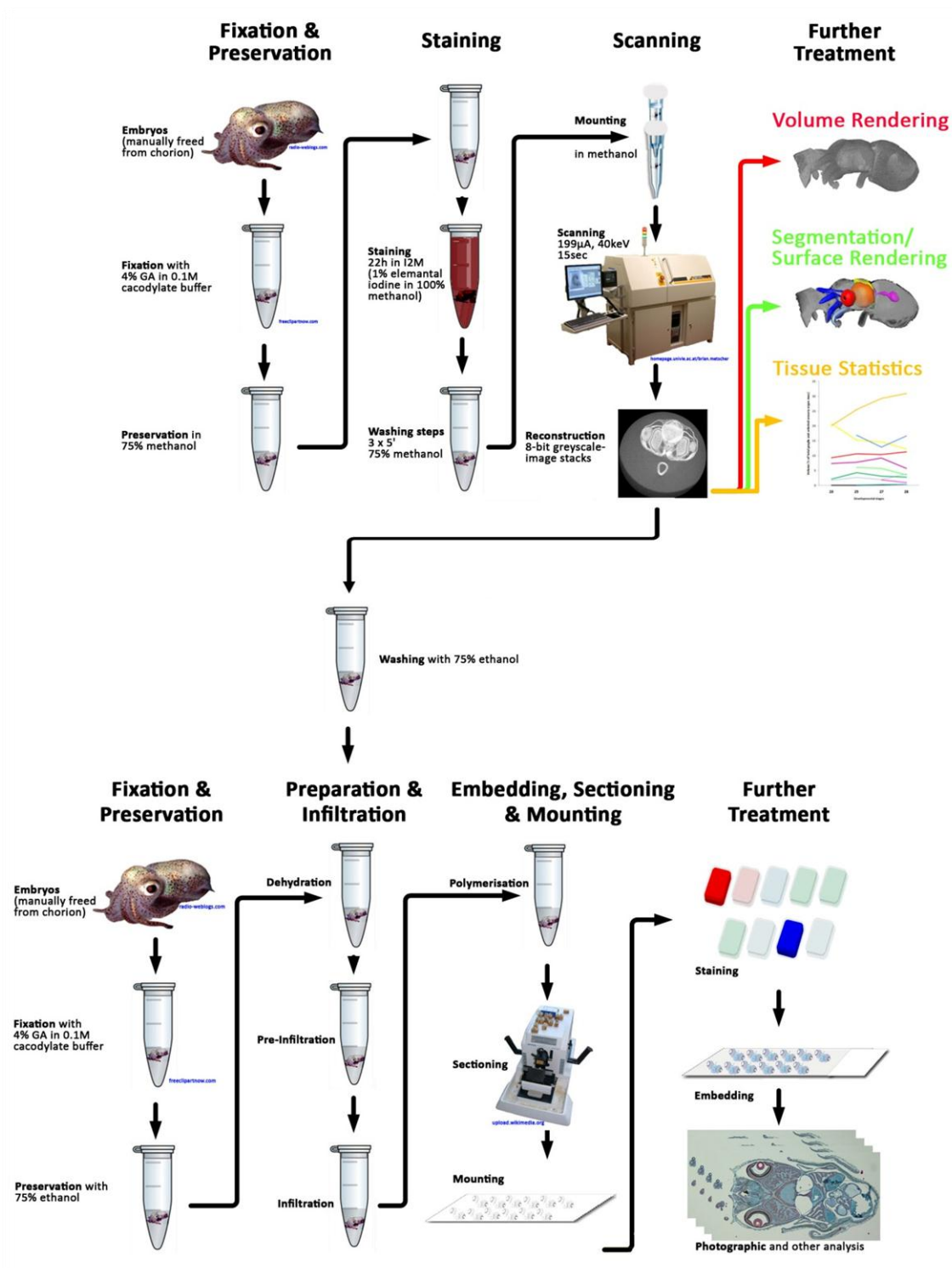


Fig. 2. Workflow combining x-ray microtomographic and histological preparation of the sample specimen. Prior to different preparing steps, the fixation with 4% GA in 0.1M cacodylate buffer is equal for all specimens. For micro-CT, the samples were stored in 75% methanol and after staining with a 1% elemental iodine-solution in methanol, they were mounted in heat-sealed pipette tubes and scanned. The images were reconstructed into 8-bit greyscale image stacks and exported to 3D-reconstruction software packages such as Amira to achieve Volume Renderings, Surface Renderings and obtain data from Tissue Statistics. Additional, more detailed information was achieved from the histological analysis. Specimens

3D-reconstruction

For 3D rendering, the stacks were imported into Amira 5.3. software (Visage Imaging, Inc., San Diego, CA, USA), where the voxel size has to be set at the beginning of the segmentation to obtain adequate data in the volumetric measurement. Individual ganglionic components were manually segmented and assigned to different “materials” within the segmentation file. These additional data sets are connected to the original image stack. Based on manual segmentation, three-dimensional surface renderings were created using the Amira *SurfaceGen* tool by selecting voxel boundaries in a data set. Segmented materials, however, can also be used to obtain quantitative information about the specific materials such as the volume of each structure, by using the *TissueStatistics* tool in Amira. These different possibilities are shown in Fig. 2. Another study focused on this aspect methodologically (Kerbl *et al.* *subm.*) and is provided in the supplementary information section of this thesis.

⇐ were embedded in Araldite following standard protocol and sectioned to serial sections with 1µm thickness. The sections were mounted on object slides and stained with toluidine blue for 30sec at 80°C. After enclosing with Araldite, they were analysed. Specimens treated for micro-CT were washed after scanning in 75% ethanol and afterwards used in histological analysis as well.

RESULTS

Embryonic development of *Euprymna scolopes*

The earliest stage investigated was stage 17, when a thin layer of extraembryonic tissue covers the yolk surface and subsequently gives rise to the external yolk sac. The blastoderm is located at the tip of the animal pole of the egg and further gives rise to the embryo. This very early phase in cephalopod development is called early organogenesis, as the ganglia as well as other organs start their development as placodes starting at stage 17 to 19. These placodes can be recognized as epithelial thickenings with histological methods.

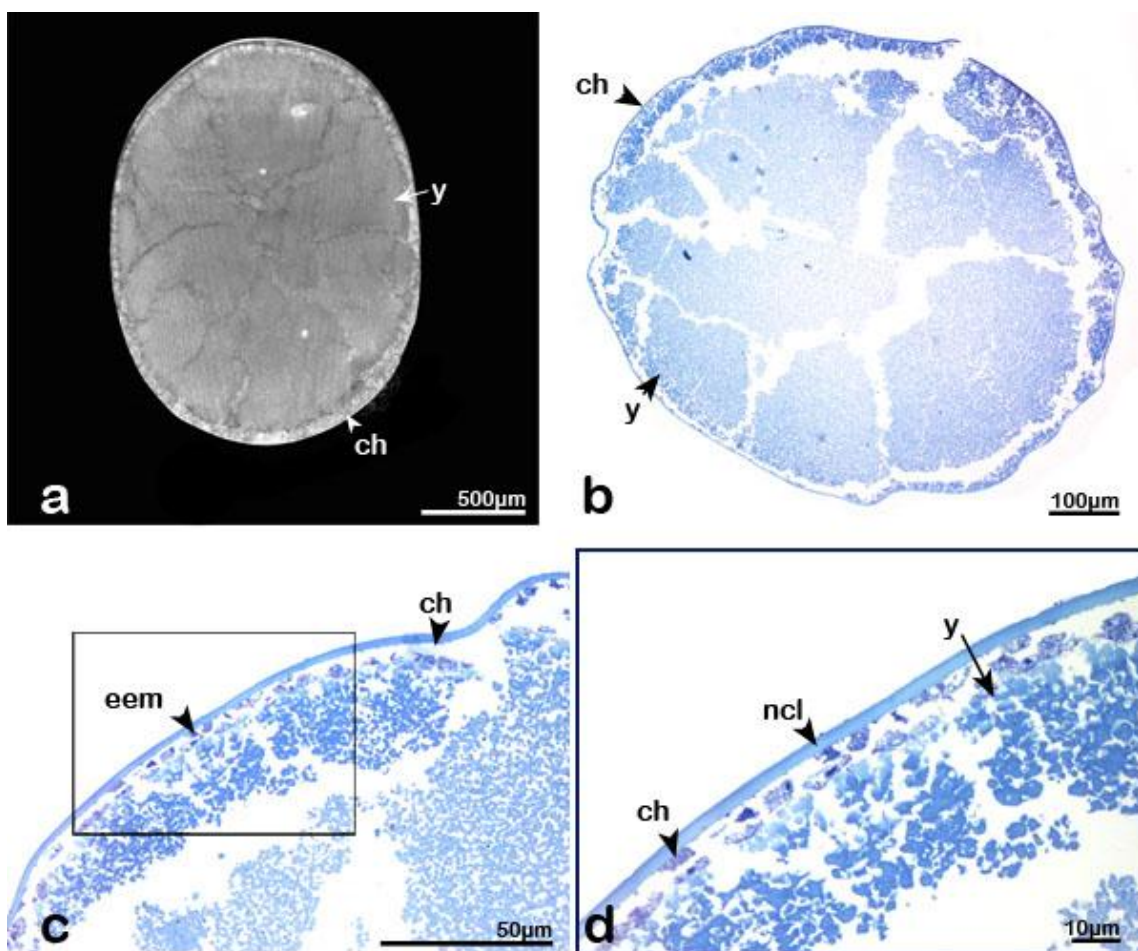


Fig. 3. Stage 17 – x-ray microtomographic and light microscopic images of the egg. **a** virtual section through a volume rendering based on a micro-CT-image stack, **b** transversal section of the egg, **c** detail of the epithelium, **d** epithelial cells. The cross section displays the large amount of yolk (y), which is broken in separate clods (**a,b**). The cortex of the yolk mass is more compact than the inner layers (**c**), which may result from its preparation. The cell layer formed by extraembryonic material (eem) and is unicellular. It covers the surface of the yolk as disjointed epithelium closely adjacent to the chorion (ch, **d**) which is closely adjacent to a noncellular layer (ncl) one to one-and-a-half times thicker than the chorion (**c, d**).

At stage 17, the egg is covered with a chorion (Fig. 3), which was removed manually in the subsequent stages (Fig. 4) to guarantee better fixation and preservation. The chorion is secreted as a membranous structure by the egg, lying closely adjacent to a noncellular protective layer (Fig. 2d) produced by the females reproductive glands (Fig. 3).

The stomodeum as front part of the digestive system starts its invagination at stage 19 between the two buds of arm pair I. It is a circular invagination about 100 to 150 μ m in diameter (Fig. 4). The ectodermal placodes of the eyes form lateral to the stomodeum dorsal to the arm buds of pair II and III. The eye placodes are approximately four times larger than the stomodeum and invaginate while forming the optic vesicles. A similar process of vesicle formation can be observed in the statocysts in a more posterior region of the body, dorsally to the arm buds of pair IV. The statocysts, though, are smaller than the eye placodes (approximately 80 to 100 μ m in diameter). The primordium of the mantle, which is situated next to the shell gland on the animal pole of the egg, is thickening (Fig. 4). Most ventral region in the embryo, five pairs of arm buds develop. In the following developmental steps, four of them (arm pair I, II, III and V) develop into arms with one side totally covered with suckers. Arm pair IV, however, develops into tentacles, where two regions can be distinguished from each other: the long, thin tentacle stalk without any suckers and the tentacle clubs, where suckers are arranged in tight rows. The first suckers can be detected at stage 22 on both the arms and the tentacles. At the posterior side of the embryo, the prospective gills are visible as little knobs below the mantle edge, approximately 50 μ m in diameter (Fig. 4). At stage 20, an ectodermal fold surrounds the invaginating eye and its edges start to fuse in the eye placode's periphery (Fig. 4). The paired fins develop laterally as thickened placodes in the mantle region, while the mantle edge is lifted from the rest of the embryonic body. There is no clear difference between the embryonic body and the external yolk sac from outer morphology, though slight differences in histology can be detected. The funnel originates from two funnel folds, which are now developing at the posterior side of the embryo and already fusing alongside their medial edges (Fig. 4). The development of the eye vesicles is finished by stage 21. The eyes are no longer detectable as invaginations, but as bulbous structures on both sides of the head region. Posterioventral to each eye, one optic lobe can be observed. This leads to a lateral enlargement of the head, which is the dominant part in the cephalopod embryo during the earlier stages. The fins refine their shape and their attachment to the mantle material decreases in size, as the distal edges loose contact. The arm buds elongate during the whole embryonic development, though not with the same rate. Arm pair IV, the prospective tentacles, grow out fastest and are the first to develop suckers on their tips. In the other arms,

there is a pattern of growth rate observable. The posterior arms (V) grow faster than the most anterior ones next to the stomodeum (I), which remain little knob-like structures during the earlier stages. At stage 21, approximately, the whole embryo starts detaching from the external yolk sac, so the connection between the internal and the external yolk sac is going to be the thin yolk neck (Fig. 4).

At stage 22, the optic lobes are a prominent mass, which is visible in the lateral protrusions on both sides inside the head in micro-computertomographic images (Fig. 5). Inside the eye vesicles, the lenses are developing, although they are not spherical yet. The mantle elongates toward the anterior part of the body and while increasing its length, it is covering the prospective organs of the mantle cavity such as the gills. The mouth is still located between the two arms of arm pair I, and has not yet been moved in the center of the arm crown. At the posterior side of the body, the funnel is now a tube-like structure and its whole complex resembles a "W". The statocysts are invaginated completely and are not visible from the outside (Fig. 5). The lenses increase in size during the next developmental stage (23) and are now approximately 50µm in diameter (Fig. 4). Between the gills, which are covered to approximately 50% by the mantle, the anal papilla develops. The arm crown is contracting, so the distance between the two arms of arm pair I decreases. Both of them are now located dorsally to the mouth opening, which is shifted to the center of the arm ring, dorsal to the yolk neck. The animal-vegetative axis of the embryo and the external yolk sac gets bent, so the head of the cephalopod is forming a right angle with the external yolk sac. The yolk neck is a thin connection between anterior and posterior structures inside the animal, which are tightly packed amongst other tissues such as the nervous system. Inside the mantle, the internal yolk sac has formed one lobe (Fig. 5). At stage 24, an epidermal fold overgrows the eye. This fold is going to become the primary lid during further development. The gills and the anal papilla are completely covered by the mantle and located now inside the mantle cavity (Fig. 5). The internal yolk sac has formed two lobes. Blood vessels and the branchial hearts are visible as well. The organ of Hoyle, which is a gland supposed to help in the process of hatching from the egg, is visible now, too. It is located at the posterior tip of the mantle in embryos and looks like a downward-pointed arrowhead (Fig. 5). At its tip, a terminal spine is developing later (stage 26).

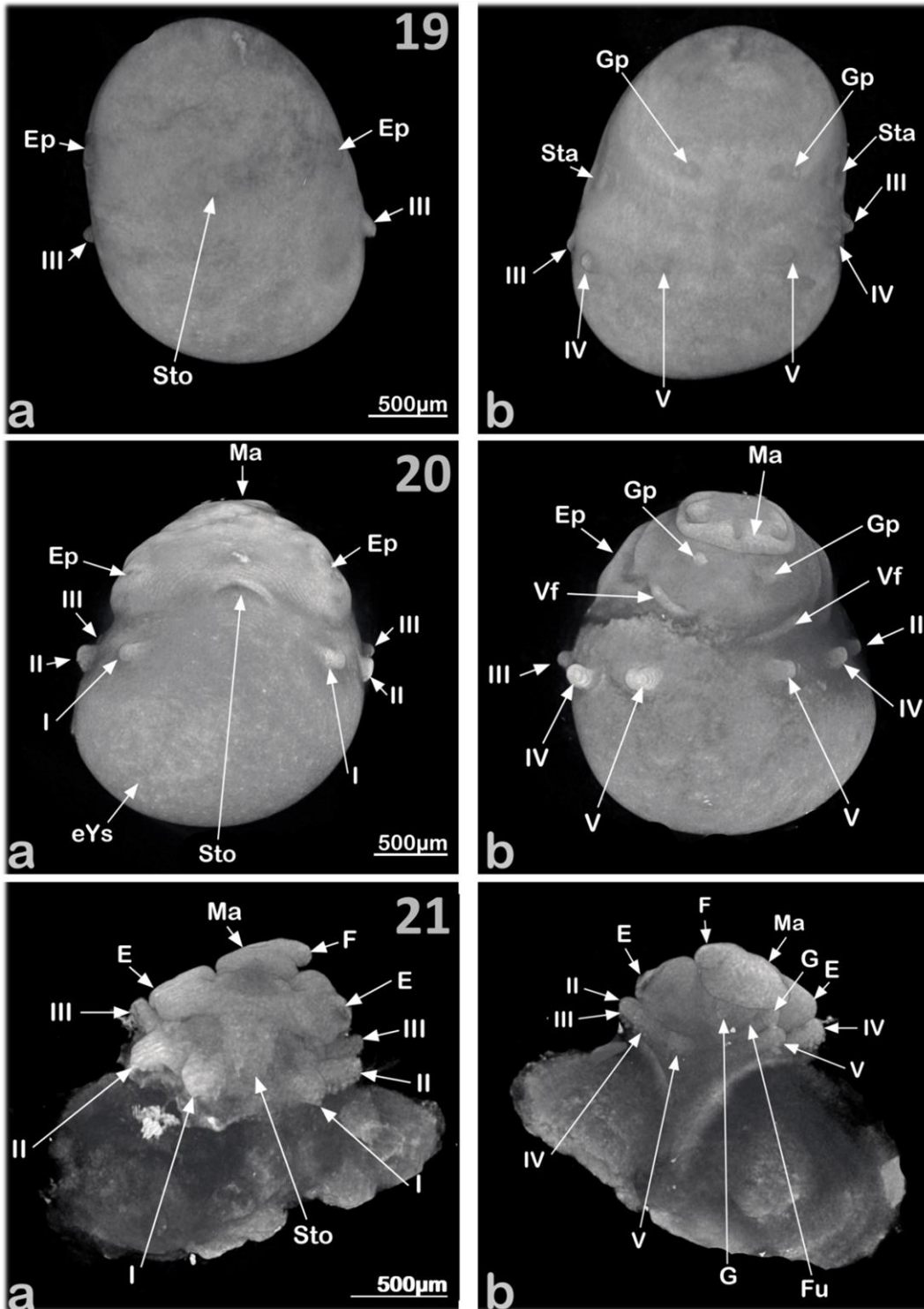


Fig. 4. Stages 19 to 21 – Volume renderings of developmental stages in *Euprymna scolopes*. **a** from anterior, **b** from posterior. During the early stages of development, the embryonic body is not yet pulled clear of the external yolk sac (eYs). The arm buds (I-V) and the eyes (E) are the most obvious structures as well as the mantle (Ma) and the stomodeum (Sto). Primordia of the gills (G) and the funnel (Fu) are also visible. The head region of the embryo dominates the total body, whereas the posterior region is small. Ep – eye placode, F – fin, Gp – gill placodes, Sta – statocyst, Vf – ventral fold.

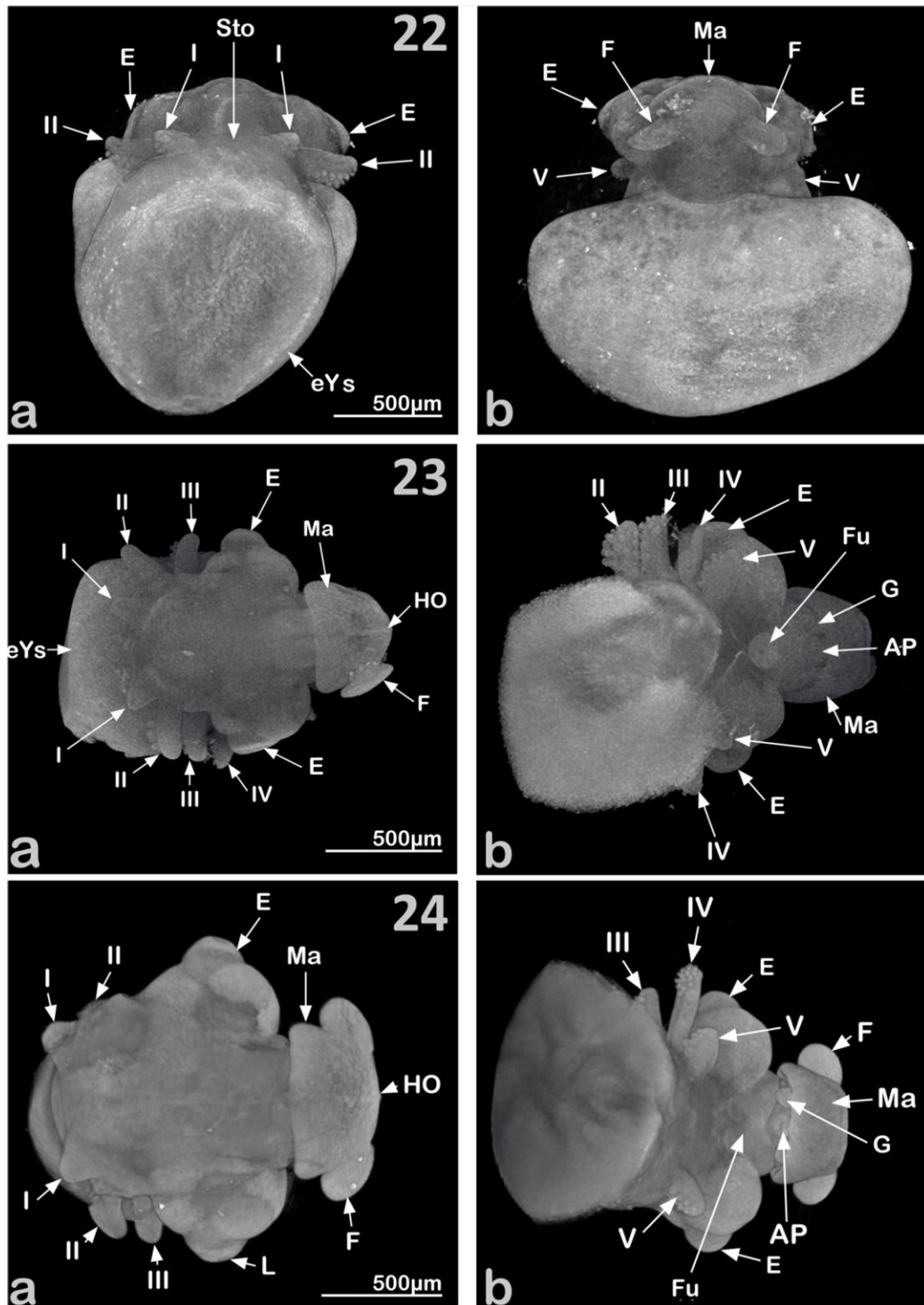


Fig. 5. Stages 22 to 24 – Volume renderings of developmental stages in *Euprymna scolopes*. 22 a from anterior, b from posterior; 23 and 24 a from dorsal, b from ventral. The mantle (Ma) starts overgrowing the prospective mantle cavity and its organs such as the gills (G), the anal papilla (AP), and the posterior part of the funnel (Fu). At stage 22, the arms (I, II, III, V) and the tentacle (IV) clubs start developing suckers. The embryo bends its axis towards the yolk, so the external yolk mass lies in front of the embryonic body in succeeding developmental steps. E – eye, F – fin, HO – organ of Hoyle, L – lense, Sto – stomodeum

The lenses are spherical at stage 25, and the fins have nearly reached their adult shape as well (Fig. 6). When the mantle edge starts to overlap with the posterior edge of the funnel, the gills are forming the first filaments. The statocysts are equipped with sensory cells (with cilia) and statoliths. Special structures located laterally in the neck region between mantle and head are olfactory tubercles (Fig. 6). At stage 26, the mantle has reached its extension, so it is covering all but the anterior tip of the funnel. The internal yolk sac inside the body is forming another set of lobes, so there are two large and two small lobes (Fig. 6). Next to the pigmentation of the retina and the iris, the chromatophores on the body surface appear as well. They are first visible on the dorsal surface of the head as yellow-orange dots. During further developing steps, the number of chromatophores on the ventral surface increases. From stage 27 on, prominent organs of the mantle cavity such as the gills and the blood vessels are completely developed (Fig. 6) and ready to assume their tasks. Especially the large blood vessels in the head region are conspicuous, as they have a diameter of 20 to 100 μ m (Fig. 6).

At stage 29, the ink sac is filled with the dark substance and can therefore be detected as small black spot from the outside when using a light microscope. In contrast to the internal yolk sac, which increases its size towards hatching, the external yolk sac gets reduced and partly concealed between the arms (Fig. 7). It will soon be absorbed in the first days after hatching from the egg.

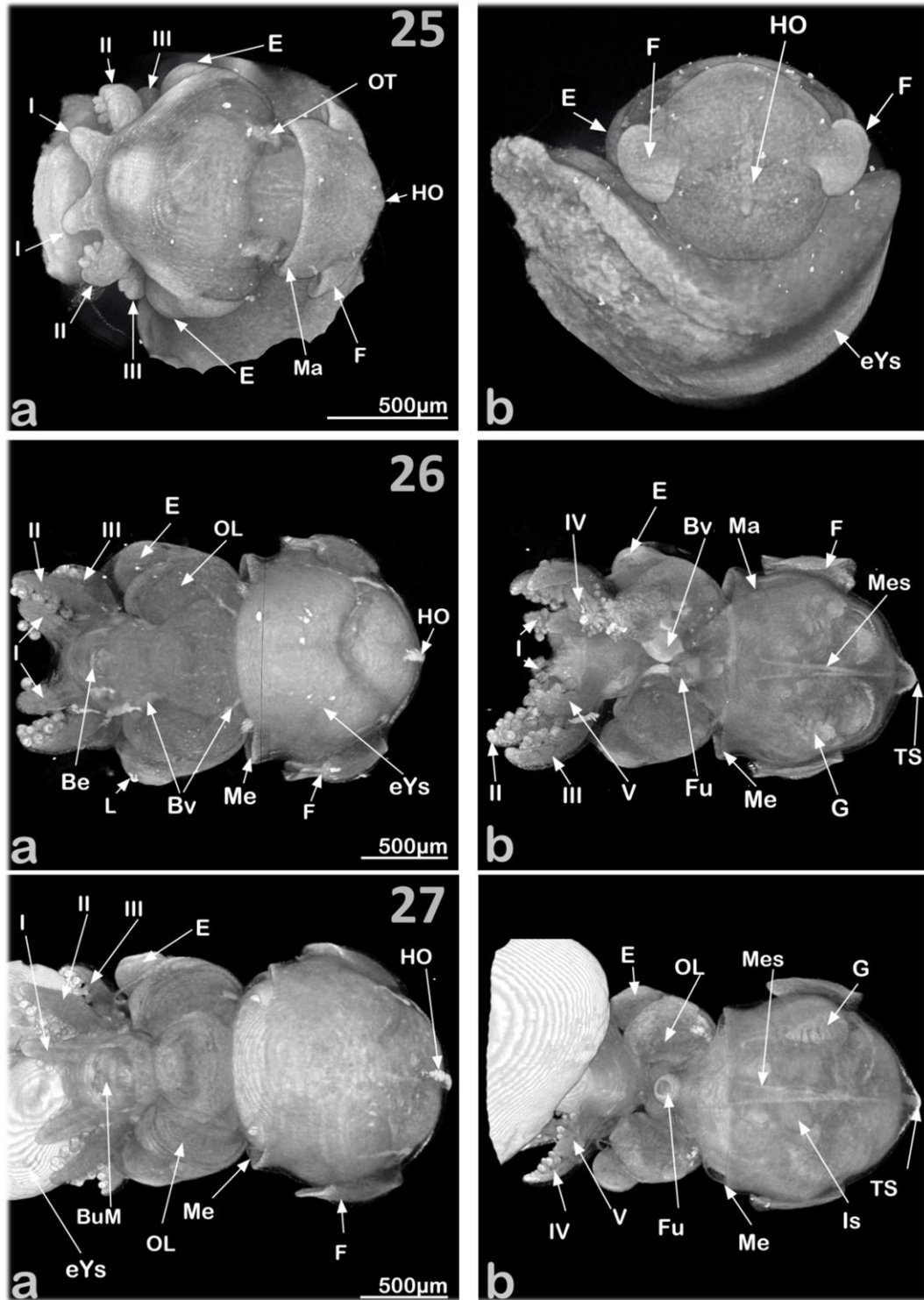


Fig. 6. Stages 25 to 27 – Volume renderings of developmental stages in *Euprymna scolopes*. **a** from dorsal, **b** from ventral. With micro-CT, the blood vessels (Bv) can be detected as they get larger during development. At the posterior tip of the mantle (Ma), the organ of Hoyle (HO) develops. At its tip, the terminal spine (TS), which is used in the hatching process as well, can be detected. Through the mantle musculature, the organs of the now formed mantle cavity are visible such as the ink sac (Is), the gills (G) and the mesentery (Mes). The external yolk sac (eYs) gets absorbed into the interior one (iYs) and decreases its size. I-V – arms I to V, Be – beak, BuM – buccal mass, E – eye, F – fin, Fu – funnel, Me – mantle edge, OL – optic lobe, OT – olfactory tubercle

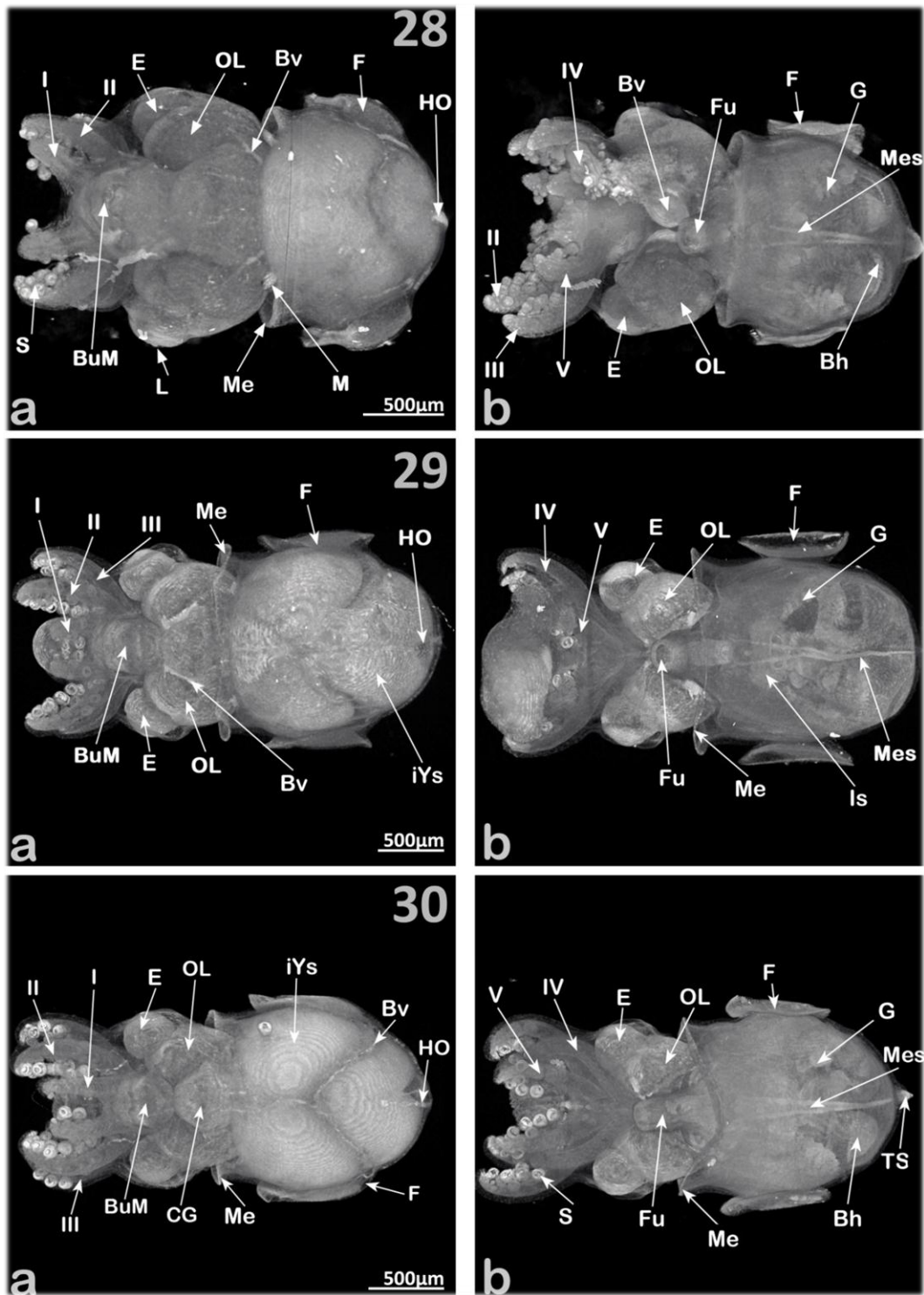


Fig. 7. Stages 28 to 30 – Volume renderings of developmental stages in *Euprymna scolopes*. **a** from dorsal, **b** from ventral. The gills (G) develop their filaments as visible in 28b. Some parts of the circulatory systems such as the branchial hearts (Bh) and the blood vessel (Bv) are visible. The internal yolk sac (iYs) has formed two larger and two smaller lobes. The number of suckers (s) on the arms (I-V) increases until they were covered with two to three suckers per row. Chromatophores, which cover the embryo at hatching stage, are not visible in x-ray microtomographic images. BuM – buccal mass, CG – cerebral ganglion, E – eye, F – fin, Fu – funnel, HO – organ of Hoyle, Is – Inc sac, L – lense, M – muscle, Me – mantle edge, Mes – mesentery, OL – optic lobe, TS – terminal spine

Nervous system development

Ganglionic placode formation and accumulation around the oesophagus (stage 19-22)

The first histological evidence of the nervous system can be detected at stage 19, when the placodes of the cerebral, pedal and palliovisceral ganglia as well as the optic lobes appear as epithelial thickenings (Fig. 8). These can be seen in cross sections. The invagination of the stomodeum, the eyes and the statocysts can be used as landmarks. The cerebral ganglia are small, punctual thickenings of the ectoderm, which are shifted to the inside of the embryo soon and have a maximum extension of about 70µm in diameter at the embryonic surface (Fig. 8). They are located on both sides of the stomodeum and slightly on the dorsal side. In contrast to the ectodermal cells of the embryo, the ganglionic cells are larger (approximately 15µm) and have larger and rounder nuclei (10µm, Fig. 8). These are not as dense as the surrounding ones, but in some cases different stages of mitosis can be observed. Lateral to the stomodeum, the eye placodes form as thickened epithelial areas and start invaginating (Fig. 8). In contrast to the stomodeum, the prospective retina is already formed by a multilayered epithelium, about 30 to 35µm in height. The eye placode is separated from the yolk and other tissue with a thin membrane, which is less than 5µm thick. Adjacent to this membrane, the optic lobes develop as thin strings of ganglionic cells with an posteroventral orientation. Here as well, the cells and their nuclei aberrate from the ones of the surrounding tissue. The highest amount of prospective nervous tissue can be found in the arm buds, which are formed by an internal core of nerve cells with large and round nuclei and an outer layer of a multilayered epithelium (Fig. 8). A thin membrane is separating the nervous tissue of the arm bud and the epithelium from the yolk. This membrane is unicellular and cell nuclei are unregularly found.

Additional parts of the central nervous system, the palliovisceral and the pedal ganglion form both anterior and posterior of each statocyst (Fig. 9). All three components first appear as thickened epithelial regions. In contrast to the ganglionic placodes, which still are on the surface of the embryo, the statocyst already starts invaginating and relocating into the embryos interior. The palliovisceral ganglion is located anterior to the statocyst and small (approximately 20µm in diameter) and resembles a sphere of few cells with light nuclei (Fig. 9).

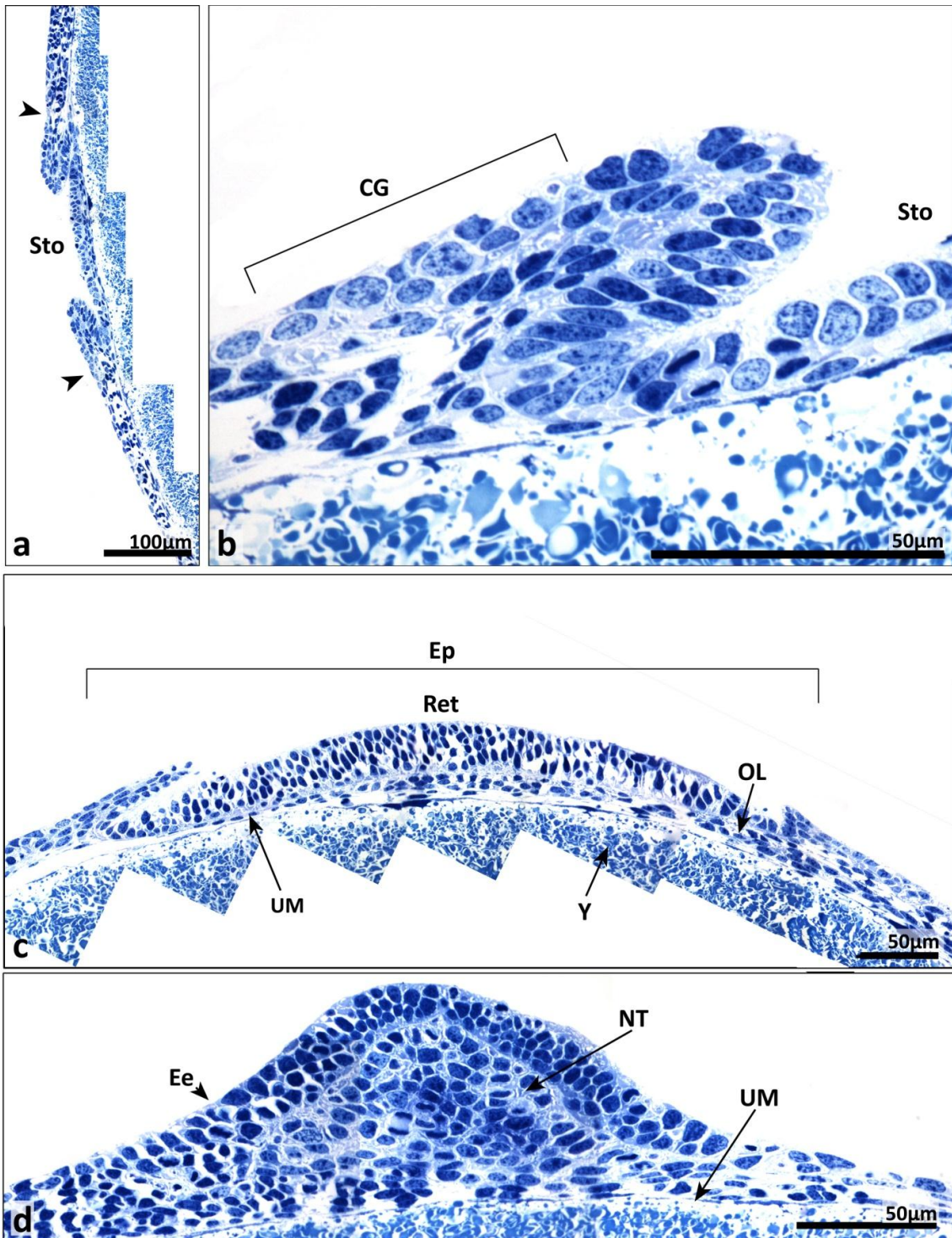


Fig. 8. Stage 19 – Ganglionic placodes formed at the anterior embryonic surface in *Euprymna scolopes* (light microscopic images). **a** partial transversal section focusing on the stomodeum (Sto) and the cerebral ganglionic (CG) placodes, **b** cerebral ganglion (CG) in detail, **c** eye placodes (Ep) with primordium of the optic lobe (OL), **d** nervous tissue (NT) preceding the arm nerves. Image **c** is composed of 7 single images to achieve a higher resolution. In contrast to the surrounding cell nuclei, the nuclei of ganglionic cells are larger and their content is less dense. The retina (Ret) is visible as multilayered epithelium. In contrast to the placodes of the cerebral ganglia, the optic lobe primordia are formed as thin strings leading to the posterior part of the embryo. Ee – embryonic material (here in the region of the arm bud), UM – unicellular membrane, Y – yolk

The most anterior portion of the statocyst has similar attributes, as it is prospective sensory epithelium, too. The pedal ganglion on the other hand is located posterior to the statocyst and covers a large area (at least 100µm in diameter). Most of the ganglionic tissues are still on the surface and not yet shifted to the embryos interior (Fig. 9).

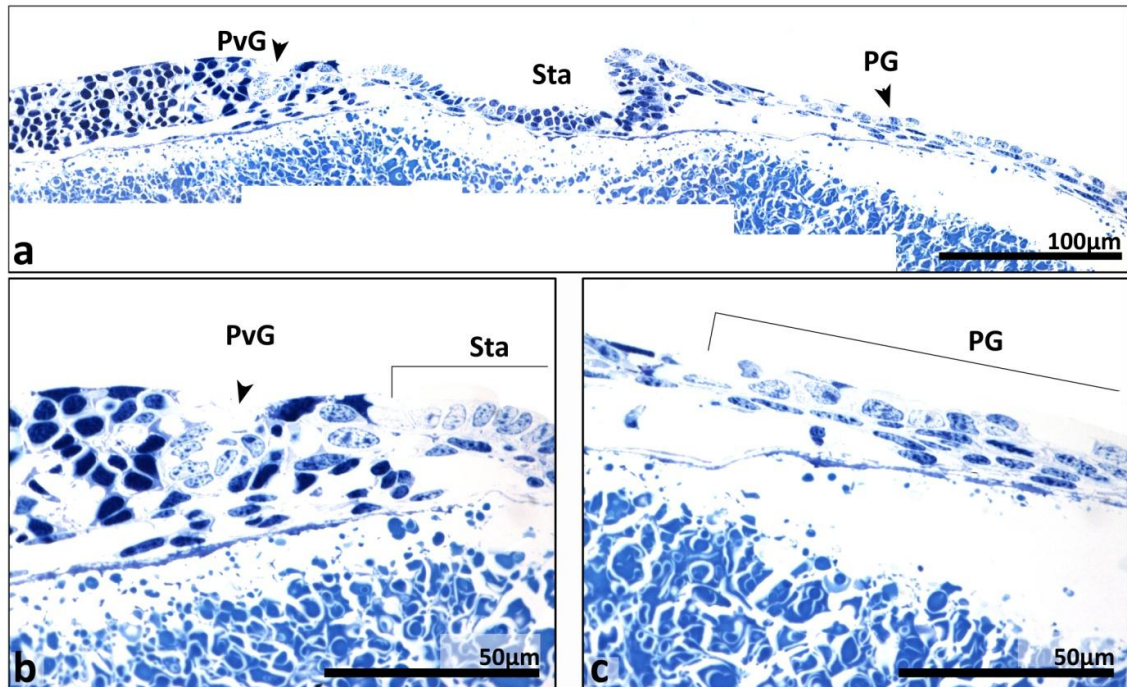


Fig. 9. Stage 19 – Ganglionic placodes formed at the posterior embryonic surface in *Euprymna scolopes* (light microscopic images). **a** partial transversal section focusing on the statocyst (Sta) primordium and the placodes of the pedal (PG) and palliovisceral ganglion (PvG), **b** palliovisceral ganglion (PvG) placodes at the anterior part of the statocyst (Sta) invagination, **c** pedal ganglion (PG) posterior to the statocyst placode. Image a is pieced together from 7 individual images. The cells of the ganglionic placodes are easy to distinguish from the surrounding cells. The pedal ganglionic placodes cover a larger area than the palliovisceral ones (c), which are small invaginations (b). While the primordium of the pedal ganglion is at least as large as the primordium of the optic lobes, the palliovisceral placode is much smaller than all the other prospective ganglia.

Next to ganglionic formation and the invagination from the surface, the individual ganglia accumulate around the oesophagus. The still paired cerebral, pedal and palliovisceral ganglia as well as the optic lobes start forming a circumoesophageal ring totally encompassing the gullet. In this ring, the cerebral ganglia form the dorsal part and both the palliovisceral and the pedal ganglia form the ventral part, whereas the optic lobes are the lateral sections (Fig. 10).

At stage 21 to 22, at least the two cerebral ganglia and the pedal and palliovisceral ganglion are fused together. While the cerebral ganglion is located just below to the head surface epithelium and above the front part of the digestive system, the pedal ganglia maintain their

position anterior to the statocysts and below the yolk neck. The palliovisceral ganglia, posterior to the pedal ganglia, are shifted more dorsal due to the statocysts. Although the paired ganglia have fused to one ganglion by now, the neuropile has not been developed clearly (Fig. 10).

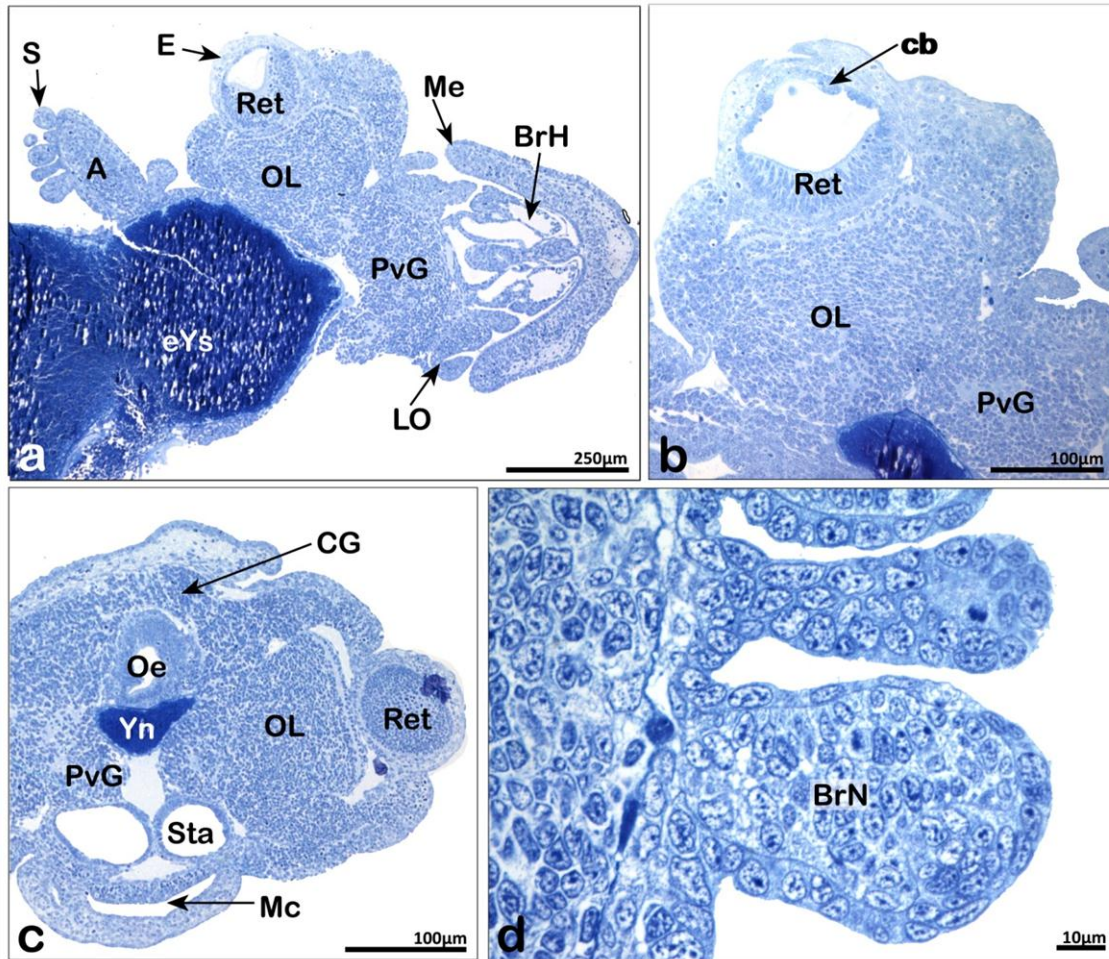


Fig. 10. Stages 21 to 22 – Ganglionic accumulation around the oesophagus in *Euprymna scolopes* (light microscopic images). **a** parasagittal section through the embryo at the level of the palliovisceral ganglion (PvG), **b** detail of the optic lobe (OL) and the eye (E), **c** cross section depicting the ganglia accumulated around the oesophagus, **d** detail of the brachial nerves (BrN). The neuropil is not yet differentiated in and between the individual ganglionic components. In the optic lobes (OL), the inner plexiform layer is already formed (b, c), as are small short connectives between the palliovisceral (PvG) and the cerebral ganglia (CG). The oesophagus (Oe) still has a large diameter, as the ganglia are not yet congregated too much. The nervous material inside the arms (A) is undifferentiated as well as in the central ganglionic parts. BrH – branchial heart, cb – ciliary body, eYs – external yolk sac, LO – light organ, Mc – mantle cavity, Me – mantle edge, s – sucker, Sta – statocyst, Yn – yolk neck

Neuropile development and lobe differentiation (stage 23-25)

The first signs of the neuropile can be observed between stages 22 and 23 and neuropile formation starts in the posterior-most parts of the suboesophageal mass (Fig. 11). Therefore, congregations of nervous fibers can be found first in the palliovisceral ganglion and parts of the

pedal ganglion, as these already start to differentiate into lobes. Lobes are formed as the ganglionic masses fuse together and create specialized regions characterized by a ganglion-like structure (an internal layer of nerve fibers and a surrounding layer of pericarya). The specialized regions are based on neuropile outgrowth. The lobes differentiation is the second important step following ganglionic accumulation, where special regions in the brain are formed out of the more or less completely fused mass of ganglia. Here, the lobes in the supraoesophageal mass are more clearly distinguishable from each other than the lobes in the suboesophageal mass in later stages. The number of lobes is higher in the supraoesophageal mass, which is mostly built by the cerebral ganglia. Although the supraoesophageal mass is not showing any signs of neuropile development until now, the outer and the inner plexiform layers can be detected adjacent to the eye (Fig. 11). Inside the arms, the peripheral nervous system is differentiating into a ganglion-like structure as well, as the nervous fibers consolidate in the center of the arms surrounded by the pericarya-layer (Fig. 11). The brachial ganglion is formed by the consolidating brachial nerves anterior to the pedal ganglion. The tentacle nerves later join the pedal ganglion, but innervate the ganglion more posterior than the arm nerves. Additionally, the first signs of the peripheral nervous system, such as the stellate ganglia, can be seen in the mantle material (Fig. 11). The connection to the central nervous system, in particular to the palliovisceral ganglion, develops later (stages 26 to 28). In the supraoesophageal mass, the neuropile is developed in the same pattern as in the suboesophageal mass, starting at its posterior- and ventralmost edge. Therefore the lobes of the basal lobe complex, especially the ventral posterior, dorsal posterior and ventral anterior basal lobe are developed at approximately stage 25 (Fig. 12). Most of the lobes situated more anterior to them are roughly formed as well, although their final shape is not defined yet. Prior to that, a widely spread net of connectives between the lobes and the different masses of the central nervous system is developed (Fig. 12). These connectives are going to increase their diameter and shorten due to a further concentration of the ganglionic components.

Further lobe differentiation (stage 26-hatching)

Next to the differentiation of the lobes, the connections between the ganglionic masses via commissures and connectives grow out as well. Anterior to the supraoesophageal mass, a buccal ganglion develops by stage 26 (Fig. 13). This ganglion consists of two portions, one dorsal and the other one ventral of the oesophagus. While the dorsal one is originally formed as a paired primordium, which fuses to form one mass, the origin of the ventral one could not be clearly detected in this study.

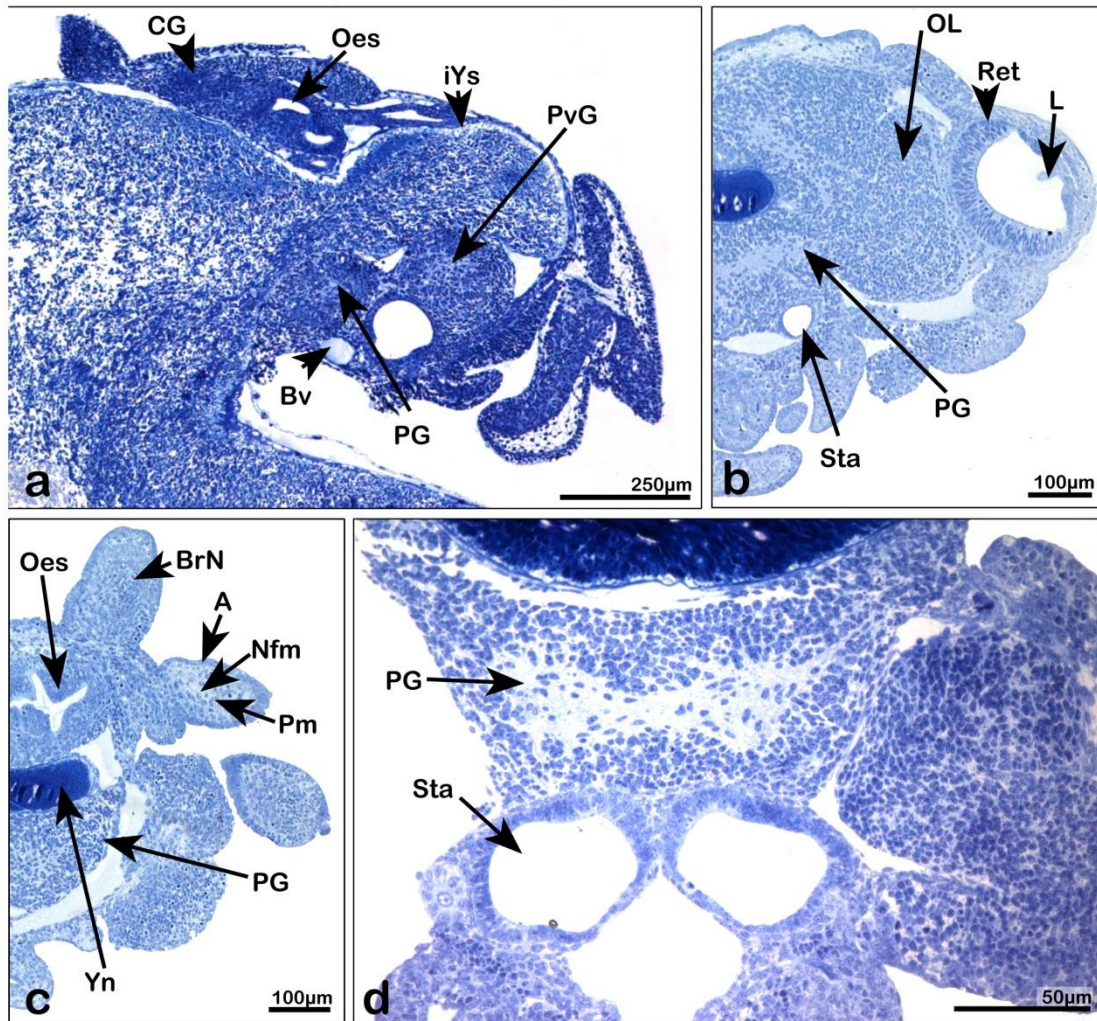


Fig. 11. Stages 23 to 24 – Beginning of neuropile differentiation in the suboesophageal mass of *Euprymna scolopes* (light microscopic images). **a** sagittal section focusing on the central ganglionic system, **b** cross section depicting neuropile outgrowth in the sub- and the supraoesophageal mass, **c** cross section through some arms (A) and the pedal ganglion (PG), **d** parahorizontal section through the statocysts (Sta) and the pedal ganglion (PG). The suboesophageal mass as well as the nervous tissue in the arms (BrN – brachial nerve) is first to differentiate into an inner layer of nervous fibers (Nfm – nervous fiber material) and the surrounding layer of pericarya (Pm – pericaryan material), **c**). The optic lobes (OL), though forming a big portion of the brain, do not show a differentiation besides the plexiform layer (**b**). The concentration of the brain is not as high as in the hatching squid, as the oesophagus (Oes) and the yolk neck (Yn) are still large in diameter. Bv – blood vessel, CG – cerebral ganglion, iYs – internal yolk sac, L – lense, PvG – palliovisceral ganglion, Ret - retina

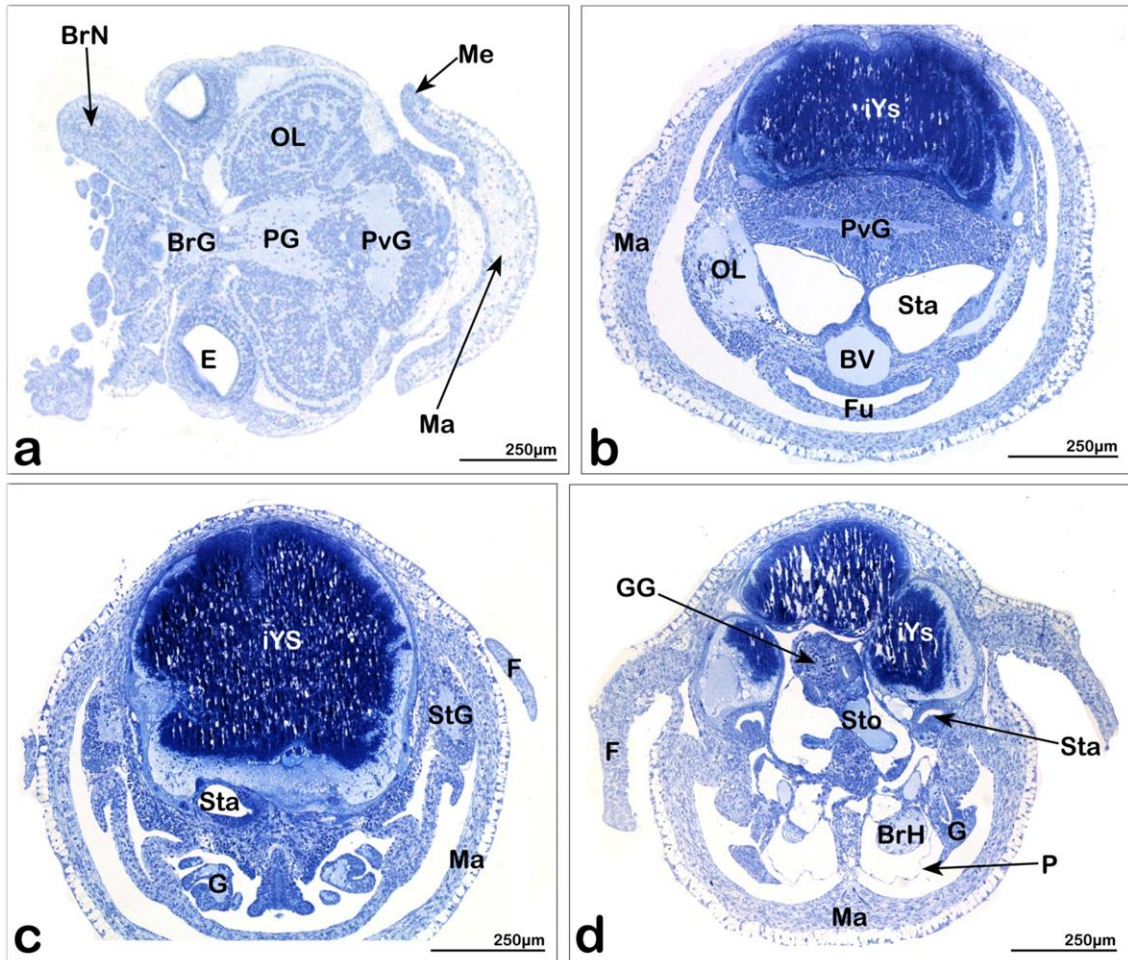


Fig. 12. Stage 25 – Neuropile differentiation in the supraoesophageal mass in *Euprymna scolopes* (light microscopic images). **a** parasagittal section through the brain, **b** cross section at the level of the palliovisceral ganglion (PvG), **c** cross section at the level of the stellate ganglia (StG), **d** cross section at the level of the gastral ganglion (GG). Cross sections reveal patterns of neuropile formation best. At this stage, the strong connection between the brachial (BrG) and the pedal ganglion (PG) can be seen (**a**). Other parts of the peripheral nervous system such as the stellate ganglia (StG) and the gastral ganglion (GG) are detectable as well. The complex neuropile network in the optic lobes (OL) starts developing too (**a**). The branchial hearts (BrH) in the mantle cavity as well as the blood vessels (BV) in the more anterior parts of the body can be detected due to their homogenous filling. BrN – brachial nerve, E – eye, F – fin, Fu – funnel, G – gill, iYS – internal yolk sac, Ma – mantle, Me – mantle edge, P – pericard, Sta – statocyst, sto - stomach

In the mayor part of the supraoesophageal mass, the anterior lobe complexes are developed by stage 27, approximately. By then, the lobular layout already resembles the hatching squid and is assumed to alter just marginally. The arm nerves, although connected at the base via the brachial ganglion, form kind of a basket more anterior in the head region with forming connectives (Fig. 13). The arm nerves have the typical character of a fused ganglionic series (one small ganglion lying closely adjacent to each other), as the component of nervous fibers in the center is surrounded by a layer of pericarya, similar to the ganglia and the lobes. The

connectives, though, miss the pericarya-layer and consist of nervous fiber material only (Fig. 13). As the stellate ganglia further differentiate, the gastral ganglion located next to the stomach is visible at stages 27 to 30. In contrast to the connection between stellate ganglia and palliovisceral ganglion, which is of nervous fiber material only, a link between the gastral ganglion and the central nervous system could not be detected. Although the gastral ganglion could not be detected in earlier developmental stages, it is clearly distinguished due to its two different layers as a ganglion.

The central nervous system of a hatching *Euprymna scolopes*

The brain of the hatching squid already is a very complex structure. The most anterior subset of the suboesophageal mass, the brachial ganglion, has been developed by fusion of the posteriormost bases of the armnerves. The tentacular nerves connect to it more posterior than the arm nerves and are separated from the others in their specialized pouches (Fig. 14). There are strong connectives between the brachial ganglion, the medial suboesophageal mass (pedal ganglion) and both the superior buccal lobe and the inferior medial frontal lobe of the supraoesophageal mass. The connection among the components of the suboesophageal mass are stronger than between the supra- and the suboesophageal masses. The suboesophageal mass is not differentiated in as many lobes as the supraoesophageal mass, but the pedal and the palliovisceral ganglion (meaning the medial suboesophageal and the palliovisceral lobe) respectively, are clearly detectable due to the separated neuropile structures (Fig. 14). In the supraoesophageal mass, more different lobes can be distinguished easy and are drawn together to describe at least four lobe complexes: the frontal lobe complex as the anteriormost part, the vertical lobes forming the dorsal part, the basal lobe complex being the most posterior part as well as forming the border towards the oesophagus, and finally the subvertical lobe complex, situated in the very middle of all the other masses (Fig. 14).

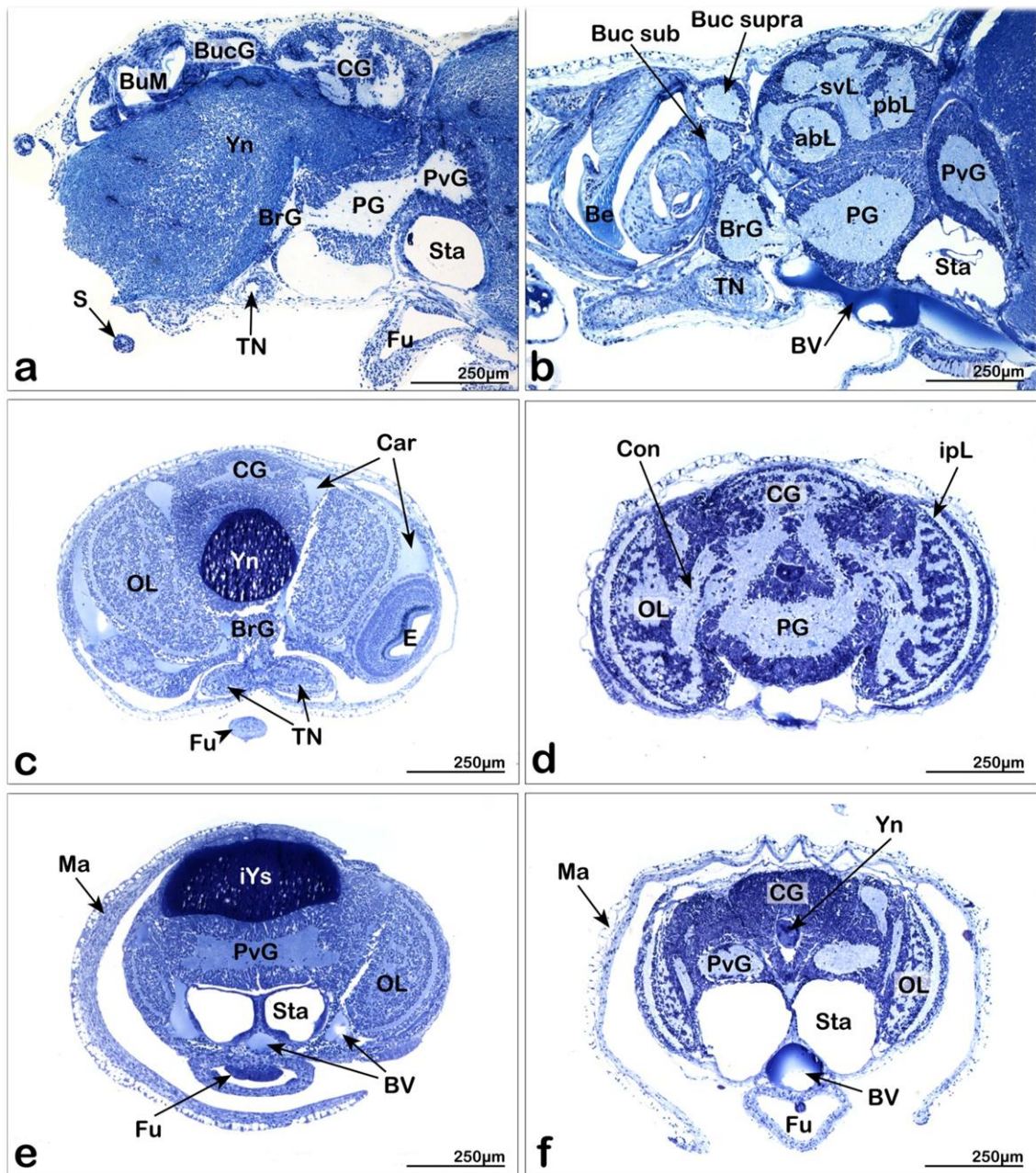


Fig. 13. Stages 26-29 – Ganglionic layout during the later stages of embryonic development in *Euprymna scolopes* (light microscopic images). a, c, e stage 26; b, d, f stage 29 in parasagittal (a, b) and cross sections at the level of the optic lobes (OL, c, d) and the palliovisceral ganglion (PvG, e, f). Most of the lobes in the supraoesophageal mass are already visible at stage 26, but the further differentiation goes on until stage 29 and even further. The characteristic treelike formation of the neuropile in the optic lobes (OL) has been formed at stage 25, but gets more and more complex in succeeding developmental stages (c, d). The brain is enclosed in a cartilage capsule (Car, c, e) and well supplied by large blood vessels (Bv, e, f). abL – anterior basal lobe, Be – beak, BrG – brachial ganglion, BucG – buccal ganglion, Buc sub – suboesophageal buccal ganglion, Buc supra – supraoesophageal buccal ganglion, BuM – buccal mass, CG – cerebral ganglion, Con – connective, E – eye, Fu – funnel, ipL – inner plexiform layer, Ma – mantle, pbL – posterior basal lobe, PG – pedal ganglion, s – sucker, Sta – statocyst, svL – subvertical lobe, TN – tentacular nerve, Yn – yolk neck

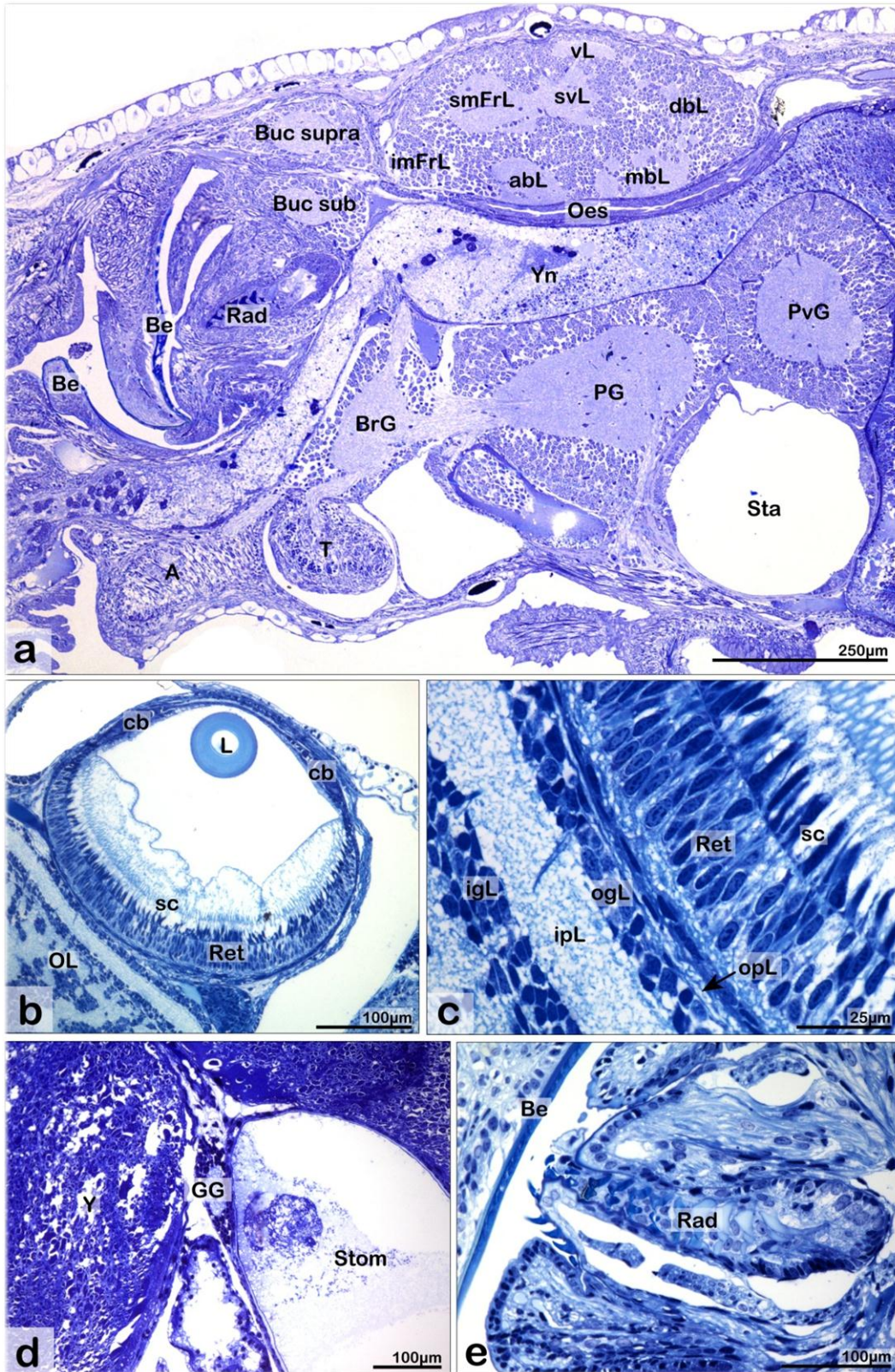


Fig. 14. Hatching stage (30) – Ganglionic layout and important sensory organs in *Euprymna scolopes* (light microscopic images). **a** sagittal section of the brain, **b** horizontal section through the eye, **c** detail of the retina (Ret) and the cortex of the optic lobe (OL), **d** gastral ganglion (GG) situated next to the stomach, **e** radula (Rad) as important part in the anterior digestive tract. In a sagittal section, several lobes of the supraoesophageal mass can be revealed, including lobes of the frontal (imFrL – inferior median frontal lobe, smFrL – superior

The optic lobes, which are situated adjacent to this central mass and connected to it via strong connective, have developed the richly branching inner structure of the neuropile, which is remarkable for their interior. The cortex, nevertheless, displays another images, as a strictly succession of plexiform and granular layers. While the outer plexiform layer, which is closest to the eye, is thin and its structure hard to follow over the whole optic lobe, the inner plexiform layer extends to about 20 μ m between the outer and the inner granular layer (Fig. 14). The eyes themselves are well developed at hatching stage and show a vertebrate-analog picture. The lense is spherical and the retina built from at least three different layers. Using semithin sections (1 μ m) it is not possible to discriminate between different cell types in this dense packing. At the basal pole of the retinal receptor cells, a complex net of blood vessels and nerves connects the eyes to the optic lobes. Ciliar bodies can be detected anterior and posterior of the lense as muscular thickenings at least 25 μ m high and extending over approximately 100 μ m (Fig. 14). These sensory organs are located directly next to the central ganglionic system such as the statocysts, which are situated ventral to the palliovisceral mass and posterior to the pedal mass.

Volumetric measurements of the developing sepiolid brain

The total body volume increases dramatically during stages 24 to 28. This is consistent with the gain of ganglionic volume in the brain, which is at stage 24 approximately a third of the total body mass. In contrast to the increase in total volume, the relative volume of the central ganglionic system is decreasing favoring the internal organs and the internal yolk sac, which becomes more and more important in the last embryonic developmental stages (Fig. 15).

The different components of the central ganglionic system as there are the cerebral, the pedal, the palliovisceral ganglia as well as the optic lobes, display different growing speed. The supraoesophageal mass and the optic lobes gain volume fastest and both of them together

⇐ median frontal lobe), the vertical (vL – vertical lobe), the subvertical (svL – subvertical lobe) and the basal lobe complex (abL – anterior basal lobe, mbL – median basal lobe, dbL – dorsal basal lobe). The eyes display a complex retina (Ret) and the lenticular apparatus (cb – ciliary body, L – lense). The gastral ganglion (GG) is small and adjacent to the stomach (Stom), whereas there is no connection to the central ganglionic system visible. A – arm, Be – beak, BrG – brachial ganglion, Buc sub – suboesophageal buccal ganglion, Buc supra – supraoesophageal buccal ganglion, igL – inner granular layer, ipL – inner plexiform layer, Oes – oesophagus, ogL – outer granular layer, opL – outer plexiform layer, PG – pedal ganglion, PvG – palliovisceral ganglion, sc – sensory cell, Sta – statocyst, T – tentacle, Yn – yolk neck

form about 50% of the total central ganglionic mass. Their internal structure serves an additional surface extension not visible in the suboesophageal mass. This can be demonstrated in a slope as well. Although starting from nearly the same value (0,04 and 0,01 mm³, respectively), the slopes are quite different. At stages 26-28, the supraoesophageal mass is at least three times larger than the suboesophageal one. This ratio remains nearly unchanged until the squids are hatching. Again, the internal surface extensions are not considered in this volumetric approach (Fig. 15).

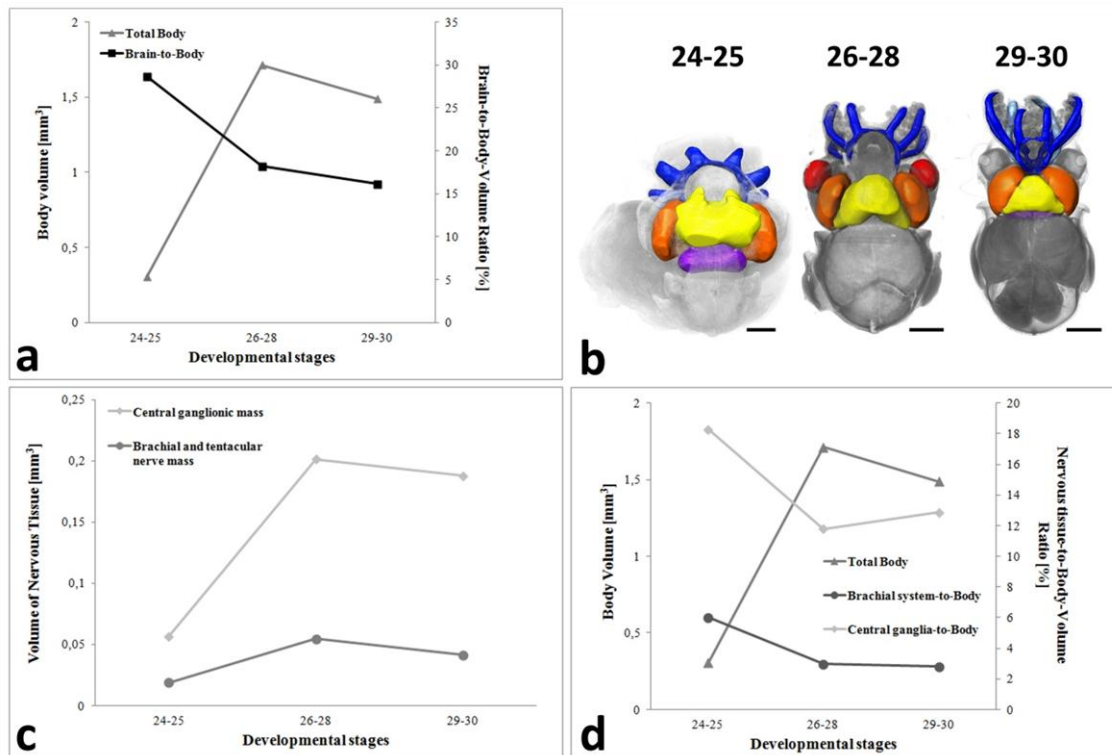


Fig. 15. Volumetric calculations of different ganglionic components of *Euprymna scolopes* at various developmental stages. **a** total body volume and brain-to-body volume ratio at three developmental stage classes, **b** overview of the central ganglionic system and the brachial nerves measured in this study (scale bar is 250µm), **c** volumetric increase in the central ganglionic and the brachial and tentacular masses during development, **d** growth slopes of the central ganglionic and the brachial system in contrast to increase of total boy volume. In **b**, the cerebral ganglion is shown in yellow, optic lobes in orange, eyes in red, palliovisceral ganglion in violet and brachial nerves and ganglion in blue. The increase in total body volume is possible due to the small sample size. Nevertheless, the flattening of the slope towards hatching time is similar in all components measured here. The decrease of the ganglionic volume in contrast to the total body can also be seen in the images depicted in (b), where the posterior part of the body gains importance.

The brachial ganglion with the connections to the brachial and the tentacular nerves are part of the peripheral nervous system, but closest related to the central nervous system. Its total

volume is about four times smaller than that of the central ganglionic parts, but most dominant in the whole peripheral nervous system, which generally develops later than the more central parts. Additionally, this slope is consistent with the growth curve of the total body volume as well (Fig. 15). All three slopes (total body volume and the nervous tissue-to-body-ratios) display a saturation level at the end of embryonic development. This is important for interspecific comparisons, because much more nervous tissue can be found in octopod arms as demonstrated in *Octopus vulgaris*.

DISCUSSION

Cephalopod nervous system development

The development of the nervous system in *Euprymna scolopes* can be classified in three stages until hatching: 1. the formation of the ganglia and their accumulation in a circumoesophageal ring (stage 19-22), 2. the formation of the neuropile and the beginning of the lobe differentiation (stages 23-25), and 3. the outgrowth of the neuropile and strengthening of the nervous connections between the individual ganglia (stages 26-30). These phases occur in other cephalopod species investigated so far as well (Meister 1972; Marquis 1989; Shigeno *et al.* 2001a, b; 2008).

Compared to *Idiosepius paradoxus* (Ortmann, 1888), *Euprymna scolopes* has a long embryonic development (21 days in *Euprymna scolopes* compared to 10 days in *Idiosepius paradoxus*, Yamamoto *et al.* 2003). Both of them, though, share the same patterns in nervous system development as mentioned above. The onset and duration of the three different phases is approximately the same as in *Euprymna* if referring to the developmental stages (Fig. 15, Yamamoto *et al.* 2003). Additionally, and maybe different to the other species investigated so far, the sepiolid central nervous system at hatching stage resembles the adult one well (Yamamoto *et al.* 2003). In contrast to the smaller *Idiosepius* with its thin and elongated body, *Euprymna* displays a more stout shape. This “compaction” can be seen in the central nervous system as well. It is more contracted in *Euprymna*, whereas the posterior suboesophageal mass (mostly the palliovisceral ganglion) in *Idiosepius* stretches much more to the posterior end of the animal (Yamamoto *et al.* 2003).

In contrast to the sepiolid squids, nervous system development starts earlier (approximately stage 14) in *Sepioteuthis lessoniana* Férussac, 1831 (Shigeno *et al.* 2001b) and *Todarodes pacificus* Steenstrup, 1880 (Shigeno *et al.* 2001a), which both belong the former teuthid group (Fig. 15). *Sepioteuthis lessoniana* is a myopsid squid due to its eyes displaying a cornea as is *Loligo vulgaris* Lamarck, 1798, whereas *Todarodes pacificus* is belonging to the oegopsid group (as its eyes does not have any cornea). In contrast to the sepiolids described before, “teuthids” are pelagic life forms without a strong relation to the substrate except for the spawning period (e. g. Boyle & Rodhouse 2005). Therefore, it might be suggested that they need at least the suboesophageal mass to be fully developed for orientation and regulation of muscle contraction (Shigeno *et al.* 2001a, b).

Octopods and *Octopus vulgaris* Cuvier, 1797 in special diverge from the pattern seen in decapodiform cephalopods (Marquis 1989). Phase one starts at stage 14, which is equal to *Sepioteuthis lessoniana*, but four stages earlier than *Euprymna scolopes* and *Loligo vulgaris*. It is more prolonged than in the former “teuthid” group and sepiolids (Fig. 16), going on for more eight to nine stages in contrast to three to five we see in other groups. As *Octopus* is considered to have the most complex brain in all cephalopods (Young 1988), this longer period of ganglionic formation and the longer time needed for the accumulation around the oesophagus may be related to this complexity. As the study done by Marquis (1989) showed, the second phase is prolonged as well, and therefore the third phase is not completed by the time the embryo hatches from the egg. As there are few studies about the nervous system development short after hatching in some octopods (e. g. Yamazaki *et al.* 2002), it is just a suggestion to state that this last phase of the development may go on after hatching to a higher extend than in the decapodiform species.

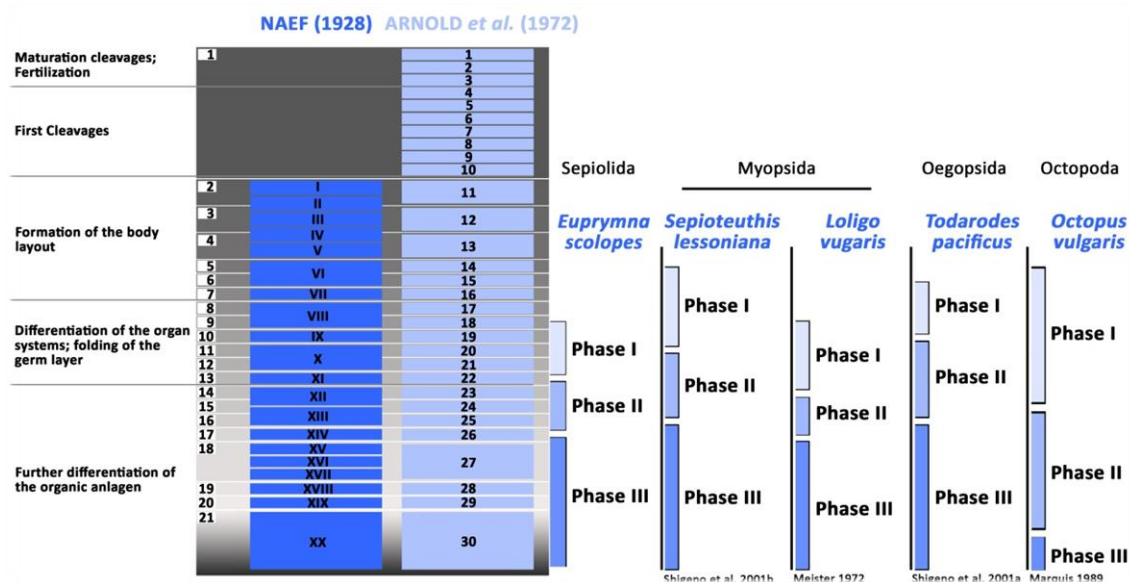


Fig. 16. Developmental patterns of the cephalopod nervous system – Comparison of different species. Whereas older studies characterized the embryonic stages after Naef 1928, newer studies use tables changed according to the specific conditions (e. g. Arnold *et al.* 1972 for *Euprymna scolopes*). The temporal pattern of nervous system development is similar in sepiolid species and deviates just a bit in other decabrachiate species. Although the three phases can be discriminated in octopods as well, their temporal arrangement is quite different. As not much is known about the triggers of the processes, the main reason for the variation is still unknown.

The sequence of processes during these first stages of nervous system development such as the ganglion formation and the accumulation around the oesophagus is quite similar in all

species investigated so far. However, triggers of these processes as well as details about their regulation are still unknown. Different molecules have been suggested to play a role in the accumulation of the ganglia (e. g. Baratte & Bonnaud 2009, Wollesen *et al.* 2009), but studies conducted so far just detected substances important for the lobe formation (Baratte & Bonnaud 2009) or possibly the processes of postembryonic development (Wollesen *et al.* 2009; Wollesen *et al.* 2010a). Another possibility is nitric oxide. This molecule is also known as a signalling molecule in vertebrate nervous systems (Peunova *et al.* 2001, 2007). Few studies have been conducted in cephalopods during the last decades (Di Cosmo *et al.* 2000; Tu & Budelmann 2000; Di Cristo *et al.* 2007), proving that nitric oxide synthase, one of the main substances in its regulation, is expressed in other organs such as the ink glands, too (Scheinker *et al.* 2005). As nitric oxide is found in many vertebrates as well as in various invertebrates (Moroz *et al.* 1996; Colasanti *et al.* 2010), it is suggested that its task as signalling molecule is conserved in bilaterians (Colasanti & Venturini 1998).

Another question not yet resolved is the innervation of the arm crown in cephalopods. Answering it should the debate of whether the arms and tentacles in cephalopods are derivatives of the molluscan foot (equal to the funnel) or if they are appendages of the head comparable to the gastropods tentacles. Previous histological studies preferred the main innervation by the cerebral ganglion, pointing out the cerebro-brachial-connective as main connection for information exchange (e. g. Young 1975). These studies were conducted mainly in *Loligo vulgaris*, which is not considered to be too highly derived from the other cephalopod groups such as *Octopus*. However, a different study in *Nautilus* showed a connection to the pedal ganglion as being more pronounced (Shigeno *et al.* 2008). Due to it being the only living form with the external chambered shell, *Nautilus* is often thought to be the most basal cephalopod and displaying ancient characters. As the branching point between the ancestors of coleoids and nautiloids date back at least 400 million years to the Devonian period (Kröger *et al.* 2011), *Nautilus* had a long time of separated evolution and should not be thought of being basal to all coleoids any more. In *Euprymna scolopes*, the brachial ganglion is formed by fusion of the brachial nerve basis and afterwards connected to both the supra- and the suboesophageal masses. Prior to entering the supraoesophageal mass, it seems as if the nerve cord branches off and leads towards both the superior buccal lobe and the inferior median frontal lobe (Fig. 17). This can especially be seen in sagittal as well as cross sections of embryos at hatching stage. The earliest evidence for the connection could be seen at stage 25, when both cerebro-brachial- and brachio-pedal connectives are already formed (Fig. 17). This can be seen in “teuthids” (Nixon & Young 2003) and sepiids (Mangold 1989).

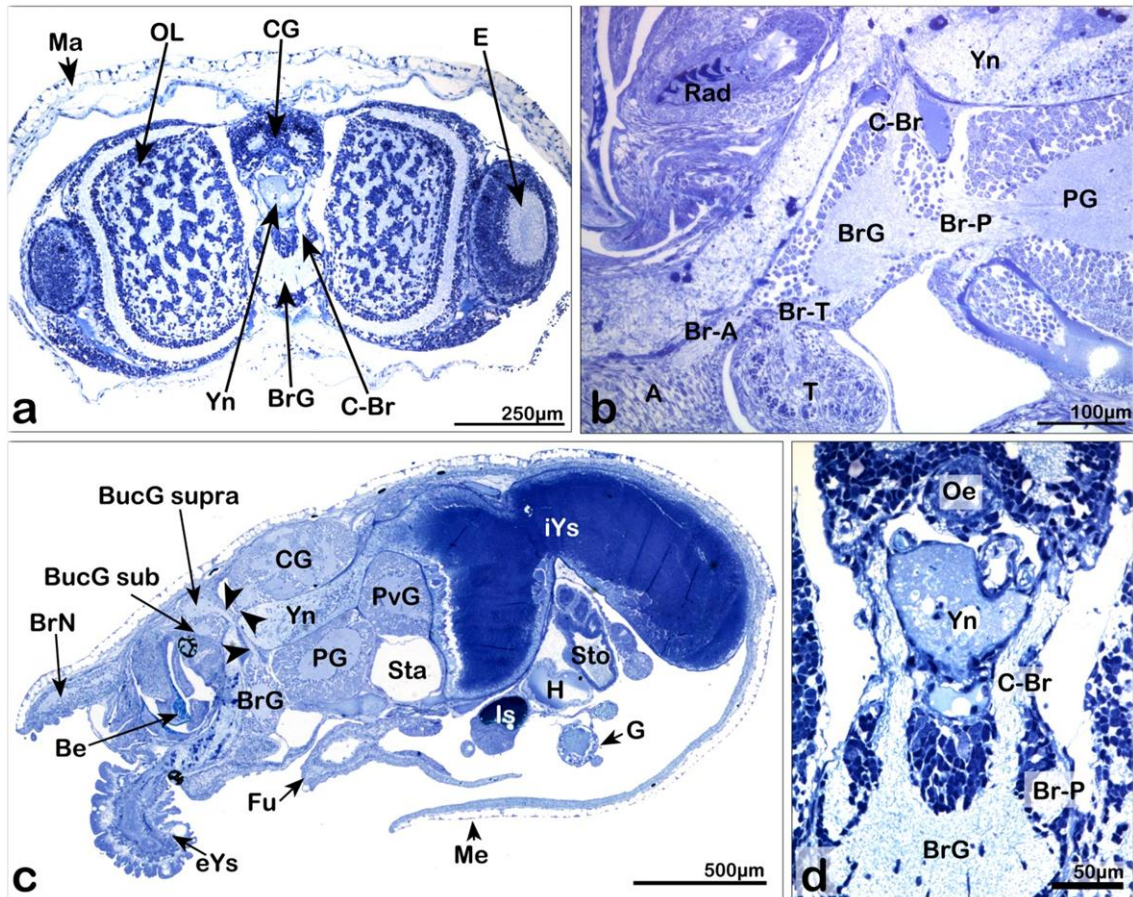


Fig. 17. Connectives between the brachial ganglion and other parts of the sub- and the supraoesophageal mass (light microscopic images). **a** cross section at the cerebro-brachial connective (C-Br), **b** sagittal section depicting the brachial ganglion (BrG) and its various connections to other parts of the nervous system, **c** sagittal section focussing on the cerebro-brachial connective, **d** detail of the cerebro-brachial connective in a cross section. Starting in the brachial ganglion (BrG), there are connections to both the arms (Br-A) and the tentacles (Br-T) and connectives to the pedal (Br-P) and the cerebral ganglion (C-Br). The connective to the supraoesophageal mass branches and leads towards the frontal lobe and the superior buccal mass (**c**, indicated by arrowheads). The cerebro-brachial connective embraces the yolk neck (Yn) as well as the oesophagus (Oe, **d**), whereas the connectives between the brachial (BrG) and the pedal ganglion (PG) are formed as several thick nervous bundles (**a**, **d**). Be – beak, BrN – brachial nerve, BucG sub – suboesophageal buccal ganglion, BucG supra – supraoesophageal buccal ganglion, CG – cerebral ganglion, E – eye, eYs – external yolk sac, Fu – funnel, G – gill, H – heart, Is – ink sac, iYs – internal yolk sac, Ma – mantle, Me – mantle edge, OL – optic lobe, PvG – palliovisceral ganglion, Rad – radula, Sta – statocyst, Sto - stomach

Patterns of neuropile differentiation in cephalopod central nervous systems

As mentioned above, neuropile differentiation is one of the major events in the development of the nervous system in *Euprymna scolopes* and in other cephalopods. The onset of this process is visible in the palliovisceral ganglion which is nearly completely forming the palliovisceral lobe. Situated ventral to the oesophagus, this mass constitutes the posterior-

most part of the suboesophageal mass. From its neuropile layer thick nervous fiber bundles lead to the club-shaped stellate ganglia located next to the body musculature. Subsequently, the neuropile grows out first in the other regions of the suboesophageal mass, but there is not a differentiation in as many lobes as in the supraoesophageal mass. In the hatching sepiolid, the lobes of the suboesophageal mass are larger than the ones of the supraoesophageal mass.

The neuropile in the optic lobe is highly developed as well. As lateral enclosures of both the supraoesophageal and the suboesophageal masses, strong connective bundles can be detected at their inner sides (Fig. 13). The net of nervous fibers in the optic lobe branches in a highly complex system (Fig. 13, 17). This structure most possibly serves an increase of the total surface which is used to process visual perceptions.

In hatchlings of *Euprymna scolopes*, the supraoesophageal mass displays the highest complexity in its lobe network. Consistent with information from previous studies on related sepiolid species such as *Idiosepius paradoxus* (Yamamoto *et al.* 2003), there are approximately 10 to 15 lobes included in the supraoesophageal mass. Although the number of lobes in this brain region varies between the taxa, the higher complexity of the supraoesophageal mass is a common pattern in coleolids as well as in nautilids (e. g. Young 1964; Yamazaki *et al.* 2002).

The regulation of the neuropil outgrowth remains likewise mysterious for the moment. The neuropil itself is a dense network of axons, dendrites and glial branches located in the center of the ganglia or lobes, respectively. The first evidence of its formation can be found in the palliovisceral ganglion, which becomes the posterior part of the suboesophageal mass, and later in the pedal ganglion (e. g. Shigeno *et al.* 2001a, b; this study). Neuropile formation in the supraoesophageal mass is progressive sequence, too, starting in the basal lobes and finally forming inside the frontal and vertical lobe complex. But the whole formation process is delayed as compared with the suboesophageal mass. This is common in all studied cephalopod species (e. g. Marquis 1989; Shigeno *et al.* 2001a, b; 2008; Yamazaki *et al.* 2002; this study). The reason for this temporal procrastination in neuropile differentiation is unclear for now, but has been tried to answer by some studies. Shigeno *et al.* (2001a, b) for example suggested the preference of suboesophageal nervous system development due to the need of the hatching squid for the lower motoric centers located there. Following this line of argumentation, the juvenile squid needs its ability to control the funnel and the fins a lot more than displaying learning ability or performing complex tasks. This is supported by the fact, that the posterior nervous material of the suboesophageal mass is much more active than the supraoesophageal one. However, behavioural or experimental studies to support this theory are not available.

Another approach was conducted by Baratte & Bonnaud (2009) who tested the involvement of acetylated α -tubulin and tyrosine hydroxylase in *in toto* expression experiments. They could prove that lobe differentiation, which is linked to neuropile outgrowth, precedes the fusion of the ganglia.

Histological methods are not able to answer questions of how the ganglia find each other and how the fusion is processed. Semithin section series as performed in this study are limited to achieve snapshots of special developmental steps in high detail with resolutions down to the cellular level, but cannot provide a series of one specimen at different time points of development. Nevertheless, selecting these special developmental steps is difficult, so an exact staging based on outer morphology easy to recognize is a prerequisite. As suggested in a former study (Kerbl *et al.*, *subm.*), the use of combined approaches is to be preferred in order to get the desired information with acceptable effort.

Nervous systems in cephalopods

The comparison of the nervous system is problematic, as these studies have been conducted on adult animals in other species, while the focus in *Euprymna scolopes* was on different embryonic stages. Nevertheless, the ganglionic layout of the hatching *Euprymna scolopes* can be roughly compared to that of other cephalopod species (Mangold 1989, Nixon & Young 2003).

Most similarities can be found between *Euprymna* and *Sepia officinalis* Linnaeus, 1758. In these two species, the arrangement of the ganglia as well as the concentration of the ganglia and the relative size is equal (Mangold 1989, Fig. 18). The supraoesophageal mass is the largest structure and also the one with the most structures inside. The pedal ganglion as median part is located directly ventral to the main component of the supraoesophageal mass. It can be discriminated from the more anterior mass (forming the brachial ganglion) and the more posterior one (forming the palliovisceral ganglion), because the neuropile forms thinner connections between them or is interrupted at all (Fig. 18). Another prominent accordance between the two species is the onset of the tentacular nerves in the brachial ganglion. It lays more posterior in the brachial ganglion than in other decabrachiate species. The tentacular nerves are not involved in the ring formed of connectives between the arm nerves (Fig. 18). The whole tentacles are structures outside the arm crown and can be redrawn in specially developed pockets lateral to the arm crown. They are also longer than the arms and are

therefore situated in loops and slings to be stored in the pouches. The connection between the cerebral ganglion and the optic lobes is massive and larger in diameter than in other species. The two buccal ganglia are closely embracing the oesophagus, whereas the suboesophageal part is sometimes lying inside of the basket formed by the arm nerves (Mangold 1989). The palliovisceral ganglion is separated from the other ganglia and the most posterior component of the central nervous system (Fig. 18).

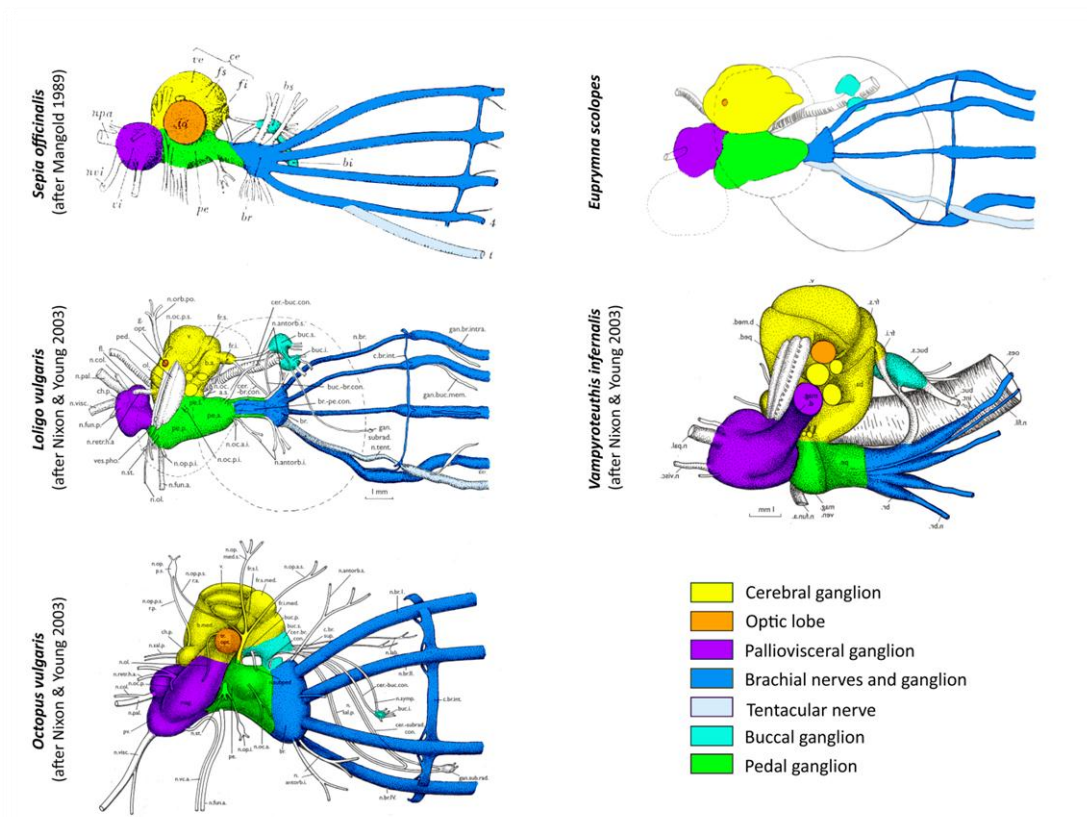


Fig. 18. Layout of cephalopod nervous systems. Although the arrangement of the ganglia in the central nervous system is similar in all species investigated, the concentration varies. In decapodiform species, the exclusion of the tentacles from the connective ring of the brachial nerves is obvious and detectable in all teuthids and sepiids as well as in *Euprymna scolopes*. This pattern cannot be detected in octopodiformes, as they do not show even rudiments of tentacular nerves.

There are also some similarities to myopsid species such as *Loligo vulgaris*. Here, the tentacular nerves insert more anterior in the brachial ganglion (nearly at the same level as the arms), and they seem to have a small connection to the connective ring. The arm nerves as well as the tentacular ones thicken significantly before the connective lead off for the ring formation (Nixon & Young 2003). The junction leading from the cerebral ganglion to the optic

lobes is small in diameter, although the optic lobes in *Loligo* as well as in *Euprymna* are the most prominent part of the brain (Fig. 18).

Different to *Euprymna scolopes* and the other decabrachiate cephalopods described so far, the central nervous system in *Octopus vulgaris* and in *Vampyroteuthis infernalis* is much more concentrated. The single ganglia cannot be resolved as separated structures anymore. Especially in *Octopus*, the fusion of the ganglia is nearly complete. As in all octopodiformes, there are just eight arm nerves and no tentacular ones any more. In *Octopus*, the borders between the central and the peripheral nervous system are melt together, so the buccal ganglia (both supra- and suboesophageal component) are fused together with the supraoesophageal and the suboesophageal masses (Fig. 18).

In *Nautilus*, the nervous system again shows another image. In contrast to *Octopus*, it is much less fused and resembles more or less an earlier stage in coleoid nervous system development. As the eyes are developed as camera-eyes in contrast to the lenticular eyes of the coleoids, the optic lobes are also not as prominent as previously seen in *Euprymna*, *Loligo*, *Sepia*, *Octopus* and *Vampyroteuthis*. The supraoesophageal and the suboesophageal masses are connected to form a thin ring embracing the oesophagus, while the palliovisceral ganglion is set a bit apart from the others. Different to decabrachiate and octobrachiate cephalopods, there is an innervation of more than eight respectively ten arms spreading from the brachial ganglion (Young 1964). There have not been a lot of studies on the brachial innervations, but each of the up to 90 tentacles is innerved separately.

With all this information, there is a chance to construct a row of central nervous system complexity starting with *Nautilus* and leading through teuthids, sepiids and sepiolids towards *Octopus* (Young 1988). *Euprymna* can be positioned close to *Sepia* and maybe shifted a bit closer to *Octopus* than *Loligo*, as the brain seems to be more compact than in the teuthid species. Naturally, the study of more different cephalopod species would enhance the quality of such a row of complexity. The investigation of more basal groups may help identifying the origins of the complexity of the nervous system, although most of the conservative groups closer related to *Nautilus* are extinct. Therefore, the development of recent cephalopods may render hints about complexity's origin.

***Euprymna scolopes* as model organism of decabrachiate brain development**

In cephalopods, there is no single species selected to be a model organism, representing either the basal conditions of the whole group or displaying features occurring in most of the other species. Species such as *Octopus vulgaris*, being the subject of many studies (e. g. Harrison & Martin 1965; Boyle 1976; Chrachri & Williamson 2004) following different approaches would be the first one coming to mind. Unfortunately, though, the octopod bodyplan as well as their nervous system displays a highly developed state compared to other cephalopods (Young 1988, Budelmann *et al.* 1997). Their living condition with eight arms lacking the two tentacles and the pronunciation of their extension in contrast to the size of the mantle and the head region discriminated them from most of the other cephalopods as well. This state does not affect their shape alone, but also influences the construction of their nervous system and their overall behavior. Although being of great importance for cognitive research (e. g. Mather 2008; Edelman & Seth 2009) and neuroanatomical studies (Wells 1972), they do not allow us to interpret much about the original conditions in the cephalopod group.

“Teuthids” such as *Loligo vulgaris* are quite common in cephalopod research, too, though they show some difficulties in laboratory culture (Mirow 1972; Arnold *et al.* 1974; Fioroni & Meister 1974). Similar to all cephalopods, the rearing of embryos and especially the treatment shortly after hatching is critical. This is mostly due to the uptake of the first nutrition different to the yolk, where hatchlings proved to be very picky. Just very few aquaria and research facilities (e.g. the CCMar – Center of Marine Sciences in Portugal) are able to breed cephalopods successfully by now, but it is not easy to keep either “teuthids” nor sepiolids alive for a complete lifecycle. Additionally, teuthids are forming schools of many individuals on the one hand and cover large areas by continuously swimming on the other hand (Boyle & Rodhouse 2005). Therefore they are not on display in most aquaria and zoological gardens, as their maintaining would need much more dedication than granted due to their limited life span.

Sepiolids and especially *Euprymna scolopes* are already established as model organism in symbiosis research. This is due to their unique relationship to the marine bacterium *Vibrio fischeri* (e. g. Hanlon *et al.* 1997; McFall-Ngai 1998; Lee *et al.* 2009g). There they proved to be unproblematic in rearing, although the critical stage short after hatching exists here as well. This is mainly due to the hatchlings not taken up any frozen food or specialized food, which varies between species. Nevertheless, at least at marine stations there are enough of these animals to supply recent research and at least specimens of different embryonic stages could be exported to other stations in various preservation-media. Due to their limited size, these

specimens are convenient for many methods such as histology, x-ray microtomography or confocal microscopy.

Additionally, as this study indicates, general patterns in the cephalopod development such as the embryonic development of the central nervous system are conserved. The overall layout of the lobular complexes inside the central ganglionic system seems to be similar at least in the hatching stages of different species (Marquis 1989; Shigeno *et al.* 2001a, b; Yamazaki *et al.* 2002), though the adult nervous systems are quite different concerning their ganglionic and lobular congregation. Additional studies besides the histological and x-ray microtomographic analyses such as confocal or behavioural are still missing for *Euprymna* and some other genera. This information would be needed to draw a final conclusion of whether the processes and patterns displayed in *Euprymna scolopes* can be suggested to be repeated in all other decabrachiate or coleoid species.

Micro-CT in cephalopod nervous system research

Nervous system research in cephalopods was based on traditional methods such as semithin-sectioning until now. As 3D-reconstruction techniques get more and more important in modern analyses, disadvantages of these methods are obvious. Especially in semithin sectioning, problems can appear in many steps, starting in specimen preparation before sectioning (e.g. in infiltration), during sectioning (e.g. section loss or unregular thickness) or afterwards (e.g. staining). Naturally, someone trained in working with this technique does not encounter these problems that often, but starting on new specimens often means modifying the standard protocol to obtain high-quality material. Therefore, these preparation techniques are problematic, especially, when dealing with a small sample, although achieving a high resolution. This resolution is just barely achieved by most of the modern alternatives to light microscopy such as micro-CT and confocal microscopy.

Nevertheless, these techniques get reworked all over the time, so a X-ray-microtomographic analysis was included in this study. Here I use them to illustrate the developmental stages of *Euprymna scolopes*, a more detailed check on that technique has already been conducted in another study (Kerbl *et al.*, *subm.*). Micro-CT offers a great palette of possibilities for morphological as well as anatomical investigations (Golding & Jones 2007; Golding *et al.* 2009; Metscher 2009b,a; Dinley *et al.* 2010; Lauridsen *et al.* 2011). Especially in descriptions of early developmental stages, where the massive amount of yolk hampers reconstruction from

section series, it is a comfortable method to obtain realistic images, which are more inclusive than schematic drawings. The resolution is sufficient to distinguish between different tissues and demonstrate the location of organs and organ systems inside the body. The structure of the ganglia consisting of a core of nervous fibers and a surrounding layer of pericarya can also be detected by X-ray-beams (Kerbl *et al.* subm.). So the ganglia of both the central and the peripheral nervous system can be easily isolated from the other tissues such as the mid gut gland, the oesophagus or the blood vessels. The image stacks achieved from a micro-CT-scanner can be used for either single images from the virtual cross sections or as a basis for computer-assisted 3D-reconstructions and –animations.

In the research of the cephalopod nervous system, many different techniques have been used until now, either focusing on special structures (e. g. the light organ or the central nervous system) or approaching in a more general way (e. g. whole-mount *in-situs* or complete section series). Quite similar to micro-CT-imaging, MRI-techniques (magnetic resonance imaging) can be used (Fig. 19). Instead of tungsten-sources, they are based on water molecules and their spins after excitation to achieve images of different structures, which are distinguished by their different amount of water, for example (Ziegler *et al.* 2008; Ziegler *et al.* 2010; Ziegler *et al.* 2011; Ziegler & Mueller 2011). So the resolution in soft-bodied organisms with higher water content and less mineralized structures such as mollusks is better in most cases than with micro-CT (Quast *et al.* 2001, Fig. 19). A more common approach since the development of various fluorescence-markers and antibodies is the confocal microscopy (Fig. 19), and there are quite a lot of protocols developed for invertebrate nervous systems (Wanninger 2008, 2009).

With the use of special markers, special components of the brain (e.g. just the serotonergic part of the nervous system) can be stained and therefore the combination of various subsystems can be investigated (Wollesen *et al.* 2010a; Wollesen *et al.* 2010b). Special stainings are not necessarily connected with confocal microscopy, but can be applied to specific molecules or components of tissues as well (Fig. 19). In whole-mount *in situs*, for example, the expression of different genes (Callaerts *et al.* 2002; Lee *et al.* 2003; Farfan *et al.* 2009) or the presence of molecules (Baratte & Bonnaud 2009; Wollesen *et al.* 2009) can be made visible in their *in vivo*-location. Histology achieves the highest resolution (Fig. 19) besides electron microscopy (which is connected to a very high effort for achieving information as well), but can be used to get overall information about many different structures.

Histochemical analyses are limited to a higher section thickness, as the staining are not working on epoxy resin-embedded samples and therefore not that common in cephalopod research (von Byern *et al.* 2006). Technovit, a glycolmetacrylate, can combine the advantages of both paraffin- and epoxy resin-sectioning. The practicability in working with a higher sample number, though, is problematic.

Most information we have today on the brain structure in cephalopods have been obtained using histology technique (Young 1964, 1973, 1975, 1976, 1977; Messenger 1978; Young 1978, 1988; Marquis 1989; Shigeno *et al.* 2001a, b).

The biggest advantage of micro-CT is its ability to be combined with other methods such as histological preparation. So the comprehensive view of micro-CT goes hand in hand with the high resolution down to the cellular level of histology. And as more and more protocols are developed to combine confocal as well as molecular expression studies with micro-CT in the future (e.g. Metscher & Müller 2011), a broader field of investigations will open to cephalopod research. A more detailed discussion of this method can be seen in Kerbl *et al.* (subm.), provided in the supplementary information section of this thesis.

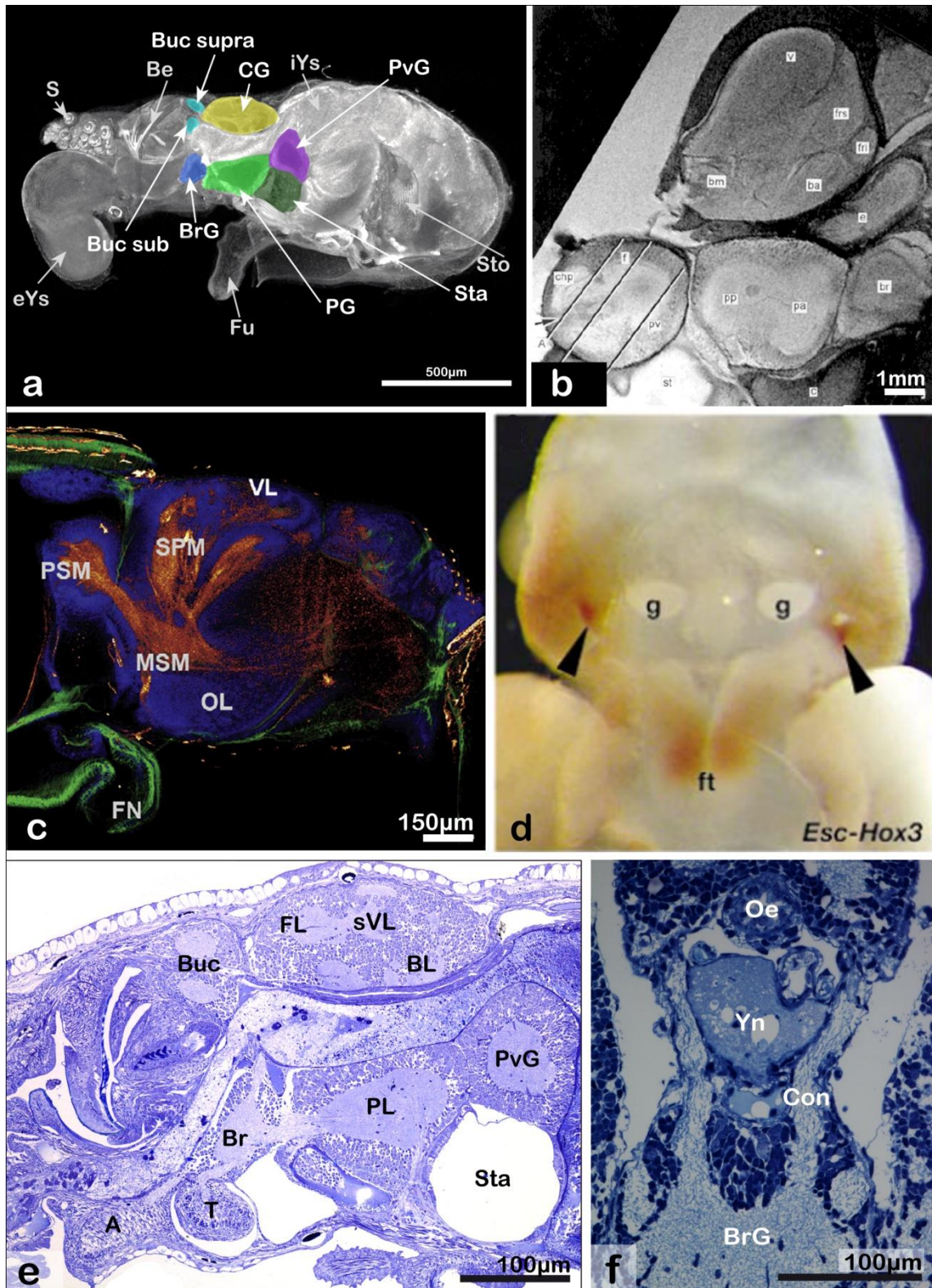


Fig. 19. Methods used in investigations of the cephalopod nervous system. **a** micro-CT-image of the total cephalopod hatchling, **b** μ MRI-image of the central nervous system using cobalt-labelling (Quast *et al.* 2001), **c** confocal investigation using phalloidin staining in vibratome sections (Wollesen *et al.* 2009), **d** whole-mount in situ-expression of Hox3 in *Euprymna scolopes* (Lee *et al.* 2003), **e** semithin sagittal section through the central nervous system depicting the major components, **f** cross section of the cerebro-brachial connective. All these

⇐ methods help to reveal a special part of the cephalopod nervous system. A combined approach of using more techniques would be best for such investigations, although not all techniques can be combined to any other. In this study, the combination of micro-CT and histology proves to be a rather elegant solution to perform a combined approach. A – arm, BL – basal lobes, Buc – buccal ganglion, Buc sub – suboesophageal buccal ganglion, Buc supra – supraoesophageal buccal ganglion, BrG – brachial ganglion, CG – cerebral ganglion, Con – connective, eYs – external yolk sac, FL – frontal lobes, FN – funnel, ft – funnel tube, Fu – funnel, g – gill, iYs – internal yolk sac, MSM – middle suboesophageal mass, Oe – oesophagus, OL – optic lobe, PG – pedal ganglion, PSM – posterior suboesophageal mass, PvG – palliovisceral ganglion, s – sucker, SPM – supraoesophageal mass, Sta – statocysts, Sto – stomach, svL – subvertical lobe, T – tentacle, VL – vertical lobe, Yn – yolk neck

CONCLUSION

The nervous system in *Euprymna scolopes* is similar to those of other decapodiform cephalopods such as *Sepioteuthis lessoniana* and *Todarodes pacificus* (Shigeno *et al.* 2001a, b) in its layout and in the sequence of steps forming the brain out of ganglionic placodes. The whole development can be roughly distinguished in three phases: The ganglionic formation and accumulation of the ganglia around the oesophagus (stage 19-21), the neuropile formation and lobe differentiation (stage 22-25) and the neuropile outgrowth and final differentiation (stage 26-30). I therefore suggest a common pattern in all cephalopods, although this pattern is altered in different groups during separated evolutionary pathways. Structures in the nervous system are not helpful in finding out more about the placement of cephalopods inside the molluscan group, which has been in discussion recently (Kocot *et al.* 2011; Smith *et al.* 2011). The cephalopod brain is much too complex and derivated from the general molluscan central nervous system to clearly detect homologies. Although there is no systematic value in the use of the nervous system, the structure as well arises a lot of interest. The eyes, for example, are similar to those of vertebrates in many points and are considered the highest developed in invertebrates. For that reason, finding out more about the basal conditions in cephalopods may help understanding the general process of the development of highly complex structures or the conditions leading towards such an innovation.

ACKNOWLEDGEMENTS

I want to thank M Walzl for supervising my diploma thesis and help wherever needed. I also want to acknowledge T Schwaha, St Handschuh, T Wollesen, B Metscher, M-T Nödl, and A Wanninger for fruitful discussions and technical help during the whole project. Additionally, I am grateful to D Gruber, W Klepal and the CIUS of the University of Vienna as well as L Rudoll of the Department of Integrative Zoology (University of Vienna) for their support and the provision of equipment. G Nickel is thanked for lecturing this thesis. This would not have been possible without the comradeship of my colleagues at the department, namely A Batawi, B Gratzner, S Hindinger, M Hüffel, St Jahnel, St Kummer, M Lintner, C Manzini, M Moosbrugger, B Schädli, B Sonnleitner and F Wehrberger, as well as my friends “from the very beginning” V Burtscher, A Engleder, T Hansal, K Hischenhuber, N Kraus, A Leeb, M Madsen, I Maiditsch, J Pulgram, A Rausch, J Rose, S Schneider and K Stejskal. Naturally, my family and none-biologist-friends have to be named here as well. Thanks for your support and help!

REFERENCES

- Adamo, S. & R. Hanlon** (1996). Do cuttlefish (Cephalopoda) signal their intentions to conspecifics during agonistic encounters? Animal Behaviour **52**: 73-81.
- Agin, V., R. Poirier, R. Chichery, L. Dickel & M. P. Chichery** (2006). Developmental study of multiple memory stages in the cuttlefish, *Sepia officinalis*. Neurobiology of Learning and Memory **86**: 264-269.
- Allcock, A. L., I. R. Cooke & J. M. Strugnell** (2011). What can the mitochondrial genome reveal about higher-level phylogeny of the molluscan class Cephalopoda? Zoological Journal of the Linnean Society **161**: 573-586.
- Arnold, J. M., C. T. Singley & L. D. Williams-Arnold** (1972). Embryonic Development and Post-Hatching Survival of the Sepiolid Squid *Euprymna scolopes* under Laboratory conditions. The Veliger **14**(4): 361-364.
- Arnold, J. M., W. C. Summers, D. L. Gilbert, R. S. Manalis, N. W. Daw & R. J. Lasek** (1974). A Guide to Laboratory Use of the Squid *Loligo pealei*. Woods Hole, Massachusetts, Marine Biological Laboratory. 74pp.
- Baratte, S. & L. Bonnaud** (2009). Evidence of early nervous differentiation and early catecholaminergic sensory system during *Sepia officinalis* embryogenesis. Journal of Comparative Neurology **517**: 539-549.
- Bonnaud, L., D. Pichon & R. Boucher-Rodoni** (2005). Molecular approach of decabrachia phylogeny: is *Idiosepius* definitely not a sepiolid. Phuket Marine Biological Center Research Bulletin **66**: 203-212
- Boyle, P. & P. Rodhouse** (2005). Cephalopods. Ecology and Fisheries, Oxford, Blackwell Science. 452pp.
- Boyle, P. R.** (1976). Receptor units responding to movement in the octopus mantle. Journal of Experimental Biology **65**(1): 1-9.
- Budelmann, B. U. & J. Z. Young** (1987). Brain pathways of the brachial nerves of *Sepia* and *Loligo*. Philosophical Transactions of the Royal Society of London Series B Biological Sciences **315**: 345-352.
- Budelmann, B. U., R. Schipp & S. Boletzky** (1997). Cephalopoda. In: **Harrison, F. W. & A. J. Kohn** (eds.): Microscopic Anatomy of Invertebrates, volume 6A: Mollusca II, pages 119-414. New York, Wiley-Liss.
- Callaerts, P., P. N. Lee, B. Hartmann, C. Farfan, D. W. Choy, K. Ikeo, K. F. Fischbach, W. J. Gehring & H. G. de Couet** (2002). HOX genes in the sepiolid squid *Euprymna scolopes*: implications for the evolution of complex body plans. Proceedings of the National Academy of Sciences of the United States of America **99**(4): 2088-2093.
- Chrachri, A. & R. Williamson** (2004). Cholinergic modulation of L-type calcium current in isolated sensory hair cells of the statocyst of octopus, *Eledone cirrhosa*. Neuroscience Letters **360**(1-2): 90-94.
- Claes, M. F. & P. V. Dunlap** (2000). Aposymbiotic culture of the sepiolid squid *Euprymna scolopes*: role of the symbiotic bacterium *Vibrio fischeri* in host animal growth, development, and light organ morphogenesis. Journal of Experimental Zoology **286**(3): 280-296.
- Colasanti, M. & G. Venturini** (1998). Nitric oxide in invertebrates. Molecular Neurobiology **17**(1-3): 157-174.
- Colasanti, M., T. Persichini & G. Venturini** (2010). Nitric oxide pathway in lower metazoans. Nitric Oxide **23**(2): 94-100.
- Di Cosmo, A., C. Di Cristo, A. Palumbo, M. d'Ischia & J. B. Messenger** (2000). Nitric oxide synthase (NOS) in the brain of the cephalopod *Sepia officinalis*. Journal of Comparative Neurology **428**(3): 411-427.

- Di Cristo, C., G. Fiore, V. Scheinker, G. Enikolopov, M. d'Ischia, A. Palumbo & A. Di Cosmo** (2007). Nitric oxide synthase expression in the central nervous system of *Sepia officinalis*: An in situ hybridization study. European Journal of Neuroscience **26**(6): 1599-1610.
- Dinley, J., L. Hawkins, G. Paterson, A. D. Ball, I. Sinclair, P. Sinnett-Jones & S. Lanham** (2010). Micro-computed X-ray tomography: a new non-destructive method of assessing sectional, fly-through and 3D imaging of a soft-bodied marine worm. Journal of Microscopy **238**(2): 123-133.
- Edelman, D. B. & A. K. Seth** (2009). Animal consciousness: a synthetic approach. Trends in Neurosciences **32**(9): 476-484.
- Farfan, C., S. Shigeno, M. T. Nodl & H. G. de Couet** (2009). Developmental expression of apterous/Lhx2/9 in the sepiolid squid *Euprymna scolopes* supports an ancestral role in neural development. Evolution & Development **11**(4): 354-362.
- Fioroni, P. & G. Meister** (1974). *Loligo vulgaris* LAM. Gemeiner Kalmar. Stuttgart, Gustav Fischer Verlag. 69pp.
- Golding, R. E. & A. S. Jones** (2007). Micro-CT as a novel technique for 3D reconstruction of molluscan anatomy. Molluscan Research **27**(3): 123-128.
- Golding, R. E., W. F. Ponder & M. Byrne** (2009). Three-dimensional reconstruction of the odontophoral cartilages of Caenogastropoda (Mollusca: Gastropoda) using micro-CT: Morphology and phylogenetic significance. Journal of Morphology **270**(5): 558-587.
- Guerrero-Ferreira, R. C. & M. K. Nishiguchi** (2007). Biodiversity among luminescent symbionts from squid of the genera *Uroteuthis*, *Loliolus* and *Euprymna* (Mollusca: Cephalopoda). Cladistics **23**: 497-506.
- Hanlon, R.** (2007). Cephalopod dynamic camouflage. Current Biology **17**(11): 400-404.
- Hanlon, R. T., M. F. Claes, S. E. Ashcraft & P. V. Dunlap** (1997). Laboratory culture of the sepiolid squid *Euprymna scolopes*: A model system for bacteria-animal symbiosis. Biological Bulletin **192**: 364-374.
- Harrison, F. M. & A. W. Martin** (1965). Excretion in the Cephalopod, *Octopus dofleini*. Journal of Experimental Biology **42**: 71-98.
- Kerbl, A., S. Handschuh, M.-T. Nödl, B. Metscher, M. Walzl & A. Wanninger** (subm.). Micro-CT as non-destructive technique to determine ganglionic growth during cephalopod development. Journal of Experimental Marine Biology and Ecology.
- Kimbell, J. R., M. J. McFall-Ngai & G. K. Roderick** (2002). Two genetically distinct populations of Bobtail Squid, *Euprymna scolopes*, exist off the island of O'ahu. Pacific Science **56**(3): 347-355.
- Kocot, K. M., J. T. Cannon, C. Todt, M. R. Citarella, A. B. Kohn, A. Meyer, S. R. Santos, C. Schander, L. L. Moroz, B. Lieb & K. M. Halanych** (2011). Phylogenomics reveals deep molluscan relationships. Nature **477**(7365): 452-456.
- Kröger, B., J. Vinther & D. Fuchs** (2011). Cephalopod origin and evolution: A congruent picture emerging from fossils, development and molecules. Bioessays **33**: 602-613.
- Lauridsen, H., K. Hansen, T. Wang, P. Agger, J. L. Andersen, P. S. Knudsen, A. S. Rasmussen, L. Uhrenholt & M. Pedersen** (2011). Inside out: modern imaging techniques to reveal animal anatomy. PLoS One **6**(3): e17879.
- Lee, P. N., P. Callaerts, H. G. de Couet & M. Q. Martindale** (2003). Cephalopod Hox genes and the origin of morphological novelties. Nature **424**(6952): 1061-1065.
- Lee, P. N., P. Callaerts & H. G. de Couet** (2009a). Culture of Hawaiian bobtail squid (*Euprymna scolopes*) embryos and observation of normal development. Cold Spring Harbor Protocols **2009**(11): pdb prot5323.
- Lee, P. N., P. Callaerts & H. G. de Couet** (2009b). The embryonic development of the Hawaiian bobtail squid (*Euprymna scolopes*). Cold Spring Harbor Protocols **2009**(11): pdb ip77.
- Lee, P. N., M. J. McFall-Ngai, P. Callaerts & H. G. de Couet** (2009c). Whole-mount in situ hybridization of Hawaiian bobtail squid (*Euprymna scolopes*) embryos with DIG-labeled

- riboprobes: I. DNA template preparation and in vitro transcription of riboprobes. Cold Spring Harbor Protocols **2009**(11): pdb prot5321.
- Lee, P. N., M. J. McFall-Ngai, P. Callaerts & H. G. de Couet** (2009d). Preparation of genomic DNA from Hawaiian bobtail squid (*Euprymna scolopes*) tissue by cesium chloride gradient centrifugation. Cold Spring Harbor Protocols **2009**(11): pdb prot5319.
- Lee, P. N., M. J. McFall-Ngai, P. Callaerts & H. G. de Couet** (2009e). Confocal immunocytochemistry of embryonic and juvenile Hawaiian bobtail squid (*Euprymna scolopes*) tissues. Cold Spring Harbor Protocols **2009**(11): pdb prot5320.
- Lee, P. N., M. J. McFall-Ngai, P. Callaerts & H. G. de Couet** (2009f). Whole-mount in situ hybridization of Hawaiian bobtail squid (*Euprymna scolopes*) embryos with DIG-labeled riboprobes: II. Embryo preparation, hybridization, washes, and immunohistochemistry. Cold Spring Harbor Protocols **2009**(11): pdb prot5322.
- Lee, P. N., M. J. McFall-Ngai, P. Callaerts & H. G. de Couet** (2009g). The Hawaiian bobtail squid (*Euprymna scolopes*): a model to study the molecular basis of eukaryote-prokaryote mutualism and the development and evolution of morphological novelties in cephalopods. Cold Spring Harbor Protocols **2009**(11): pdb emo135.
- Mangold, K.** (1989). Cephalopodes. In: **Pierre-Paul Grassé** (eds.): Traité de zoologie, anatomie, systématique, biologie. Tome V, Fascicule 4. Paris, Ed. Masson. 804pp.
- Marquis, F.** (1989). Die Embryonalentwicklung des Nervensystems von *Octopus vulgaris* Lam. (Cephalopoda, Octopoda), eine histologische Analyse. Verhandlungen der Naturforschenden Gesellschaft in Basel **99**: 23-76.
- Martin, R. & D. Rungger** (1966). Zur Struktur und Entwicklung des Riesenfasersystems erster Ordnung von *Sepia officinalis* L. (Cephalopoda). Zeitschrift für Zellforschung **74**: 454-463.
- Martin, R.** (1969). The structural organization of the intracerebral giant fiber system of cephalopods. Zeitschrift für Zellforschung **97**: 50-68.
- Mather, J. A.** (2008). Cephalopod consciousness: Behavioural evidence. Consciousness and Cognition **17**(1): 37-48.
- McFall-Ngai, M. J.** (1998). Pioneering the Squid-*Vibrio* Model. American Society for Microbiology News **64**(11): 639-645.
- McFall-Ngai, M. J., S. V. Nyholm & M. G. Castillo** (2010). The role of the immune system in the initiation and persistence of the *Euprymna scolopes-Vibrio fischeri* symbiosis. Seminars in Immunology **22**(1): 48-53.
- Meister, G.** (1972). Organogenese von *Loligo vulgaris* Lam. (Mollusca, Cephalopoda, Teuthoidea, Myopsida, Loliginidae). Zoologische Jahrbücher. Abteilung für Anatomie und Ontogenie der Tiere **89**: 247-300.
- Messenger, J. B.** (1978). The nervous system of *Loligo* IV. The peduncle and olfactory system. Philosophical Transactions of the Royal Society of London Series B Biological Sciences **285**: 275-309.
- Metscher, B. D.** (2009a). MicroCT for developmental biology: a versatile tool for high-contrast 3D imaging at histological resolutions. Developmental Dynamics **238**(3): 632-640.
- Metscher, B. D.** (2009b). MicroCT for comparative morphology: simple staining methods allow high-contrast 3D imaging of diverse non-mineralized animal tissues. BMC Physiology **9**: 11.
- Metscher, B. D.** (2010). X-ray microtomographic imaging of vertebrate embryos. In: **J. Sharpe, R. Wong & R. Yuste**: Imaging in Developmental Biology: A Laboratory Manual. Cold Spring Harbor, Cold Spring Harbor Press. 883pp.
- Metscher, B. D. & G. B. Müller** (2011). MicroCT for molecular imaging: Quantitative visualization of complete three-dimensional distributions of gene products in embryonic limbs. Developmental Biology **240**(12): 2301-2308.
- Mirow, S.** (1972). Skin color in the squids *Loligo pealii* and *Loligo opalescens*. II. Iridophores. Zeitschrift für Zellforschung und Mikroskopische Anatomie **125**(2): 176-190.

- Moroz, L. L., D. Chen, M. U. Gillette & R. Gillette** (1996). Nitric oxide synthase activity in the molluscan CNS. Journal of Neurochemistry **66**(2): 873-876.
- Moynihan, M.** (1983). Notes on the behavior of *Euprymna scolopes* (Cephalopoda: Sepiolidae). Behaviour **85**(1/2): 25-41.
- Naef, A.** (1913). Studien zur generellen Morphologie der Mollusken. 2. Teil. Das Cölomsystem in seinen topographischen Beziehungen. Ergebnisse und Fortschritte der Zoologie **3**: 329—462.
- Naef, A.** (1928). Die Cephalopoden. Part II: Embryologie. Fauna Flora Golf Neapel **35**: 1-357.
- Nixon, M. & J. Z. Young** (2003). The brains and lives of cephalopods. Oxford ; New York, Oxford University Press. 408pp.
- Nyholm, S. V., E. V. Stabb, E. G. Ruby & M. J. McFall-Ngai** (2000). Establishment of an animal-bacterial association: recruiting symbiotic vibrios from the environment. Proceedings of the National Academy of Sciences of the United States of America **97**(18): 10231-10235.
- Packard, A.** (1972). Cephalopods and fish: The limits of convergence. Biological Reviews **47**: 241-307.
- Peunova, N., V. Scheinker, H. Cline & G. Enikolopov** (2001). Nitric oxide is an essential negative regulator of cell proliferation in *Xenopus* brain. Journal of Neuroscience Methods **21**(22): 8809-8818.
- Peunova, N., V. Scheinker, K. Ravi & G. Enikolopov** (2007). Nitric oxide coordinates cell proliferation and cell movements during early development of *Xenopus*. Cell Cycle **6**(24): 3132-3144.
- Pozzo-Miller, L. D., J. E. Moreira & R. R. Llinas** (1998). The first-order giant neurons of the giant fiber system in the squid: electrophysiological and ultrastructural observations. Journal of Neurocytology **27**(6): 419-429.
- Quast, M. J., H. Neumeister, E. L. Ezell & B. U. Budelmann** (2001). MR microscopy of cobalt-labeled nerve cells and pathways in an invertebrate brain (*Sepia officinalis*, Cephalopoda). Magnetic Resonance in Medicine **45**(4): 575-579.
- Salvini-Plawen, L.** (1980). A reconsideration of systematics in the mollusca (phylogeny and higher classification). Malacologia **19**(2): 249-278.
- Salvini-Plawen, L. & G. Steiner** (1996). Synapomorphies and plesiomorphies in higher classification of Mollusca. In: **J. D. Taylor**: Origin and Evolutionary Radiation of the Mollusca. Oxford, Oxford University Press: 29-52.
- Scheinker, V., G. Fiore, C. Di Cristo, A. Di Cosmo, M. d'Ischia, G. Enikolopov & A. Palumbo** (2005). Nitric oxide synthase in the nervous system and ink gland of the cuttlefish *Sepia officinalis*: Molecular cloning and expression. Biochemical and Biophysical Research Communications **338**(2): 1204-1215.
- Shears, J.** (1988). The use of a sandcoat in relation to feeding and diel activity in the sepiolid squid *Euprymna scolopes*. Malacologia **29**(1): 121-133.
- Shigeno, S., H. Kidokoro, K. Tsuchiya, S. Segawa & M. Yamamoto** (2001a). Development of the Brain in the Oegopsid squid, *Todarodes pacificus*: An atlas up to the hatching stage. Zoological Science **18**: 527-541.
- Shigeno, S., K. Tsuchiya & S. Segawa** (2001b). Embryonic and paralarval development of the central nervous system of the loliginid squid *Sepioteuthis lessoniana*. Journal of Comparative Neurology **437**(4): 449-475.
- Shigeno, S., T. Sasaki, T. Moritaki, T. Kasugai, M. Vecchione & K. Agata** (2008). Evolution of the cephalopod head complex by assembly of multiple molluscan body parts: Evidence from *Nautilus* embryonic development. Journal of Morphology **269**(1): 1-17.
- Smith, S. A., N. G. Wilson, F. E. Goetz, C. Feehery, S. C. Andrade, G. W. Rouse, G. Giribet & C. W. Dunn** (2011). Resolving the evolutionary relationships of molluscs with phylogenomic tools. Nature **480**(7377): 364-367.

- Strugnell, J & M. K. Nishigushi** (2007). Molecular phylogeny of coleoid cephalopods (Mollusca: Cephalopoda) inferred from mitochondrial and six nuclear loci: A comparison of alignment, implied alignment and analysis methods. Journal of Molluscan Studies **73**: 339-410
- Tu, Y. & B. U. Budelmann** (2000). Effects of nitric oxide donors on the afferent resting activity in the cephalopod statocyst. Brain Research **865**(2): 211-220.
- Tublitz, N. J., M. R. Gaston & P. K. Loi** (2006). Neural regulation of a complex behavior: body patterning in cephalopod molluscs. Integrative and Comparative Biology **46**(6): 880-889.
- von Byern, J., L. Rudoll, N. Cyran & W. Klepal** (2006). Histochemical characterization of the adhesive organ of three *Idiosepius* spp. species. Biotechnic & Histochemistry **83**(1): 29-46.
- Wanninger, A.** (2008). Comparative lophotrochozoan neurogenesis and larval neuroanatomy: recent advances from previously neglected taxa. Acta Biologica Hungarica **59** Suppl: 127-136.
- Wanninger, A.** (2009). Shaping the things to come: ontogeny of lophotrochozoan neuromuscular systems and the tetraneuralia concept. Biological Bulletin **216**(3): 293-306.
- Warnke, K., J. Plötner, J. I. Santana, M. J. Rueda & O. Llinàs** (2003). Reflections of the phylogenetic position of *Spirula* (Cephalopoda): Preliminary evidence from the 18S ribosomal RNA gene. Berliner Paläobiologische Abhandlungen **3**: 253-260.
- Wells, M.** (1972). Octopus Neuroanatomy. Nature **236**(5342): 123-123.
- Wilson, D. M.** (1959). Nervous control of movement in cephalopods. Journal of Experimental Biology **37**: 57-72.
- Wollesen, T., R. Loesel & A. Wanninger** (2009). Pygmy squids and giant brains: mapping the complex cephalopod CNS by phalloidin staining of vibratome sections and whole-mount preparations. Journal of Neuroscience Methods **179**(1): 63-67.
- Wollesen, T., S. F. Cummins, B. M. Degnan & A. Wanninger** (2010a). FMRFamide gene and peptide expression during central nervous system development of the cephalopod mollusk, *Idiosepius notoides*. Evolution & Development **12**(2): 113-130.
- Wollesen, T., B. M. Degnan & A. Wanninger** (2010b). Expression of serotonin (5-HT) during CNS development of the cephalopod mollusk, *Idiosepius notoides*. Cell and Tissue Research **342**(2): 161-178.
- Yamamoto, M., Y. Shimazaki & S. Shigeno** (2003). Atlas of the embryonic brain in the pygmy squid, *Idiosepius paradoxus*. Zoological Science **20**(2): 163-179.
- Yamazaki, A., M. Yoshida & K. Uematsu** (2002). Post-hatching development of the brain in *Octopus ocellatus*. Zoological Science **19**(7): 763-771.
- Young, J. Z.** (1932). On the cytology of the neurons of cephalopods. Philosophical Transactions of the Royal Society of London Series B Biological Sciences **297**: 1-57.
- Young, J. Z.** (1964). The central nervous system of *Nautilus*. Philosophical Transactions of the Royal Society of London Series B Biological Sciences **249**: 1-45.
- Young, J. Z.** (1973). The central nervous system of *Loligo* I. The optic lobe. Philosophical Transactions of the Royal Society of London Series B Biological Sciences **267**: 263-301.
- Young, J. Z.** (1975). The nervous system of *Loligo* II. Suboesophageal centres. Philosophical Transactions of the Royal Society of London Series B Biological Sciences **274**: 101-167.
- Young, J. Z.** (1976). The 'cerebellum' and the control of eye movements in cephalopods. Nature **264**: 572-574.
- Young, J. Z.** (1977). The nervous system of *Loligo* III. Higher motor centres: The basal supraoesophageal lobes. Philosophical Transactions of the Royal Society of London Series B Biological Sciences **276**: 351-398.
- Young, J. Z.** (1978). The nervous system of *Loligo*. V. The vertical lobe complex. Philosophical Transactions of the Royal Society of London Series B Biological Sciences **285**: 311-354.

- Young, J. Z.** (1985). Cephalopods and neuroscience. Biological Bulletin **168 (suppl.)**: 153-158.
- Young, J. Z.** (1988). Evolution of the cephalopod brain. In: **K. M. Wilbur, A. S. Tompa, N. H. Verdonk & J. A. M. van den Biggelaar**: Paleontology and Neontology of Cephalopods, volume **12**, pages 215-228. Academic Press Inc.
- Young, R. E., M. Vecchione & K. M. Mangold** (2012). Cephalopod glossary. Available at tolweb.org/notes/?noe_id=587, last time checked 10.03.2012
- Ziegler, A., C. Faber, S. Mueller & T. Bartolomaeus** (2008). Systematic comparison and reconstruction of sea urchin (Echinoidea) internal anatomy: a novel approach using magnetic resonance imaging. BMC Biology **6**: 33.
- Ziegler, A., M. Ogurreck, T. Steinke, F. Beckmann & S. Prohaska** (2010). Opportunities and challenges for digital morphology. Biology Direct **5**: 45.
- Ziegler, A., M. Kunth, S. Mueller, C. Bock, R. Pohmann, L. Schröder, C. Faber & G. Giribet** (2011). Application of magnetic resonance imaging in zoology. Zoomorphology **130**(4): 227-254.
- Ziegler, A. & S. Mueller** (2011). Analysis of freshly fixed and museum invertebrate specimens using high-resolution, high-throughput MRI. Methods in Molecular Biology **771**: 633-651.

SUPPLEMENTARY INFORMATION

SUPPLEMENTS I: Kerbl, A., S. Handschuh, M.-T. Nödl, B. Metscher, M. Walzl & A. Wanninger (subm.). Micro-CT as non-destructive technique to determine ganglionic growth during cephalopod development. Journal of Experimental Marine Biology and Ecology

Micro-CT as non-destructive technique to determine ganglionic growth during cephalopod development

Alexandra Kerbl^{1,✉}, Stephan Handschuh^{2,3}, Marie-Therese Nödl², Brian Metscher², Manfred Walzl¹ & Andreas Wanninger¹

¹ Department of Integrative Zoology, University of Vienna, Althanstraße 14, 1090 Vienna, Austria

² Department of Theoretical Biology, University of Vienna, Althanstraße 14, 1090 Vienna, Austria

³ Konrad Lorenz Institute for Evolution and Cognition Research, Adolf Lorenz Gasse 2, 3422 Altenberg, Austria

✉Corresponding author: Alexandra Kerbl, Department of Integrative Zoology, University of Vienna, Althanstraße 14, 1090 Vienna, Austria. Email: alexandra.kerbl@univie.ac.at, Tel: +43 1 4277 76318

HIGHLIGHTS

We tested micro-CT-protocols for their applicability to soft-bodied organisms

Resulting data proved to be useful in 3D-reconstruction and other techniques

Main features of such data include perfect alignment and no distortions

3D-images with 2µm voxels can resolve specific structures of 2mm cephalopod embryos

Micro-CT can be used for the study of rare and museum samples without altering them

ABSTRACT

Cephalopods are of considerable interest in many different fields of biology, particularly in behavioral studies and physiology, which is partially due to their sophisticated nervous system. Until now, most investigations on the internal organization have been based on serial sectioning techniques. Here, we demonstrate the state-of-the-art-technique of X-ray microtomography (micro-CT) for 3D imaging of soft-bodied organisms without mineralized structures. As a model for this study, we chose the Hawaiian bobtail squid *Euprymna scolopes* Berry, 1913, a species that has recently been considered as model organism for decabrachiate development. The nervous system and its development have been the subjects of many molecular and gene expression-based investigations in cephalopods, although basic information about the structures is missing. We therefore focused our study on ganglionic growth during embryonic developmental stages. We show that micro-CT in combination with contrast-enhancing substances such as iodine or phosphotungstic acid can provide detailed 3D information on the anatomy of an entire cephalopod embryo as well as on selected structures such as the ganglionic system, which is easily recognized in most of the specimens. Additionally, this technique simplifies computer-assisted 3D-reconstructions and modeling due to the perfectly aligned, distortion-free image stacks produced by the micro-CT scans. In particular, we want to point out one key advantage of non-destructive micro-CT applications, namely its great potential when combined with other research techniques such as histology, immunocytochemistry, and gene expression studies.

KEYWORDS

X-ray microtomography, *Euprymna scolopes*, nervous system, development, contrast-enhancement, volumetric measurements, 3D-renderings

ABBREVIATIONS

BrG brachial ganglion, BrN brachial nerve, BuG buccal ganglion, BuM buccal mass, BV blood vessel, CG cerebral ganglion, E eye, F funnel, Fi fin, GG gastral ganglion, H heart, igl inner granular layer, Int intestine, iYS internal yolk sac, J jaws, L lense, Ma mantle, Oe oesophagus, ogl outer granular layer, OL optic lobe, opl outer plexiform layer, PG pedal ganglion, PvG palliovisceral ganglion, Ret retina, St statocyst, StG stellate ganglion, TN tentacular nerves, YN yolk neck

INTRODUCTION

Cephalopods exhibit a highly complex central nervous system (CNS) in protostomes as well as a diverse suite of behavioral patterns. Their CNS is believed to have evolved by fusion of paired ganglia homologous to those found in their potential sister group, the gastropods (Salvini-Plawen, 1980; Salvini-Plawen and Steiner, 1996), although recent studies show a different relationship between the molluscan groups (Kocot et al., 2011; Smith et al., 2011). Thus, the cephalopod “brain” may comprise the fused cerebral, brachial, pedal, palliovisceral, and buccal ganglia of a proposed last common gastropod-cephalopod ancestor. The most prominent parts of the cephalopod central nervous system are the paired, laterally situated optic lobes, which may occupy up to two thirds of the total mass of the cephalopod CNS. In addition, so-called stellate ganglia are found that innervate the mantle musculature (Messenger, 1978; Shigeno and Yamamoto, 2002; Wollesen et al., 2010; Young, 1973, 1975, 1977, 1978). In contrast to vertebrates, where the brain develops from a neural tube (neurulation), cephalopod ganglia form as individual placodes in the blastoderm of the embryo, which fuse during subsequent development (Marquis, 1989; Shigeno et al., 2001a). Although a large body of information exists on the internal organization of cephalopods (Alagarswami, 1966; Arnold, 1965; Asokan and Kakati, 1991; Marquis, 1989; Marthy, 1975; Shigeno and Yamamoto, 2002; Shigeno et al., 2001b; Shigeno et al., 2001a; Young, 1965, 1973, 1975, 1977, 1978), these accounts were mainly based on conventional techniques such as serial sections and light microscopy, while only a few studies have focused on the early development of the cephalopod nervous system (Marquis, 1989; Shigeno et al., 2001b; Shigeno et al., 2001a).

Euprymna scolopes is a sepiolid squid and a potential emerging model organism for developmental studies in decabrachiate cephalopods. Currently, it serves as model together with the bacterium *Vibrio fischeri* for the study of host-symbiont interactions (McFall-Ngai 1994; McFall-Ngai 1999; Nyholm and McFall-Ngai 2004), and its suitability for gene expression analyses has recently been demonstrated (Callaerts et al., 2002; Farfan et al., 2009; Hartmann et al., 2003). Nevertheless, neither the internal anatomy nor the development of organ systems has been investigated extensively. Two categorizations of 30 developmental stages have been conducted (Arnold et al., 1972; Lee et al., 2009c) using mostly external features. We therefore know that *Euprymna scolopes* exhibits discoidal cleavage, typical for cephalopod mollusks, whereby the embryo proper forms a disc-like structure at the animal pole. Like in other coleoids, only the ridge of the ectodermal layer envelops the yolk to form the yolk sac. The germ layers are formed after gastrulation, while the embryonic body becomes visible at the onset of organogenesis. This occurs in *Euprymna scolopes* late in stage 16 or in early stage 17, when the embryo covers approximately 60% of the egg surface. The formation of organ primordia such as ganglionic placodes can be observed at approximately these stages in other species as well (Shigeno et al., 2001b; Shigeno et al., 2001a; Shigeno et al., 2008). During the following stages, the ganglia accumulate around the esophagus and additional organs start to form and are well established at hatching (stage 30).

Despite these gross morphological data, very little is known on the development of the internal organ systems of *Euprymna scolopes*.

In this study, micro-CT images were used to reconstruct CNS development of selected developmental stages of *Euprymna scolopes*. We found that combined application of micro-CT and histology renders far more conclusive information on the overall morphology of a given study specimen than does either technique alone. In addition, we outline the possibilities of combining various imaging methods in order to obtain a more comprehensive data set of a specimen than would be possible by applying any single method. The data generated by micro-CT may form the basis for a computer-assisted 3D-reconstruction of the central nervous system as well as other soft tissues. Combined with modern imaging software including segmentation algorithms, volume measurements of both the total body and the central nervous system are possible. The micro-CT-scanned specimens are further processed to obtain histological data that allow for analyses on the cellular level.

MATERIALS & METHODS

Specimen fixation and preservation

Embryos of *Euprymna scolopes* were obtained from adults that were kept in tanks at the University of Hawaii at Manoa, Oahu. Embryos were mechanically freed from the protective egg envelopes and fixed in 4% glutaraldehyde in 0.1M cacodylate buffer (pH 7.4) overnight at 4°C. After fixation, samples were rinsed and preserved in 70% methanol.

Specimen preparation for micro-CT

For achieving a better contrast for soft tissues for X-ray microtomography, a total of 14 specimens of various developmental stages (stages from 17 to 30) were contrasted using 1% elemental iodine dissolved in 100% methanol (Metscher 2009b) for 22h and subsequently rinsed three times with 100% methanol. In addition, one specimen (stage 28) was stained with phosphotungstic acid (PTA, Metscher 2009b) to compare the contrasting ability of PTA for squid tissue. Afterwards, the specimens were mounted in 75% methanol in heat-sealed pipette tips that were sealed with UHU Pattafix and Parafilm to avoid vaporization of the mounting medium (Metscher, 2009a, 2010). In these mounts it is critical to avoid gas bubbles inside the pipette, since these may cause movements of the sample, which would render proper reconstruction of the projection images impossible.

X-ray micro-CT

For X-ray microCT imaging, we used an Xradia MicroXCT scanner (vintage 2007, Xradia Inc.,USA). The heat-sealed pipette tip was mounted on the object platform, which rotates during the scan inside the micro-CT scanner cabinet. The detector system is composed of a set of light microscopy objectives, each equipped with a scintillator crystal at its frontal lens that absorbs X-rays and converts the energy into visible light, a tube lens system, and a CCD camera. The Xradia system-specific control software was used to set the source and detector distances to achieve a geometric magnification suitable for the specimen size. Both geometric and objective magnification can be used to optimize the depiction of important details and to determine an ideal field of view. In this study we used 4x objective magnification for all specimens. The field of view for a scan is adjusted such that it covers either the total or just a part of the specimen. For specimens too large to be scanned in one scan, two regions were scanned separately and stitched together using the Xradia stitching plugin. With this method, a higher resolution can be achieved even in relatively large objects than with one individual scan. Exposure time and source voltage and current may be adjusted depending on the object and the contrasting agents applied. In our case, we used 15 sec exposure per projection image, and source settings of 60 keV and 8 W. During the scan, the specimen is rotated around its own vertical axis by slightly more than 180°. For this rotation range, 4 images were taken per 1° rotation, resulting in about 747 projection images for each scan. Thus, specimens were entirely scanned within 5-12 hrs. (Fig. I).

Image reconstruction

Tomographic cross sections were reconstructed from projection images using the included XMReconstructor software and saved as 8-bit greyscale TIFF image stacks. Exporting the data in a standard image format is necessary for later import in 3D software packages such as Amira and allows an inspection with traditional image processing applications. After reconstruction, a mfilter with kernel size 3 was used to reduce background noise. The process of reconstruction results in perfectly aligned and size-calibrated image stacks with isotropic voxels ranging in a size range of 2.5 to 3.8 microns (Fig.1).

3D reconstruction and volumetric calculations

For 3D rendering, the stacks were imported into Amira 4.1.1 software (Visage Imaging, Inc., San Diego, CA, USA) with defined voxel size. Individual ganglionic components were manually segmented and assigned to different “materials” within the segmentation file. These additional data sets are connected to the original image stack. Based on manual segmentation, three-dimensional surface renderings were created using the Amira *SurfaceGen* tool by selecting voxel boundaries in a data set. Segmented

materials, however, can also be used to obtain quantitative information about the specific materials such as the volume of each structure, by using the *TissueStatistics* tool in Amira.

Specimen preparation for histology

To test the possibility for a downstream histological preparation of the same specimen after the scanning process, the specimens were rinsed in 70% ethanol, dehydrated in a graded series of ethanol and embedded in epoxy resin (Araldite). The blocks were sectioned with a thickness of 1µm and serial sections were stained with toluidine blue for 30sec at 60°C and photographed using a Nikon Eclipse E800 microscope.

Brief description of embryonic development and stages investigated

In this study, embryos from stage 17 onwards were investigated, at a stage where the blastoderm is situated at the animal pole and the extraembryonic tissue almost completely covers the surface of the yolk. Placode formation starts stage 16-18, and brain development starts approximately at this stage (Marquis, 1989; Shigeno et al., 2001b; Shigeno et al., 2001a). At stage 19, the arm buds begin to develop as five pairs partially surrounding the yolk. Between the two buds of arm pair I, the stomodeum forms and the anlagen of the eyes, statocysts, and mantle can be observed (Fig. II). Subsequently, the fourth arm pair elongates more rapidly than the others and subsequently differentiates into the tentacles. During development, the body elongates along its dorsoventral axis, although the head with the dominant visual apparatus is more prominent than the mantle (Fig. II and III). During later organogenesis (stage 24-30), the mantle increases in size and eventually covers the gills and the anterior part of the funnel tube. The yolk is divided into the external yolk sac and an internal mass, both connected to each other via the yolk neck. Until hatching (stage 30), the external yolk sac is almost entirely absorbed by the embryo and nourishes the hatchling for about one more week (Fig. II and III).

RESULTS

Development of the nervous system

Micro-CT proved to be unsuitable for a detailed reconstruction of the ganglionic system in stages younger than stage 24. The palliovisceral and the pedal ganglion as well as the cerebral ganglion are the first components of the central nervous system that can be recognized with microCT and they form most of the supraoesophageal and the suboesophageal masses. On X-ray micrographs, the ganglia in stages higher than 24 can be distinguished due to their specific organization: the nervous fibers form a less X-ray

dense inner layer, while the neuropil and the perikarya form a more X-ray-dense layer surrounding the fibers (Fig. IV). At stage 24, the primordia of the everse lenticular eyes are already connected to the brain via the optic tract region and the optic lobes. The optic lobes gain in size and become the largest lobes of the CNS. They can be identified by the tree-like arrangement of fibers and perikarya, which can be detected after stage 25 (Fig. II and III). The main components investigated were the cerebral, palliovisceral, pedal, and the optic lobes, which form the central nervous system. Additionally, the brachial ganglion and the nerves in the arms and tentacles were considered, as these structures are directly adjacent to the brain. Data of all these components could be obtained from embryos of stage 24 until hatching (Fig. II, III and V).

Additionally, the two most proximate sensory organs, the eyes and statocysts, were measured. The peripheral nervous system consists of the pair of stellate ganglia, the buccal ganglia, and the gastric ganglion (Fig. II, III & IV). They form later in development at approximately stage 26 and could not be observed in the earliest stages investigated.

The nervous system of hatchlings constitutes about a third of the body volume, with the CNS as largest component in the anterior part of the embryo. The internal yolk sac increases in size and is situated in the visceral part of the embryo. By reconstructing the microtomographs and applying volume rendering (using the tool *Voltex* in Amira 4.1.1), a much more detailed representation of the original specimen can be achieved, providing information also on internal structures. Thus, the gills or the internal yolk sac can be observed as well as blood vessels, which are displayed due to their high electron density (Fig. IVe - i). Nevertheless, a higher resolution up to cellular detail can be obtained by histological sections following the scanning procedure (Fig. VI).

Volumetric measurements

To demonstrate the suitability of micro-CT data for volumetric measurements, we used the scanned specimens to calculate the volumes of distinct ganglionic components. In the volumetric calculations, the components of the CNS and some parts of the peripheral nervous system were considered, although we mainly focused on the cerebral ganglion and the optic lobes. The cerebral ganglion, containing the highest integration center, shows a decrease in volume relative to that of the total brain. The pedal and the palliovisceral ganglia do not undergo changes in size relative to the body volume throughout the development as far as it was investigated here. Each component remains at less than 10 percent of the total ganglionic volume.

Considering all developmental stages, there is a decrease in the total ganglionic volume relative to the body volume, with the growth curve leveling off towards the older stages. The same pattern can be observed in the total body volume, when the graph seems to be reaching a saturation level (Fig. Va & b).

The cerebral ganglia and the optic lobes are already prominent ganglionic components in earlier stages (24-25) of development and form the supraoesophageal mass as well as the lateral connections between the supraoesophageal and the suboesophageal masses. However, their growth pattern is different. The optic lobes increase far more rapidly in size than the cerebral ganglion, and, interestingly, both ganglionic structures level off remarkably in the later developmental stages relative to the growth of the total body. When expressed in relative numbers as percentage of the total body volume, the volume curves of both ganglia still increase, although the optic lobes still grow faster (Fig. Vc & d).

DISCUSSION

Gross development of the ganglia in *Euprymna scolopes*

The nervous system of cephalopods is rather concentrated, and even in more basal cephalopods such as *Nautilus* consists of highly concentrated and fused ganglia (Young, 1965). The coleoid cephalopod *Euprymna scolopes* belongs to the Sepiolida, where the brain is organized in a rather complex way. Due to the limitations in spatial resolution or eventually due to lack of stained contrast between the relevant structures, a detailed analysis of stages earlier than 24 was not possible. Therefore, information on nervous system development is restricted to the process of ganglionic growth, i.e., at stages where the individual ganglia have already condensed to a circumesophageal ring. Since no information is currently available on the interior organization of *Euprymna scolopes*, these data can either be compared to data on the outer morphology from former studies (Arnold et al., 1972; Hanlon et al., 1997; Lee et al., 2009c) or the developmental processes in other cephalopod species (Marquis, 1989; Shigeno and Yamamoto, 2002; Shigeno et al., 2001b; Shigeno et al., 2001a; Shigeno et al., 2008). In early embryonic stages, the embryonic brain of *Euprymna scolopes* and other species resembles the adult brain in *Nautilus* (Young, 1988). Although the ganglia in *Nautilus* have formed the circumesophageal ring, the concentration is very low and the single components can still be discriminated (Young, 1965). During subsequent development, processes such as neuropil formation or lobe differentiation are quite similar to species such as *Sepioteuthis lessoniana* (Shigeno et al., 2001a), or *Octopus vulgaris* (Marquis, 1989). The temporal pattern, however, differs slightly, and single ganglia are fused to a higher degree in *O. vulgaris* (present study, Marquis 1989).

Micro-CT as a powerful tool to reveal information on the internal organization of soft-bodied organisms at microscopic scales

Micro-CT imaging is currently used in various fields of both engineering (Desplentere et al., 2005) and biology (Lauridsen et al., 2011). To date, micro-CT has mainly been used for visualizing bones or other mineralized hard tissues with a high X-ray density.

Nevertheless, contrast enhancing substances such as iodine or heavy metals (e.g. tungsten) result in high contrast in soft tissues as well (Metscher 2009b). As shown in previous studies, the tungsten X-ray source in standard lab CT scanners is sufficient to achieve quality data (Dinley et al., 2010), but this has not really proven to work with cephalopod tissue, even in single X-ray images (Westermann et al., 2002). In *E. scolopes*, different tissues show very similar X-ray-densities after staining and are therefore sometimes hard to discriminate when located closely to each other. Embryos of *E. scolopes* proved to be rather easily contrasted when treated with different substances such as I2M or PTA (Metscher, 2009b), since whole-mount contrasting in small Eppendorf tubes may be performed in less than a day. Since micro-CT has already been used in developmental imaging of vertebrates such as chicken and mice, where even specific cell populations can be identified if imaged under high magnification (Metscher, 2009a), we chose a similar approach with the cephalopod nervous system. If performed properly (the specimens have to be mounted inside small tubes without inclusion of air bubbles to avoid moving during the scan or drying of the object), preparation and data acquisition with micro-CT imaging is much less time consuming than using standard histological protocols, thus allowing for a higher throughput of specimens. This advantage has been pointed out by other studies as well (Dinley et al., 2010; Lauridsen et al., 2011; Ziegler et al., 2010b), together with its second major advantage, the non-destructiveness of the method on the study specimens. Accordingly, even rare specimens may be investigated without destroying them, which is highly advantageous when working with museum material. Investigations of such specimen has not been possible until now in most cases, as most techniques are associated with specimen damage or destruction. This method can further be combined with other imaging techniques as outlined in this study. Micro-CT can give a first impression of an organism or help defining a closely confined region of interest for other studies.

The combination of microCT imaging with other methods is one of the strongest advantages of this method. The iodine-contrasted and microCT-scanned specimens used in this study presented no difficulties histological preparation (such as crystals in the tissues or other perturbations). Thus, the exposure to X-ray radiation does not significantly harm the histological preservation of tissues. If thoroughly rinsed in ethanol, no deposits of iodine remain within the cephalopod tissue, and resin embedding, sectioning and staining with toluidine blue works well (Fig. VI). A combined approach is highly valuable, since semithin serial sections (1µm) allow the identification of sub-cellular details that are not accessible to resolutions of current micro-CT lab systems.

Due to the concentrated X-ray beam and the shielded scanning chamber inside the Micro-Ct-scanner, specimen size is limited. In *Euprymna scolopes*, a squid with embryos approximately 1 to 5mm in length, the use of a CT scans with rather high resolution can be performed on whole specimens. Although the different tissues inside the animal lie closely adjacent to each other, contrasting agents such as I2M allow for a relatively easy differentiation between them. In the majority of stages investigated in

this study, it was possible to distinguish between single ganglia when scanning the whole sample using a 4x objective. With higher magnifications, the differences between the surrounding muscular tissue and the nervous material in, e.g., the arms may be enhanced and may provide data on the nervous system in younger stages as well. Even if only little information on the internal organization of an animal is obtainable, a micro-CT-examination of a specimen prior to, e.g., histological sectioning, provides an overview of the inner organization of the study organism and allows for identification of potential structures of interest.

The data acquired by tomographic methods have a range of advantages. (1) Perfect alignment of virtual sections significantly facilitates subsequent segmentation procedures. (2) There are no geometric distortions, which again facilitates segmentation and allows for artifact-free volume visualization of the data set. Voxels of the tomographic image data are size-calibrated and isotropic. This encourages the use of micro-CT for quantitative investigations, while it is almost impossible to apply volumetric measurements in serial sections based on inhomogeneities and limits in section thickness, and geometric distortions. (4) Also, there are fewer problems with staining inhomogeneities in the sample, which can be a difficulty when applying volume rendering on serial section data (Handsuh et al., 2010). Staining gradients can appear in micro-CT images as well, for example in the case of an irregular penetration of the contrasting agent, but can easily be identified and balanced in the process.

In contrast to other imaging methods such as confocal microscopy, micro-CT contrasting substances can be chosen to be rather tissue-nonspecific. Therefore, an overview of different tissues can be revealed on micrographs. Conveniently, the entire brain structure with directly adjacent sensory organs such as eyes and statocysts may be revealed by one scan without further manipulation of the specimen. Although micro-CT already offers a wide range of possibilities to process different specimens, more methods are still being added to the micro-CT repertoire. The combination with modern fluorescence techniques should be possible, and a molecular imaging method has recently been developed (Metscher and Müller, 2011). The application of micro-CT to imaging gene expression could for example be used on neural patterning genes to better locate expression domains in complex organisms. According to our data, tissues are not significantly damaged, at least not on the light microscopic level. With this application, the signal inside the body may be revealed in greater detail using the images obtained by a micro-CT scanner. As the whole field of micro-CT is still developing, there are many possibilities within the scope of this technique concerning its application.

Current CT scanners offer the possibility to image specimens across a huge size range at very different resolutions. Using a conventional (medical) CT scanner, resolution is mostly limited to approximately 10 μ m voxel size (cubic) (Westermann et al., 2002). With systems such as the Xradia MicroXCT we used in this study, resolution is much higher (down to approximately 1.5 μ m), although the field of view is limited about 5 millimeters. The newer Xradia systems offer a large field option along with the high-

magnification imagers (www.xradia.com). Desktop instruments such as the Skyscan 1172 micro-CT machine (www.skyscan.be) offer a wider field of view, but lower resolutions. Due to the high X-ray doses and the prohibition to move during the scan, no live material can be used in the latter two devices. In vivo micro-CT scanners are available though, with which investigation of living material is possible if movement is reduced to a minimum (e.g., by narcotization of the study specimens). This lower resolution comes close to that achieved in magnetic resonance imaging (MRI), where orientation of water molecules is used to discriminate between different tissues (Ziegler et al., 2008; Ziegler et al., 2010a; Ziegler et al., 2011). This method has proven to be quite useful in investigations of museum specimens and of a higher number of individuals, as it does not take a lot of time to obtain the data (Ziegler and Mueller, 2011; Ziegler et al., 2009; Ziegler et al., 2010b). In cephalopods, MRI has already been used to describe nervous system components (Quast et al., 2001) and for work with palaeobiological material (Mietchen et al., 2005). The resolution, though, cannot compete to that achieved with μ CT-scanners.

CONCLUSION

Many traditional imaging techniques are not suitable for such combined use on the same sample since they are destructive. Micro-CT offers the opportunity to combine with other methods to carry out a thorough investigation of the internal organization of soft-bodied organisms at multiple spatial scales. We demonstrated that the X-ray beam of the scanner is non-damaging to soft tissue, which thus can be further processed for histological analyses. Apart from the downstream methods discussed herein, there is a rich palette of possibilities for combinations to test in the future. As an example, micro-CT applications might be combined with gene expression studies on neural patterning genes to allow for better localization of expression domains in complex organisms. The development of specific antibody staining protocols for micro-CT imaging (Metscher and Müller, 2011) was just such a step in the development of the method and will offer a versatile tool for future investigations for morphologists, developmental biologists, and researchers of many other fields. Until now, the production of serial sections has been the most detailed way to achieve this kind of information to base molecular data on. In contrast to confocal data, X-ray microtomography data reveal the structure of thicker tissues in great detail and are unaffected by autofluorescence. This is a particular concern when working with cephalopod embryos, since they contain a large amount of yolk, thus being notorious for generating high levels of autofluorescence.

ACKNOWLEDGEMENTS

Tim Wollesen (Vienna) is thanked for comments on the manuscript. Additionally, we want to thank Gerd Müller (Vienna) for providing the equipment used for micro-CT-investigations. We are grateful to the CIUS (Core Facility of Cell Imaging and

Ultrastructure research) at the University of Vienna for providing the microtome used in this study.

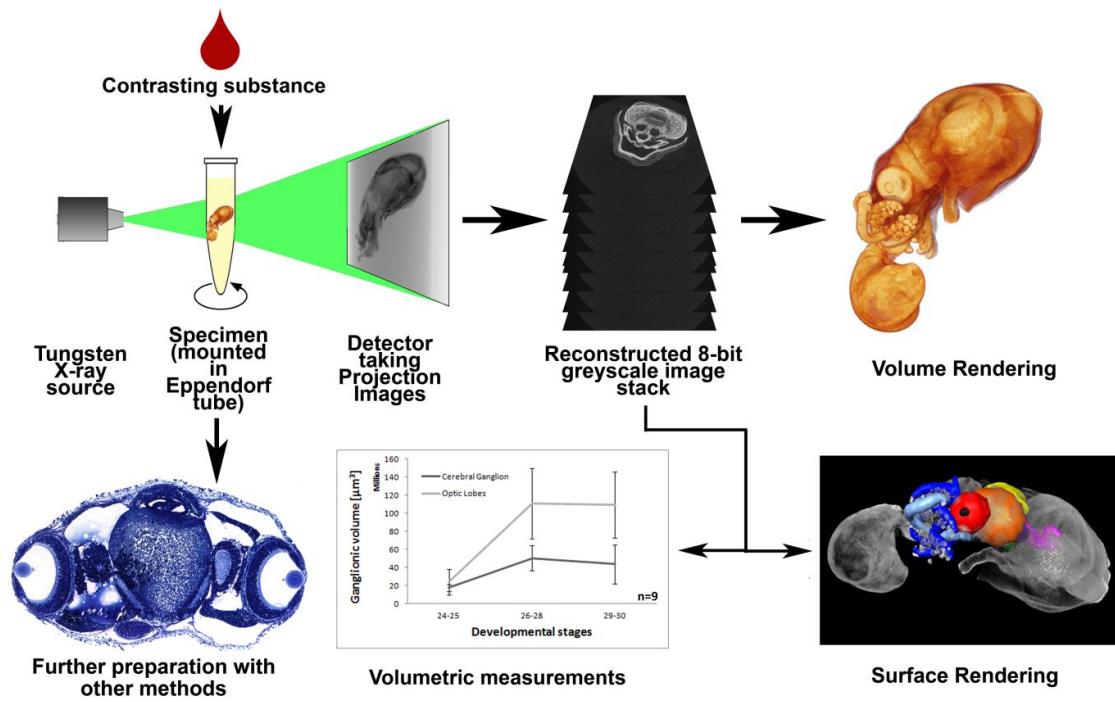
REFERENCES

- Alagarwami, K., 1966. On the embryonic development of the squid (*Sepioteuthis arctipinnis* GOULD) from the Gulf of Mannar. J. Mar. biol. Ass. India 8(2), 278-284.
- Arnold, J.M., 1965. Normal embryonic stages of the squid, *Loligo pealii* (Leseur), Department of Zoology, University of Minnesota. University of Minnesota, Minneapolis.
- Arnold, J.M., Singley, C.T., Williams-Arnold, L.D., 1972. Embryonic Development and Post-Hatching Survival of the Sepiolid Squid *Euprymna scolopes* under Laboratory conditions. The Veliger 14(4), 361-364.
- Asokan, P.K., Kakati, V.S., 1991. Embryonic development and hatching of *Loligo duvaucelii* ORBIGNY (Loliginidae, Cephalopoda) in the laboratory. Indian Journal of Fisheries 38(4), 201-206.
- Callaerts, P., Lee, P.N., Hartmann, B., Farfan, C., Choy, D.W., Ikeo, K., Fischbach, K.F., Gehring, W.J., de Couet, H.G., 2002. HOX genes in the sepiolid squid *Euprymna scolopes*: implications for the evolution of complex body plans. Proc Natl Acad Sci U S A 99(4), 2088-2093.
- Desplentere, F., Lomov, S.V., Woerdeman, D.L., Verpoest, I., Wevers, M., Bogdanovich, A., 2005. Micro-CT characterization of variability in 3D textile architecture. Composites Science and Technology 65(13), 1920-1930.
- Dinley, J., Hawkins, L., Paterson, G., Ball, A.D., Sinclair, I., Sinnett-Jones, P., Lanham, S., 2010. Micro-computed X-ray tomography: a new non-destructive method of assessing sectional, fly-through and 3D imaging of a soft-bodied marine worm. J Microsc 238(2), 123-133.
- Farfan, C., Shigeno, S., Nodl, M.T., de Couet, H.G., 2009. Developmental expression of apterous/Lhx2/9 in the sepiolid squid *Euprymna scolopes* supports an ancestral role in neural development. Evol Dev 11(4), 354-362.
- Handschuh, S., Schwaha, T., Metscher, B.D., 2010. Showing their true colors: a practical approach to volume rendering from serial sections. BMC Dev Biol 10, 41.
- Hanlon, R.T., Claes, M.F., Ashcraft, S.E., Dunlap, P.V., 1997. Laboratory culture of the sepiolid squid *Euprymna scolopes*: A model system for bacteria-animal symbiosis. Biol Bull 192, 364-374.

- Hartmann, B., Lee, P.N., Kang, Y.Y., Tomarev, S., de Couet, H.G., Callaerts, P., 2003. Pax6 in the sepiolid squid *Euprymna scolopes*: evidence for a role in eye, sensory organ and brain development. *Mech Dev* 120(2), 177-183.
- Kocot, K.M., Cannon, J.T., Todt, C., Citarella, M.R., Kohn, A.B., Meyer, A., Santos, S.R., Schander, C., Moroz, L.L., Lieb, B., Halanych, K.M., 2011. Phylogenomics reveals deep molluscan relationships. *Nature* 477(7365), 452-456.
- Lauridsen, H., Hansen, K., Wang, T., Agger, P., Andersen, J.L., Knudsen, P.S., Rasmussen, A.S., Uhrenholt, L., Pedersen, M., 2011. Inside out: modern imaging techniques to reveal animal anatomy. *PLoS One* 6(3), e17879.
- Lee, P.N., Callaerts, P., de Couet, H.G., 2009c. The embryonic development of the Hawaiian bobtail squid (*Euprymna scolopes*). *Cold Spring Harb Protoc* 2009(11), pdb ip77.
- Marquis, F., 1989. Die Embryonalentwicklung des Nervensystems von *Octopus vulgaris* Lam. (Cephalopoda, Octopoda), eine histologische Analyse. *Verhandl. Naturf. Ges. Basel* 99, 23-76.
- Marthy, H.J., 1975. Organogenesis in cephalopoda: further evidence of blastodisc-bound developmental information. *J. Embryol. exp. Morph.* 33(1), 75-83.
- Messenger, J.B., 1978. The nervous system of *Loligo* IV. The peduncle and olfactory system. *Philos Trans R Soc Lond B Biol Sci* 285, 275-309.
- Metscher, B.D., 2009a. MicroCT for developmental biology: a versatile tool for high-contrast 3D imaging at histological resolutions. *Dev Dyn* 238(3), 632-640.
- Metscher, B.D., 2009b. MicroCT for comparative morphology: simple staining methods allow high-contrast 3D imaging of diverse non-mineralized animal tissues. *BMC Physiol* 9, 11.
- Metscher, B.D., 2010. X-ray microtomographic imaging of vertebrate embryos. In: Sharpe, J., Wong, R., Yuste, R. (Eds.), *Imaging in Developmental Biology: A Laboratory Manual*. Cold Spring Harbor Press, Cold Spring Harbor.
- Metscher, B.D., Müller, G.B., 2011. MicroCT for molecular imaging: Quantitative visualization of complete three-dimensional distributions of gene products in embryonic limbs. *Dev Dyn* 240(12), 2301-2308.
- Mietchen, D., Keupp, H., Manz, B., Volke, F., 2005. Non-invasive diagnostics in fossils - Magnetic Resonance Imaging of pathological belemnites. *Biogeosciences* 2, 133-144.
- Quast, M.J., Neumeister, H., Ezell, E.L., Budelmann, B.U., 2001. MR microscopy of cobalt-labeled nerve cells and pathways in an invertebrate brain (*Sepia officinalis*, Cephalopoda). *Magnetic Resonance in Medicine* 45(4), 575-579.

- Salvini-Plawen, L., 1980. A reconsideration of systematics in the mollusca (phylogeny and higher classification). *Malacologia* 19(2), 249-278.
- Salvini-Plawen, L., Steiner, G., 1996. Synapomorphies and plesiomorphies in higher classification of Mollusca. In: Taylor, J.D. (Ed.), *Origin and Evolutionary Radiation of the Mollusca*. Oxford University Press, Oxford, pp. 29-52.
- Shigeno, S., Yamamoto, M., 2002. Organization of the nervous system in the pygmy cuttlefish, *Idiosepius paradoxus* Ortmann (Idiosepiidae, Cephalopoda). *J Morphol* 254(1), 65-80.
- Shigeno, S., Tsuchiya, K., Segawa, S., 2001b. Embryonic and paralarval development of the central nervous system of the loliginid squid *Sepioteuthis lessoniana*. *J Comp Neurol* 437(4), 449-475.
- Shigeno, S., Kidokoro, H., Tsuchiya, K., Segawa, S., Yamamoto, M., 2001a. Development of the Brain in the Oegopsid squid, *Todarodes pacificus*: An atlas up to the hatching stage. *Zoolog Sci* 18, 527-541.
- Shigeno, S., Sasaki, T., Moritaki, T., Kasugai, T., Vecchione, M., Agata, K., 2008. Evolution of the cephalopod head complex by assembly of multiple molluscan body parts: Evidence from *Nautilus* embryonic development. *J Morphol* 269(1), 1-17.
- Smith, S.A., Wilson, N.G., Goetz, F.E., Feehery, C., Andrade, S.C., Rouse, G.W., Giribet, G., Dunn, C.W., 2011. Resolving the evolutionary relationships of molluscs with phylogenomic tools. *Nature*.
- Westermann, B., Ruth, P., Litzlbauer, H.D., Beck, I., Beuerlein, K., Schmidtberg, H., Kaleta, E.F., Schipp, R., 2002. The digestive tract of *Nautilus pompilius* (Cephalopoda, Tetrabranchiata): an Xray analytical and computational tomography study on the living animal. *The Journal of Experimental Biology* 205, 1617-1624.
- Wollesen, T., Cummins, S.F., Degnan, B.M., Wanninger, A., 2010. FMRFamide gene and peptide expression during central nervous system development of the cephalopod mollusk, *Idiosepius notoides*. *Evol Dev* 12(2), 113-130.
- Young, J.Z., 1965. The central nervous system of *Nautilus*. *Philos Trans R Soc Lond B Biol Sci* 249, 1-45.
- Young, J.Z., 1973. The central nervous system of *Loligo* I. The optic lobe. *Philos Trans R Soc Lond B Biol Sci* 267, 263-301.
- Young, J.Z., 1975. The nervous system of *Loligo* II. Suboesophageal centres. *Philos Trans R Soc Lond B Biol Sci* 274, 101-167.
- Young, J.Z., 1977. The nervous system of *Loligo* III. Higher motor centres: The basal supraoesophageal lobes. *Philos Trans R Soc Lond B Biol Sci* 276, 351-398.

- Young, J.Z., 1978. The nervous system of *Loligo*. V. The vertical lobe complex. *Philos Trans R Soc Lond B Biol Sci* 285, 311-354.
- Young, J.Z., 1988. Evolution of the cephalopod brain. In: Wilbur, K.M., Tompa, A.S., Verdonk, N.H., van den Biggelaar, J.A.M. (Eds.), *Paleontology and Neontology of cephalopods*. Academic Press Inc., pp. 215-228.
- Ziegler, A., Mueller, S., 2011. Analysis of freshly fixed and museum invertebrate specimens using high-resolution, high-throughput MRI. *Methods Mol Biol* 771, 633-651.
- Ziegler, A., Faber, C., Bartolomaeus, T., 2009. Comparative morphology of the axial complex and interdependence of internal organ systems in sea urchins (Echinodermata: Echinoidea). *Front Zool* 6, 10.
- Ziegler, A., Faber, C., Mueller, S., Bartolomaeus, T., 2008. Systematic comparison and reconstruction of sea urchin (Echinoidea) internal anatomy: a novel approach using magnetic resonance imaging. *BMC Biol* 6, 33.
- Ziegler, A., Mooi, R., Rolet, G., De Ridder, C., 2010a. Origin and evolutionary plasticity of the gastric caecum in sea urchins (Echinodermata: Echinoidea). *BMC Evol Biol* 10, 313.
- Ziegler, A., Ogurreck, M., Steinke, T., Beckmann, F., Prohaska, S., 2010b. Opportunities and challenges for digital morphology. *Biol Direct* 5, 45.
- Ziegler, A., Kunth, M., Mueller, S., Bock, C., Pohmann, R., Schröder, L., Faber, C., Giribet, G., 2011. Application of magnetic resonance imaging in zoology. *Zoomorphology* 130(4), 227-254.



Graphical abstract

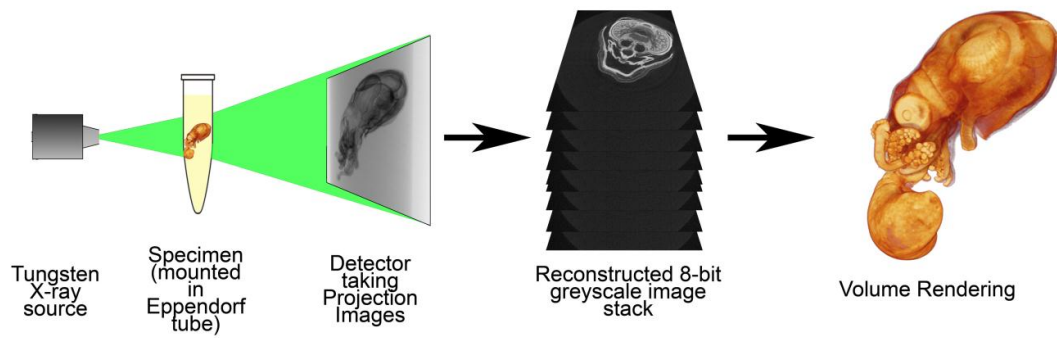


Fig. I. Workflow for microCT data acquisition, reconstruction, and visualization. During the scan, multiple single projection images of an organism are recorded at different angles, while the specimen is rotated around its own vertical axis. Due to the organization of the tissues inside the body, the detector receives X-rays with different intensities depending on the X-ray absorption in tissues. Using appropriate software, the projection images are reconstructed, yielding a greyscale image stack of virtual sections, which can be exported to create computer-assisted 3D-reconstructions (such as volume renderings using arbitrary colouring), calculate volumes, and perform further analyses. Scale bars are 500 μ m.

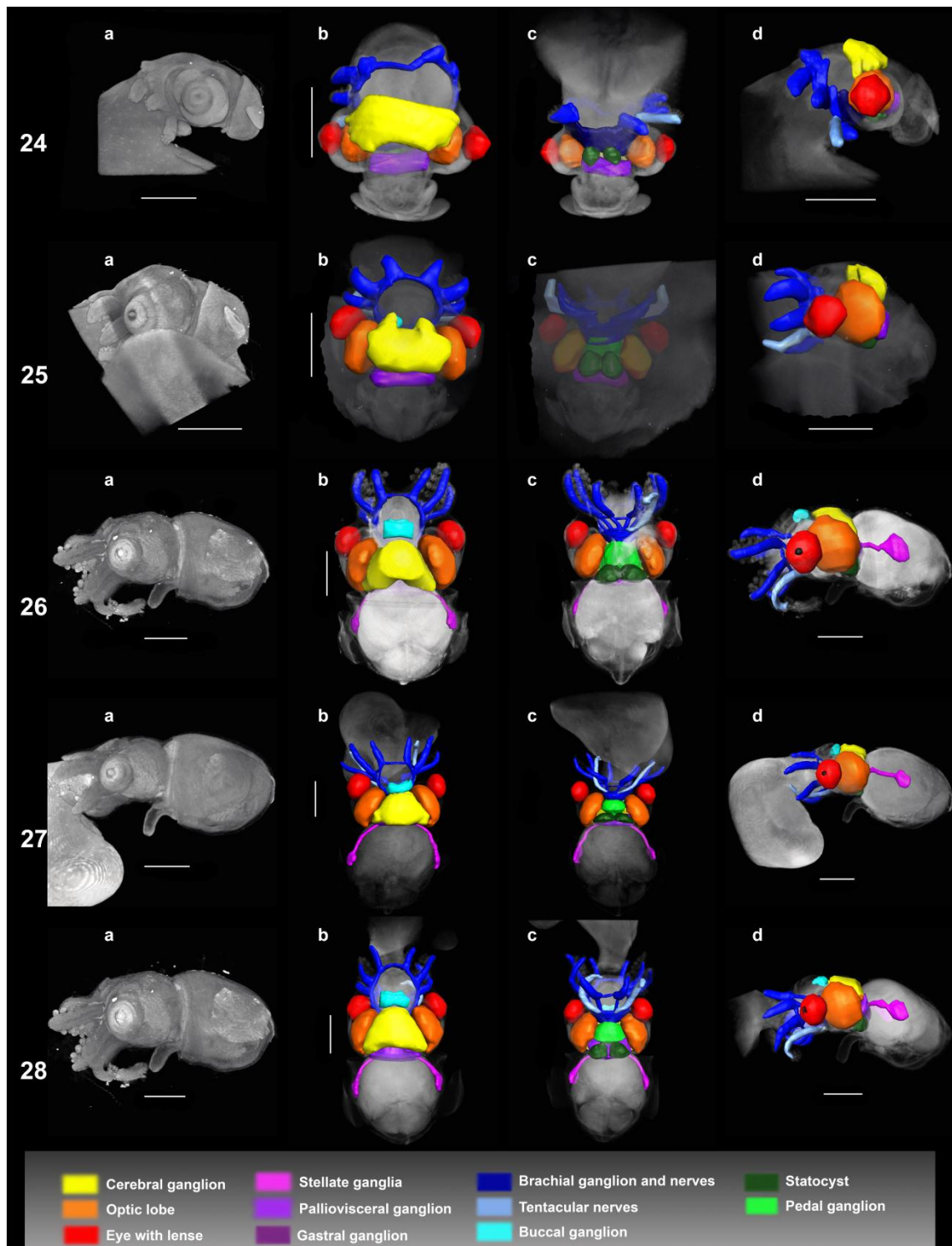


Fig. II. Volume renderings (a) and combined images of volume and surface renderings (b – dorsal, c – ventral, d – lateral), focusing on the nervous system of *Euprymna scolopes* from stage 24 to 28. The different ganglia, dominant sensory organs, and prominent nerve strands are color coded. During development, the brachial nerves are elaborated, elongate, and the optic lobes rapidly increase in volume. They remain the most prominent component in the brain of *Euprymna* and overlay the pedal, the brachial, and the palliovisceral ganglion. In the specimen of stage 25, the yolk was surrounding the whole animal, shading the ganglia when seen from the ventral side. Scale bars are 500 μ m.

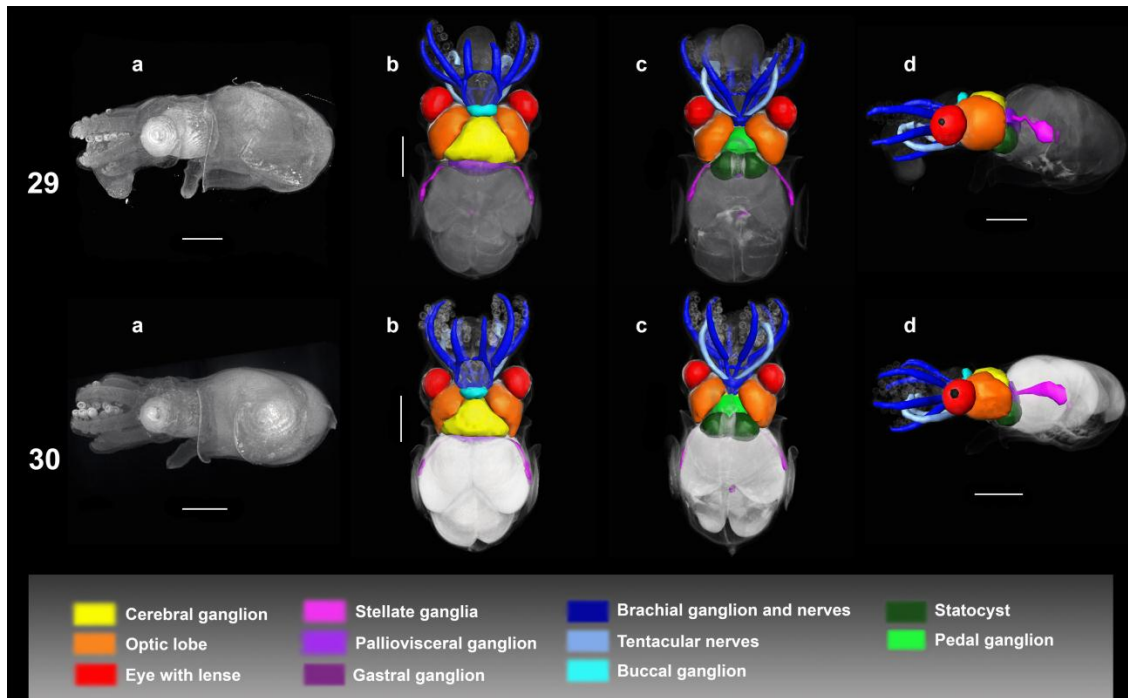


Fig. III. Volume renderings (a) and combined images of volume and surface renderings (b – dorsal, c – ventral, d – lateral) focusing on the nervous system of *Euprymna scolopes* of stage 29 and 30 (hatchling). The different ganglia, prominent sensory organs, and nerve strands are color coded. At hatching, most of the ganglionic mass is strictly concentrated in the head. From stage 29 onwards, the gastral ganglion close to the stomach can be observed. Scale bars are 500 μ m.

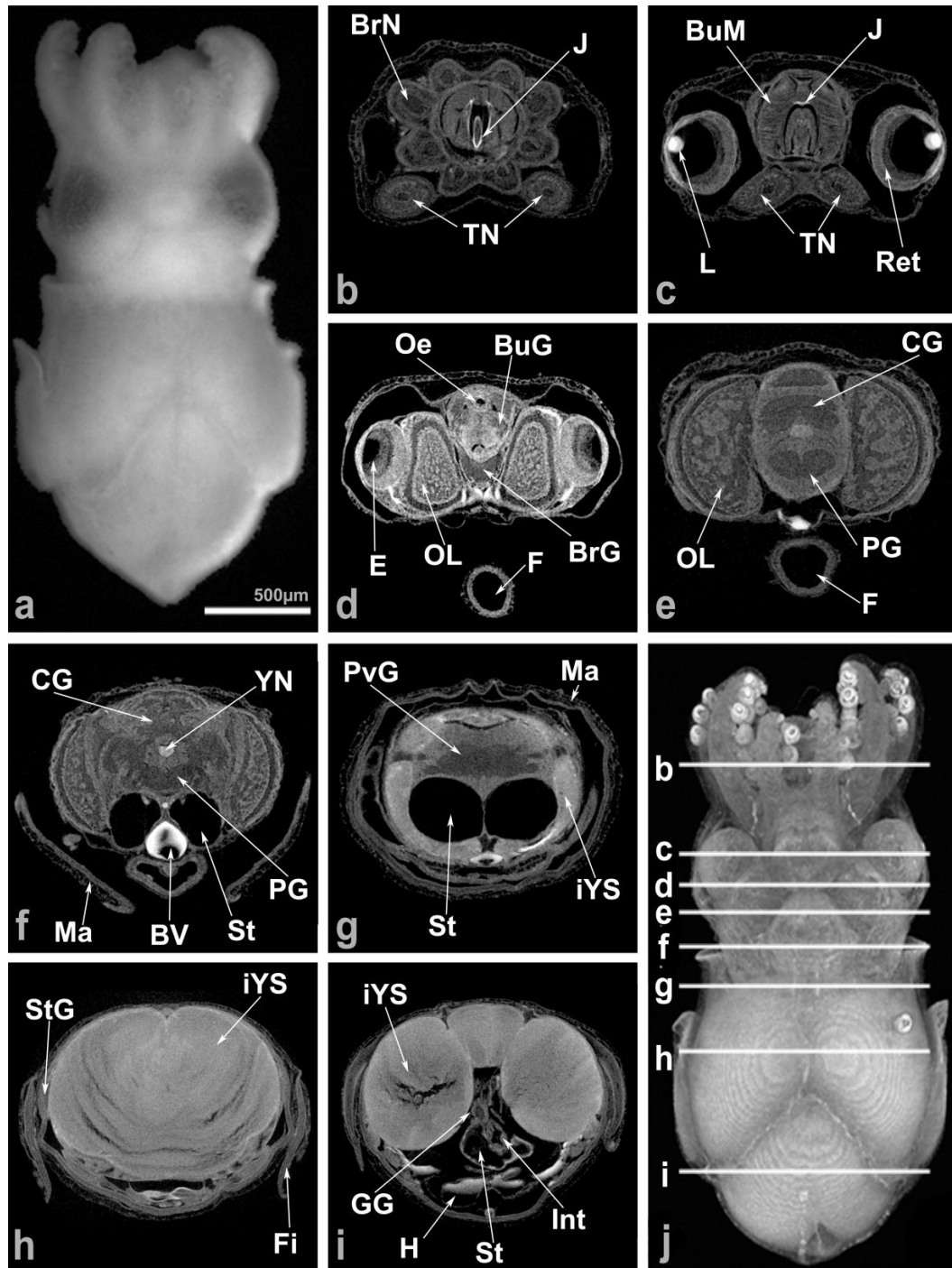


Fig. IV. X-ray microtomographic section series of a *Euprymna scolopes* hatchling. Starting from a fixed sample (a, light microscopic image), virtual sections may be viewed in the three orthogonal planes of the animal. Especially the ganglionic system (brachial and tentacular nerves) (b), eyes, buccal mass, and tentacular nerves (c), buccal ganglia, optic lobes, eyes, brachial ganglion, and funnel (d), optic lobes, cerebral ganglion, esophagus, pedal ganglion, and frontal lobe (e), palliovisceral ganglion, cerebral ganglion, optic lobes, mantle, and statocysts with statoliths (f), statocysts and palliovisceral ganglion with outgoing connections to the stellate ganglia (g), stellate ganglia and internal yolk sac (h), gastral ganglion and parts of the digestive system and heart (i) can be discriminated from the other organ systems. A volume rendering (j) offers a better insight into the specimen's internal organization than the light microscopic image (a).

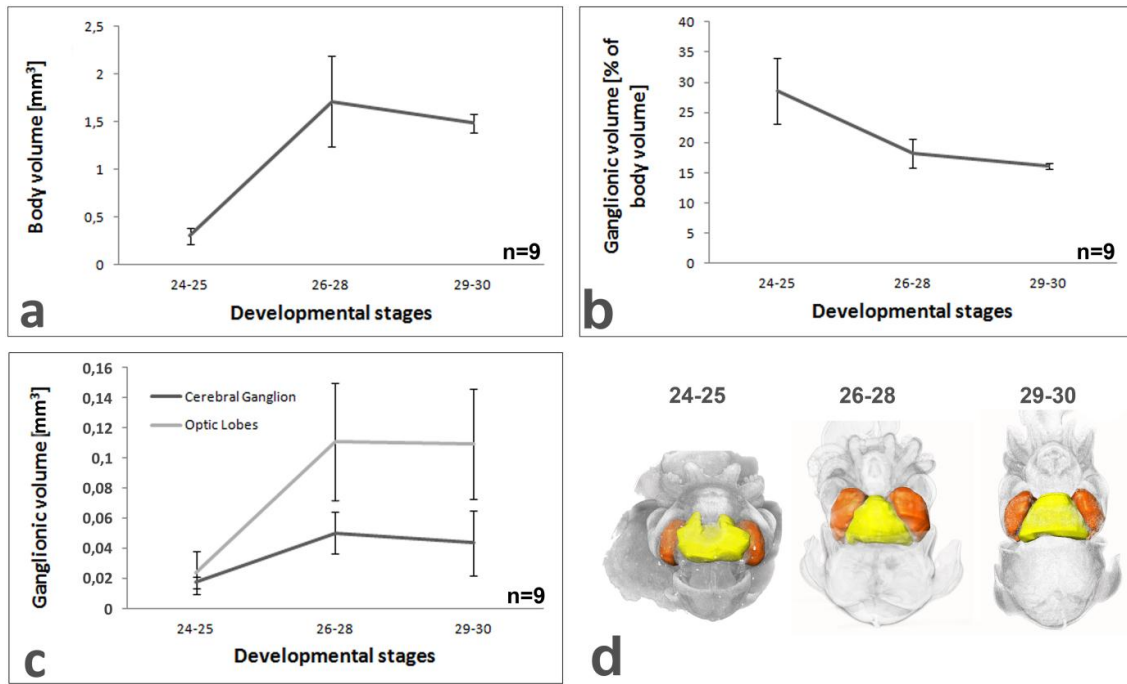


Fig. V. Growth and volumetrics of the CNS of *Euprymna scolopes*. Graphs of (a) the total body volume, (b) the ganglionic system as percentage of the total body volume and (c) the cerebral ganglion and the optic lobes in absolute numbers. (d) displays the optic lobes (orange) and the cerebral ganglion (yellow) in characteristic specimens of the chosen developmental stages. Ten individuals were investigated in this study and regrouped into four groups. The graph is formed after the arithmetic means of these groups. Standard deviations are given as well. The ganglionic system rapidly increases during the first developmental stages and decreases relative to the total body volume toward the end of embryonic development. The optic lobes gain size faster than the cerebral ganglion, as can be observed by using absolute as well as relative volumes.

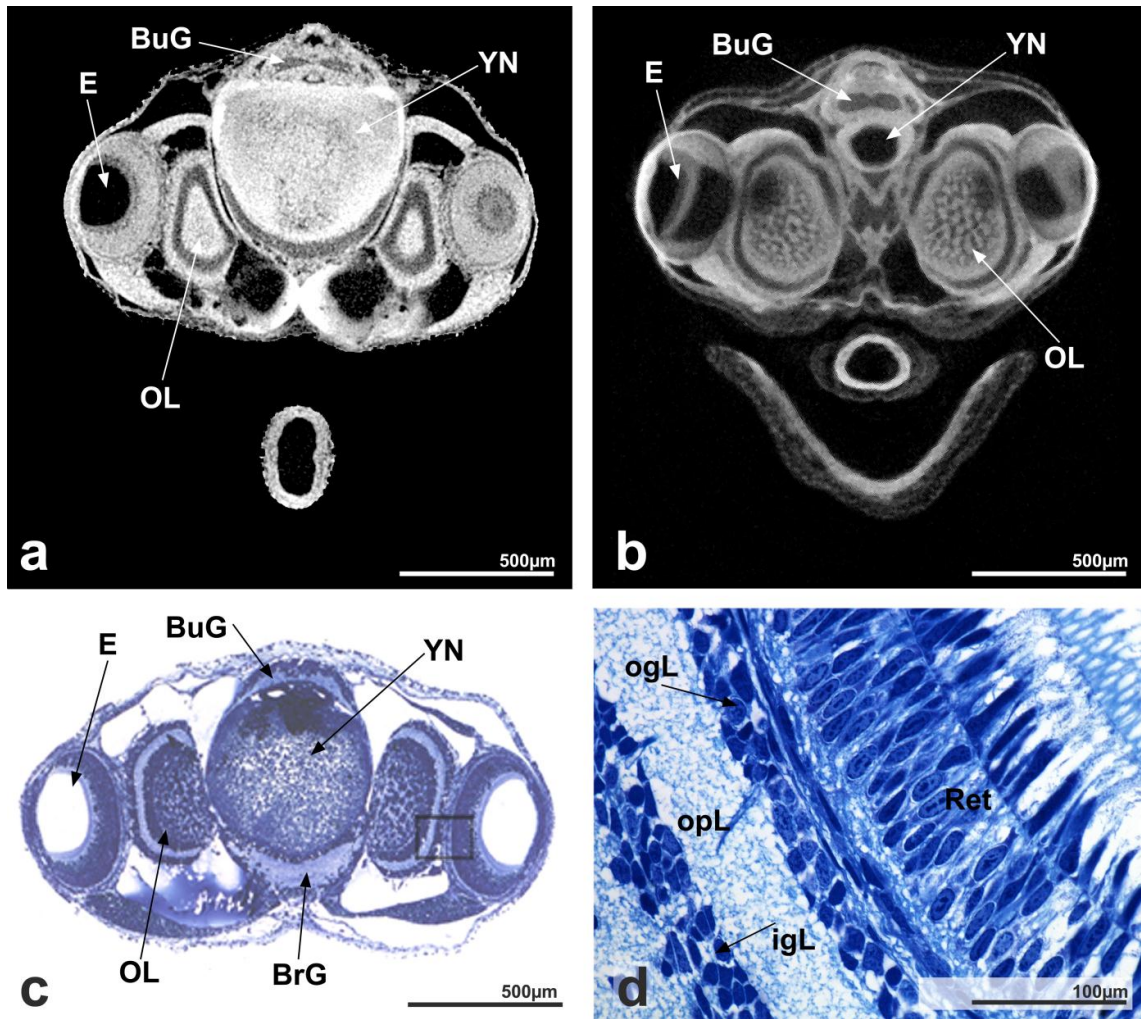


Fig. VI. Different staining and preparation of a *Euprymna scolopes* stage 28 embryo. (a) micro-CT (phosphotungstic acid (PTA); voxel size 3µm), (b) micro-CT (elemental iodine in methonal (I2M); voxel size 3µm), (c) araldite-embedded section (toluidineblue; slice thickness 1µm), (d) different layers of the retina. I2M has proven to work better with *Euprymna* embryos than PTA, since it contrasts all tissues well and allows for a better differentiation than PTA, which intensely stains the yolk, but not thin membranes. In semithin sections, resolution may go down to the cellular level and reveal fine details. The detail of the retina and the cortex of the optic lobe (d) was taken from the cross section (d) and depicts the layers of the cortex as well as cellular details of the retina.

CONTACT INFORMATION

Alexandra KERBL
Rosensteingasse 29/8
1170 Vienna, AUSTRIA
Tel. +43 6644206766
Email: alexandra.kerbl@univie.ac.at



PERSONAL INFORMATION

Date of birth: January 12th, 1988 (Vienna)
Nationality: AUSTRIA

EDUCATION

SS 2008 – WS 2011 Diploma study of zoology at the University of Vienna, Austria
SS 2008 - ? Diploma study of ecology at the University of Vienna, Austria
WS 2006 – WS 2009 Bachelor study of publicism and communication studies at the University of Vienna, Austria (completed at October 7th, 2009)
WS 2006 – SS 2008 Diploma study of biology at the University of Vienna, Austria
1998-2006 BRG IV Waltergasse, 1040 Vienna, Austria (Matriculation at June 6th, 2006)
1994-1998 Evangelische Volksschule Karlsplatz, 1040 Vienna, Austria

PRACTICAL COURSES

October 2008 – January 2009 Special practicum „Mollusca“ (Salvini-Plawen, Steiner, Redl)
October 2009 – January 2010 „Palaeodiversity of evertebrates“ (Zuschin, Pervesler, Ostrovsky)
Juli 2009 „Introduction to marine flora and fauna“, in Rovinj, Croatia (Steiner, Abed-Navandi, Gallmetzer)
November 2009 – January 2010 „Histological Project Practicum“ (Walzl, Rudoll, Handschuh)
March 2010 – June 2010 „3-D Imaging and Modeling Using MicroCT“ (Metscher, Pokorny, Handschuh)
October 2010 – January 2011 „Marine-ecologic special practicum 1+2“ (Herndl, Schagerl) with two-week field work at Calvi, Corse
April 2010 „Fieldwork in aquatic sediments“ (Herler, Zuschin) in Dahab, Egypt
March 2011 „Submicroscopic anatomy and preparation techniques“ (Klepal, Gruber, Weidinger, Cyran)

WORK EXPERIENCE

since July 2011 Work at the FWF-Project „Characterisation of the cement of *Dosima fascicularis* GRAY” under administration of Prof. Waltraud Klepal

October 2011 – February 2012 Tutor for the „Histologic project practicum“, and the project practicum „Submicroscopic anatomy and preparation techniques“, at the University of Vienna, Austria

March 2011 – July 2011 Tutor for the basic course „Baupläne 2“, at the University of Vienna

October 2010 – February 2011 Tutor for the “Histologic project practicum“, and the special practicum „Mollusca“, at the University of Vienna, Austria

CONGRESS CONTRIBUTIONS

Alexandra Kerbl

Smart from the start!? – Developmental changes in the central ganglia system of the Hawaiian Bobtail Squid (*Euprymna scolopes* BERRY, 1913) [Mollusca: Cephalopoda]

Oral presentation at the DZG Graduiertenforum at the University of Vienna, Austria at October, 23rd, 2010

Alexandra Kerbl & Stephan Handschuh

Smart from the start!? Developmental changes in the central ganglia system of the Hawaiian Bobtail Squid (*Euprymna scolopes* BERRY, 1913) [Mollusca: Cephalopoda]

Poster presentation at the Molluscan Forum 2010 in London, Great Britain at November 30th, 2010 (organized by the Malacological Society London)

Alexandra Kerbl

Development of the central nervous system in *Euprymna scolopes* [Cephalopoda: Sepiolidae]

Poster presentation at the Euroceph-Conference 2011 in Naples, Italy at April 9th, 2011 (organised by the Stazione Zoologica Anton Dohrn in Naples)

Alexandra Kerbl & Manfred Walzl

Development of the ganglionic system of the Hawaiian Bobtail Squid *Euprymna scolopes*

Poster presentation at the 2nd International Conference on Invertebrate Morphology (ICIM) in Harvard, USA at June 22nd, 2011

Alexandra Kerbl

Development of the ganglionic system of the Hawaiian Bobtail Squid *Euprymna scolopes*

Oral presentation at the DZG Graduiertenforum at the LMU Munic, Germany at October 21st, 2011

Alexandra Kerbl, Stephan Handschuh, Marie-Therese Nödl, Brian Metscher, Manfred Walzl & Andreas Wanninger

New Possibilities In Anatomical Studies. Micro-CT-protocols and their use for investigations in soft-bodied organisms

Oral presentation at the Molluscan Forum 2011 in London, Great Britain at November 30th, 2011 (organized by the Malacological Society London)

PUBLICATIONS

Alexandra Kerbl, Stephan Handschuh, Marie-Therese Nödl, Brian Metscher, Manfred Walzl & Andreas Wanninger (subm.): Micro-CT as non-destructive technique to determine ganglionic growth during cephalopod development.

ADDITIONAL QUALIFICATIONS

PADI Advanced Open Water Diver

Driving licence (class B)

Knowledge of foreign Languages: English, French

Basic knowledge of statistics

INTERESTS

Molluscs (especially cephalopods), diving, marine biology, ecology, anatomy, morphology